DISSERTATION

EVALUATING THE SUSTAINABILITY OF EMERGING AGRICULTURAL SYSTEMS

Submitted by

Reid Maynard

Department of Mechanical Engineering

In partial fulfillment of the requirements

For the Degree of Doctor of Philosophy

Colorado State University

Fort Collins, Colorado

Summer 2025

Doctoral Committee:

Advisor: Jason C. Quinn

Todd Bandhauer
Shantanu Jathar
Sybil Sharvelle

ABSTRACT

EVALUATING THE SUSTAINABILITY OF EMERGING AGRICULTURAL SYSTEMS

As the global community seeks to balance rising demands for food and energy with the planet's ecological limits, stakeholders must scrutinize production systems across sectors for opportunities to innovate and reduce impacts. Foremost among these challenges is the threat of climate change driven by greenhouse gas (GHG) emissions. In order to address these emissions, the agricultural sector will play a role as producers mitigate GHG's associated with essential food production while also rising to meet other decarbonization initiatives such as biofuel usage. To quantify these impacts, life cycle assessment (LCA) is used as a well-established method that captures the flows of resources and pollution across supply chains, translating them into impacts. These LCA results inform stakeholders of ecological tradeoffs and mitigation opportunities. By leveraging more advanced methods to differentiate between locations and to model future conditions, these tools can steer the consideration and development of emerging systems towards eco-efficient outcomes. In this dissertation, LCA is utilized in three phases to evaluate emerging agricultural systems, assessing their impacts and identifying sustainability strategies.

In the first research phase, geographically-resolved LCA was applied to compare climate impacts and water usages of new local food production systems across the contiguous United States with a centralized supply chain. Using leaf lettuce as the study crop, hydroponic systems were modeled using building energy demand software to simulate indoor plant factories and greenhouses under different local climate and grid conditions. Additionally, crop modeling software was utilized to simulate seasonal lettuce production on farms at each location. Finally,

these localized systems were compared to a modeled conventional system of California field cultivation and shipping. Results across all sites indicate that indoor production systems have substantially higher GHG emissions than the conventional supply chain owing to energy consumption from heating and dehumidification demand. Thus, consumers seeking low-impact options should eat from local farms when in-season and otherwise use conventional supply chains. However, local stakeholders may consider a food-climate-water tradeoff, since indoor hydroponic systems use far less water than outdoor systems. Technology adoption scenarios are also considered to evaluate how heating electrification and decarbonized electricity affect the GHG outcomes of indoor cultivation, providing insights for operators in this emerging sector.

Continuing to leverage geographic resolution in LCA, the second research phase considers an emerging biofuel feedstock production supply chain at the field-by-field level. In partnership with a company building a plant to convert ethanol to jet fuel, corn fields across South Dakota and Minnesota were evaluated for the 2023 harvest. Utilizing upstream supply chain modeling and the Daycent biogeochemical soil model, localized cultivation practices were translated into farm-gate carbon intensities. Stochastic modeling was then applied to compare results across hundreds of sample sites to default modeling assumptions typically utilized in biofuel LCA. Results demonstrate that this supply chain, on average, achieves lower GHG emissions than the default model suggests, stemming from local variations in energy usage, agrochemical application, and soil conservation. Further analysis suggests that producers focus on nitrogen fertilizer efficiency and land management initiatives with a particular need to ensure accurate, field-level modeling of soil dynamics. Alongside downstream decarbonization efforts, such cultivation-stage initiatives can contribute to creating aviation fuel that meets clean energy standards.

While geography-specific LCA insights are useful to understand agricultural emissions, developments across time are also poised to make significant changes in the sector. Thus, in the third research phase, dynamic LCA (DLCA) methods were applied to the outdoor lettuce cultivation model, incorporating modeled ecospheric and technospheric transformations from the present-day to 2050. Dynamic process modeling was used to evaluate how changing climate could affect crop growth. Meanwhile, background technospheric transformation and on-farm technology adoption were modeled to consider how decarbonizing supply chains and zero-emissions equipment could mitigate life cycle GHG emissions. DLCA baseline results show that 2050 emissions will be substantially reduced compared to present-day assumptions; in particular, the deployment of electrified irrigation, combined with decarbonizing generation, provides a near-term avenue for mitigation. In more optimistic technology change scenarios, emerging technologies like green-hydrogen-derived fertilizer and battery electric heavy machinery could provide further emissions reductions; stakeholders could take steps in the present to support the development and adoption of these systems, enabling ecoefficiency gains in food production.

Throughout this work, standard and enhanced LCA methods were employed to evaluate the sustainability of emerging agricultural systems that could one day meet global food and fuel demands. The results of these assessments provide quantifiable estimates that support inter-system comparisons and process improvement strategies. Thus, these methods and results can support decision-making for stakeholders across the supply chain to invest in a more sustainable agricultural future.

ACKNOWLEDGEMENTS

I would like to acknowledge the support of my committee: Dr. Bandhauer, Dr. Jathar, and Dr. Sharvelle. I particularly would like to thank Dr. Quinn for the opportunity to change my career and for his dedication to my success. Thank you to Dr. Paustian and Dr. Locatelli for their support in soil carbon modeling in Chapter 3. I would also like to thank the members of the Quinn Group and my fellow InterFEWS trainees for their advice, support, and friendship through the years.

Research Question 1 and 3 are based upon work supported by the National Science Foundation under Grant No. 1828902. Any opinions, findings, and conclusions or recommendations expressed in this material are those of the author(s) and do not necessarily reflect the views of the National Science Foundation.

Research Question 2 is based upon work supported by the U.S. Department of Agriculture, under agreement number NR233A750004G076. Any opinions, findings, conclusions, or recommendations expressed in this publication are those of the author(s) and do not necessarily reflect the views of the U.S. Department of Agriculture. In addition, any reference to specific brands or types of products or services does not constitute or imply an endorsement by the U.S. Department of Agriculture for those products or services.

TABLE OF CONTENTS

CHAPTER 1: INTRODUCTION

As atmospheric greenhouse gases continue accumulating and the effects of climate change become more apparent, global production systems must identify and adopt sustainability measures across supply chains. The reports of the International Panel on Climate Change (IPCC) evaluate the need for greenhouse gas (GHG) mitigation and climate change adaptation measures in sectors from energy to industry to agriculture[1,2]. When considered together, Agriculture, Forestry, and Other Land Use account for 22% of global GHG emissions[1]. Influenced by rapidly-changing technologies and climate adaptation necessity, emerging agricultural systems seek not only to mitigate current environmental impacts but also provide sufficient food and fuel to a growing, increasingly-affluent population. Spread across different geographies, facing different socio-economic realities, and utilizing different technological toolsets, communities will make unique decisions in how they balance agriculture and the environment. Understanding these complex systems will be essential to help these decisionmakers compare production methods and identify opportunities to improve eco-efficiency. Life cycle assessment (LCA) is a well-established methodology that quantifies environmental impacts across the entire supply chain[3]. LCA can be applied to emerging technologies to guide development and to established technologies to allow continuous improvement. When applied as a comparative tool, stakeholders can leverage LCA to guide diverse decisions like project sites, suppliers, and technology investments.

As described in the ISO 14040 Standard, LCA consists of four stages: goal and scope definition, life cycle inventory (LCI) analysis, life cycle impact analysis (LCIA), and interpretation[3]. In the first stage, the goal and scope of the project are described through a set of

design parameters, defining such aspects as the system boundary (e.g., cradle-to-factory-gate or cradle-to-grave), the input and output flows of the system, the environmental impacts considered, and the audience for the report[4]. Through this definition process, LCA practitioners set the intent for the study, informing efforts later data collection, modeling, and communication efforts. In the second stage, an LCI is created, accounting for the physical flows between the natural world (also called the "ecosphere") and various technological production systems (also called the "technosphere"). Flows into the system include energy, such as electricity and fuel, as well as materials like water and petrochemicals. Flows out of the system include the primary product, coproducts, and emissions to the air, water, and soil. By leveraging existing LCA databases like ecoinvent[5], practitioners can incorporate highly-detailed models of upstream flows, such as the air emissions of various generation technologies in a particular electrical grid. In the third stage of LCA, known as LCIA, these flows are translated to environmental impacts using established methodologies. Some impact methods reflect inputs, such as total water consumption, while other methods consider how output emissions affect the environment, such as the IPCC's global warming potential (GWP) factors to normalize GHG's like methane and nitrous oxide to carbon dioxide equivalents of climate change impact[6]. Finally, in the interpretation stage of LCA, practitioners further explore the results of these process models, considering different sensitivities, scenarios, and uncertainties to identify relevant impact contributors, explore opportunities for improvement, and compare alternatives. By iterating through these four stages, LCA practitioners quantify a product's impacts and provide stakeholders with a deeper understanding of production systems. These results can then inform important actions like product comparisons, purchasing decisions, and production process improvements.

Though LCA can be a potent sustainability decision-making tool, standard studies can have significant limitations. Notably, LCA results are highly dependent on the accuracy of LCI data. While high-value resources such as primary production data and government survey data can be employed, site-to-site variations can have a significant impact. For example, the environmental impacts of a product manufactured with a coal-heavy grid will differ from one produced using a renewable generation mix. In particular, LCI's in the agricultural sector can vary due to natural factors like soil and climate conditions as well as technological factors like fertilizer manufacturing supply chains. However, LCA practitioners often rely on the limited geographic resolution allowed by their primary and secondary data collections. Further, standard LCA's offer little temporal resolution, deferring to the static snapshot of primary data and the variable ages of studies contained within databases. In contrast, the technological systems of the 21st century are evolving rapidly. Looking again to the example of electricity, a United States-focused LCA from coal-dependent 2008 would provide little insight for a world of low-cost natural gas and renewables. Decarbonizing the global economy will require similar radical transformation across every sector; for programs and investments that span decades, decisions with static data could miss opportunities and risks posed by an evolving world. By going beyond the geographic and temporal limitations of standard analyses, LCA studies can provide insights that capture the diversity and dynamics of nature and technology.

Recognizing these shortcomings, this dissertation examines the sustainability of emerging agricultural systems with a focus on advancing LCA methods to incorporate important geographic and temporal insights. The three research phases included in this work, summarized in **Figure 1**, are: 1) a comparative climate and water LCA of localized food production and centralized food production, 2) a high-detail examination of a South Dakota and Minnesota corn

supply chain for a new jet fuel plant compared to national averages and heuristics, and 3) development of dynamic LCA methods to explore the effects of technological development and climate changes on food system sustainability over the next three decades. The following three chapters detail the background information, methods, and major findings of each phase of work. The combined phases demonstrate the importance of advanced LCA insights to evaluate the sustainability of emerging agricultural systems.

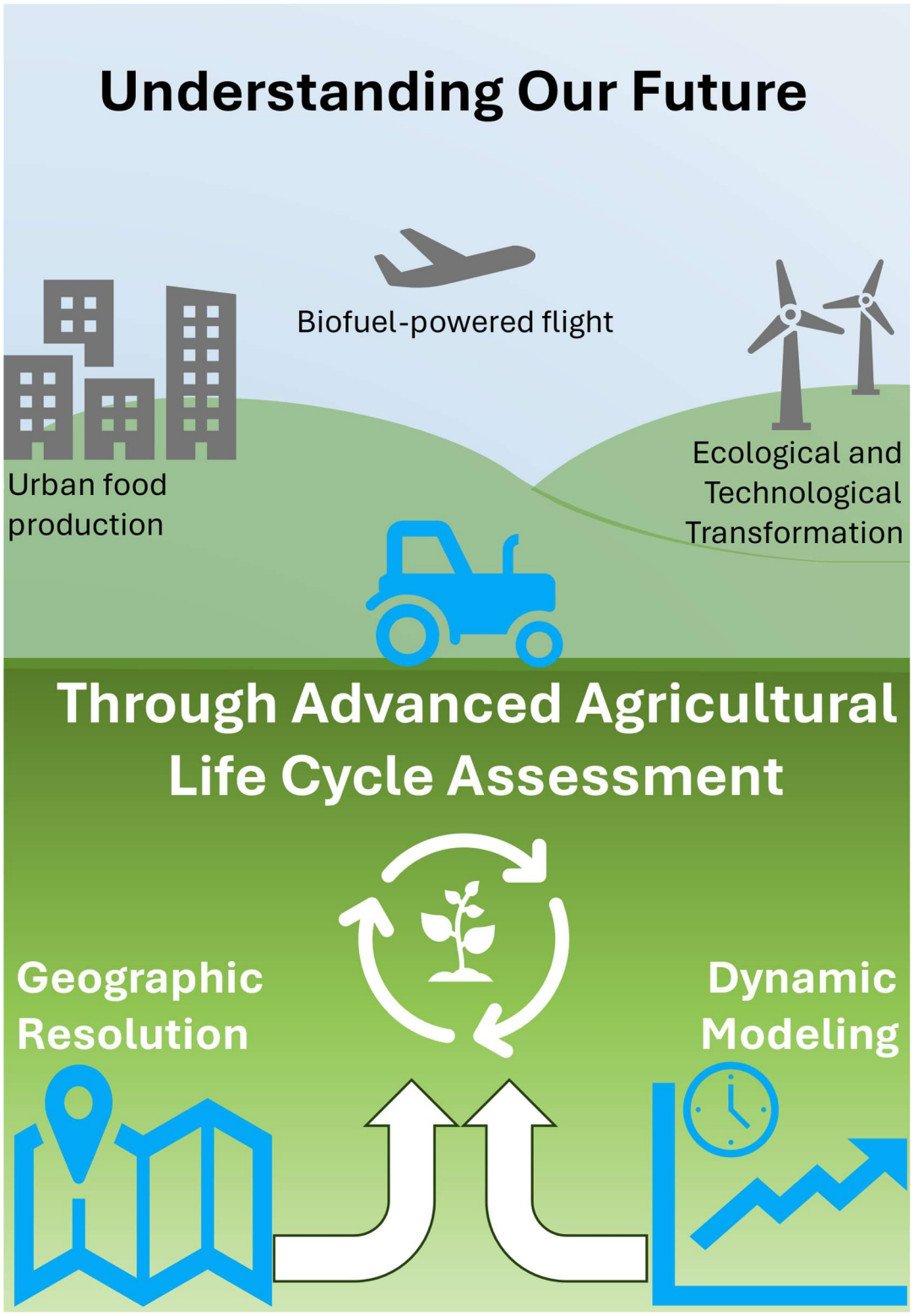

Figure 1. *Visual abstract of the emerging agricultural systems examined in this dissertation's three research phases using advanced LCA methods.*

CHAPTER 2: LCA OF LOCAL AND CENTRALIZED FOOD SYSTEMS[1]

2.1 Background

Globally, agriculture, forestry, and other land use accounts for 21% of global net anthropogenic greenhouse gas (GHG) emissions[7], and food systems including supply chains account for 26% of global emissions[8,9]. These impacts are large enough that achieving the 1.5 °C and 2 °C Paris Agreement targets may not be possible without decarbonizing the agricultural sector[10]. The sustainability challenges will continue to grow as increasing population and affluence grows the demand for more GHG intensive foods[10]. Under these pressures, the global food system will need to adapt technologies, practices, and policies.

One frequently explored option to improve food sustainability is the adoption of local production systems. The Milan Urban Food Policy Pact, for example, identifies urban and peri-urban production as a recommended action for its 211 signatory cities to consider[11]. Such urban production, however, encapsulates diverse techniques and technologies, from community gardens to year-round Controlled Environment Agriculture (CEA) facilities[12]. CEA systems have come under increased scrutiny; while their hydroponic systems can reduce land and water demands, these facilities can have far greater energy demands than conventional systems[13]. Such energy intensity, and the associated emissions, could outweigh the supposed environmental benefits of local production such as reduced "food-miles"[14]. Without systemic considerations, an assumption of local sustainability could have detrimental climate impacts.

---

[1] This chapter has been published as a peer-reviewed journal article: R. Maynard, J. Burkhardt, and J. C. Quinn, "Sustainability of lettuce production: A comparison of local and centralized food production," Journal of Cleaner Production, vol. 428, p. 139224, Nov. 2023, doi: 10.1016/j.jclepro.2023.139224.

Life cycle assessments (LCA) consider the resource inputs and environmental releases throughout a product's life cycle; thus, LCA can serve as a tool to holistically compare different food systems. Previous literature has used LCA to estimate the emissions from urban agriculture. Some studies focus on understanding and improving the environmental performance of CEA facilities[15] while others compare systems with different supply chains. Goldstein et al., for example, compared multiple CEA and soil facilities in the northeastern United States to conventional production and shipping, finding that high-yield, high-energy-input facilities had a greater environmental impact than conventional production[14]. Similarly, Casey et al. compared agricultural production in shipping container modules to soil cultivation supply chains connecting London consumers to British, Spanish, and Californian producers[16]. They found that local CEA production on the existing British grid mix only reduced GHG emissions compared to air-freighted Californian produce. Though previous work sheds light on the sustainability of urban agriculture and how particular systems perform, it often focuses on particular locations with a limited geographic resolution. As such, the literature does not yet provide a tool to facilitate more general CEA sustainability discussions.

This study addresses a gap in the literature by developing location-flexible models for multiple production systems and incorporating geographic resolution in climate, growing conditions, transportation distances, and electricity generation. A primary objective of this paper is to estimate and compare the carbon and water footprints of local and centralized crop production systems in the continental United States. The output will provide communities and local policymakers with clear environmental sustainability comparisons between local and centralized food production. Lettuce is chosen as the model crop as its production is highly centralized in the U.S. and leafy greens are a common crop grown in hydroponic indoor systems;

therefore, lettuce enables a full-spectrum view of the complex localized-centralized production comparison. Four systems are examined: plant factories and greenhouses, because these local systems provide year-round produce at a high energy cost; conventional California production, because California currently supplies a majority of U.S. lettuce[17] and provides the crop year-round[18]; and local seasonal soil cultivation, because this system represents a common local food alternative. The LCA results of these four systems reflect the food-energy-water sustainability nexus of local food production compared to conventional food production across the contiguous U.S.

2.2 Methods

2.2.1 Goal and scope

To compare the four production alternatives, this study's life cycle assessments were performed following ISO Standard 14040[3] consisting of four phases: goal and scope definition, life cycle inventory analysis, life cycle impact assessment, and interpretation. The goal of the project was to provide policymakers and consumers with insights on the sustainability of local and centralized food options while providing insights to producers on potential sustainability improvement opportunities. Thus, the study's scope focused on a product of 1 kg of fresh lettuce. To provide a consistent comparison between local and centralized production systems, the system boundary included production, post-harvest processing, and transportation to the store, as illustrated in **Figure 2**. Beyond this "cradle-to-store-gate" point, the storage and usage phases of lettuce were assumed to be identical between the four supply chains; thus, these stages were excluded from this comparative analysis. To provide expanded geographical insight, the geographic scope included 924 sites across the contiguous United States.

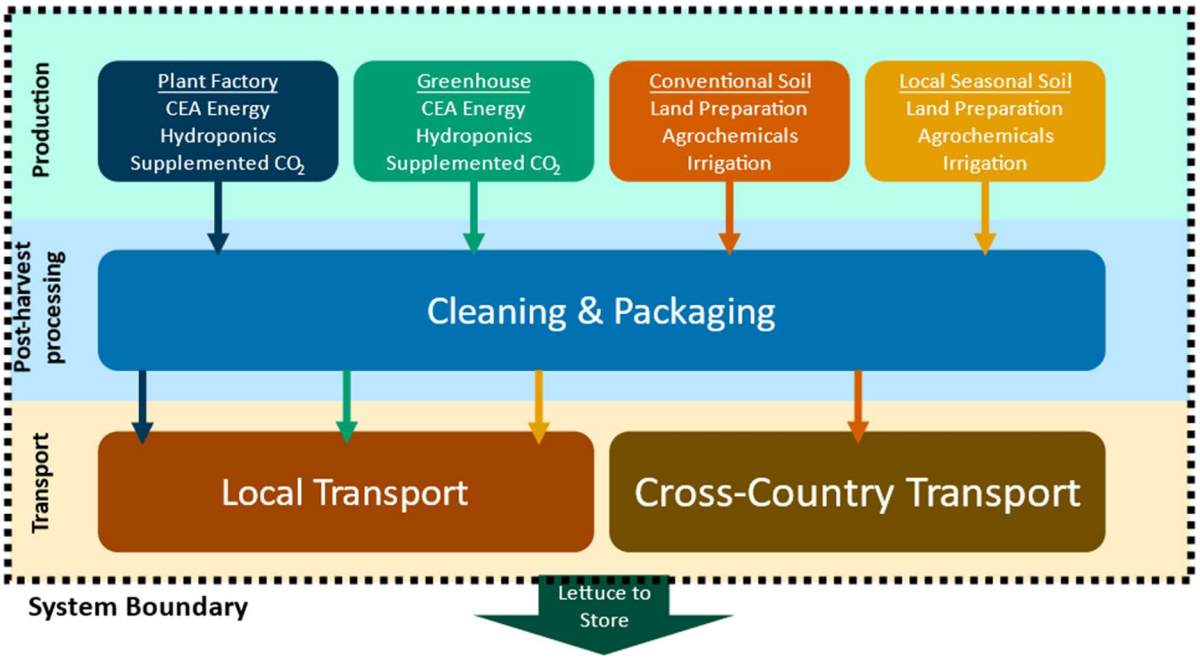

***Figure 2**. A visual summary of the unit processes modeled in this work for four systems: local plant factory, local greenhouse, conventional production and shipping from California, and local seasonal soil production.*

2.2.2 Life cycle inventory analysis

The life cycle inventory analysis (LCI) phase was performed for all four systems to determine flow values like yields from production stages, energy consumption at all stages, and material inputs. For the plant factory and greenhouse models, the production stage was simulated using the United States Department of Energy's EnergyPlus software to calculate the electricity and heat inputs necessary to grow hydroponic lettuce indoors[19]. Existing published CEA experimental data were used to estimate material inputs of water[20], fertilizer[21], and supplemental carbon dioxide[22,23]. For the California centralized model, the production stage utilized United States Department of Agriculture Statistical Data[24], agricultural Extension office guidance documents[18], and existing literature data[25,26] to determine model inputs. For local seasonal soil production, the UN Food and Agriculture Organization's AquaCrop model[27] was used to estimate per hectare yield and irrigation demand in different climates. These intermediate outputs were then combined with data from the California conventional model to estimate farm machinery

usage, irrigation system usage, and fertilizer usage. Post-harvest processing and packaging, including washing, initial cooling, and plastic packaging, was then modeled identically for each of the four production systems based on existing literature[25,28] and California Extension guidance[18,29]. Finally, transportation by refrigerated truck was modeled for each of the production systems. Local systems used a 10 km estimate[14], while the California conventional model utilized Morgan et al.'s Google Maps API Python tool[30] to estimate transport distances. Further details on these models, including summary input data tables, are included in **Appendix A Section A1** and validation of model design assumptions are included in **Appendix A Section A2**.

2.2.3 Life cycle impact assessment

In the life cycle impact assessment (LCIA) phase, data from the LCI models were translated to environmental impacts. The impact categories selected were global warming potential on a 100-year timeframe (GWP-100), owing to agriculture's significant contribution to global GHG emissions, and water consumption, examining the food-water nexus which can factor into agricultural decision making. The water intensity of the system included all blue water and excluded green and gray water impacts[31]. To determine characterization factors for most flows, OpenLCA[32] was utilized to access the ecoinvent 3.7.1 database[5], with processes summarized in **Appendix A Section A3**. The IPCC AR6 method[6] was utilized for GWP-100, while the ReCIPE 2016 midpoint (H)[33] was used for water consumption. Two additional resources were utilized for geographically resolved electricity flow characterization factors: the U.S. EPA eGRID GHG emissions factors at the subregion level[34] were utilized for electricity in plant factory and greenhouse systems, while electricity water footprints were calculated using North American Electric Reliability Corporation (NERC) region consumption factors[35]. Through

applying these characterization factors in a spreadsheet model, category indicator results were characterized for each of the four supply chain models.

2.2.4 Interpretation

In the interpretation phase of the LCA, the impact results were analyzed to provide comparative insights on the four supply chains for consumers, policymakers, and producers. To provide a geographically diverse overview to consumers and policymakers of sustainability trends, GHG and water impact results were compared for the four largest cities in the United States: New York City, NY; Los Angeles, CA; Chicago, Il; and Houston, TX. Further, for each of these cities, a one-at-a-time GWP sensitivity analysis was performed, adjusting inventory inputs by ± 20% to observe the effect on impact results. Beyond these four cities, an additional 920 simulated sites were considered with results interpolated on maps to show regional trends. To illustrate such patterns, impact results were mapped and interpolated in ArcGIS Pro[36]. Between stations, ordinary kriging was applied with a spherical semi-variogram model and default inputs. For extents and masking, the United States Census Bureau States Boundary File[37], sans Alaska, Hawaii, and Puerto Rico, was used. Percent clip stretch symbology was then applied with default inputs, and colors and labels were manually adjusted to provide a clear display and discussion of results. Additionally, to provide insights to policymakers and producers on future industry trends, a series of scenario analyses were performed to examine CEA GHG intensity with new technology implementations. These analyses included electrifying dehumidification in greenhouses, using a geothermal heat pump with a consistent COP of 3.1[38] in greenhouses and plant factories, and sourcing 100% of electricity from wind or nuclear generation at a GWP of 13 kg CO2e MWh^{-1} [39].

2.3 Results and Discussion

2.3.1 Life cycle comparison overview

The results show energy-intensive local CEA systems have the highest global warming impact of the four agricultural systems evaluated in this paper; soil-based systems have the lowest impact, even when including conventional system transportation footprints. **Figure 3** provides an overview with results for the four largest U.S. cities; **2A** shows how CEA impacts range between 3 and 6 kg CO_2e kg^{-1} compared to the California and local soil systems which are detailed and magnified in **2B**, ranging between 0.3 and 1 kg CO_2e kg^{-1}. The impacts on water use, however, are generally reversed, as shown in **Figure 4**. Across locations, the hydroponic CEA systems require less water per kilogram of lettuce produced than the conventional system. This analysis incorporates all of the water requirements including the indirect water footprints such as those associated with energy production. Local soil water footprints vary, but generally fall below conventional footprints depending on local seasonal precipitation.

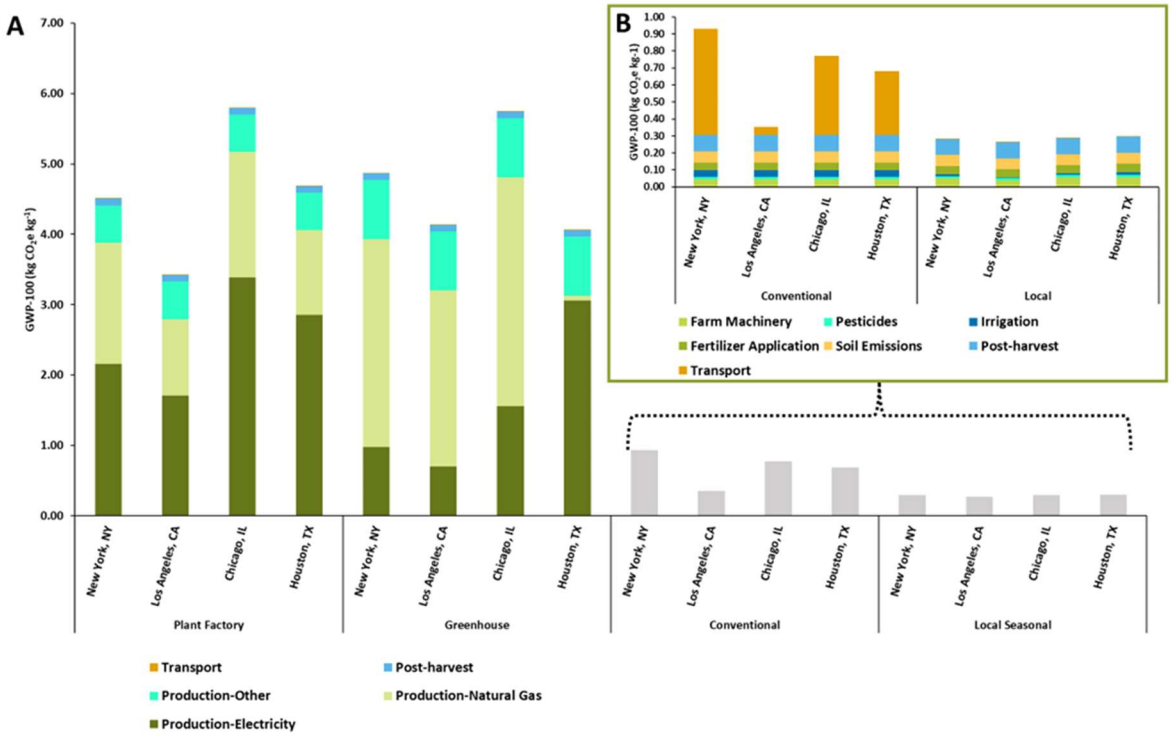

Figure 3. *Cradle-to-shelf GHG emissions of leaf lettuce production for four system types in the four largest United States cities. a. Emissions of local CEA systems, with total emissions of soil-based systems for comparison. b. Magnified and detailed emissions of soil-based systems.*

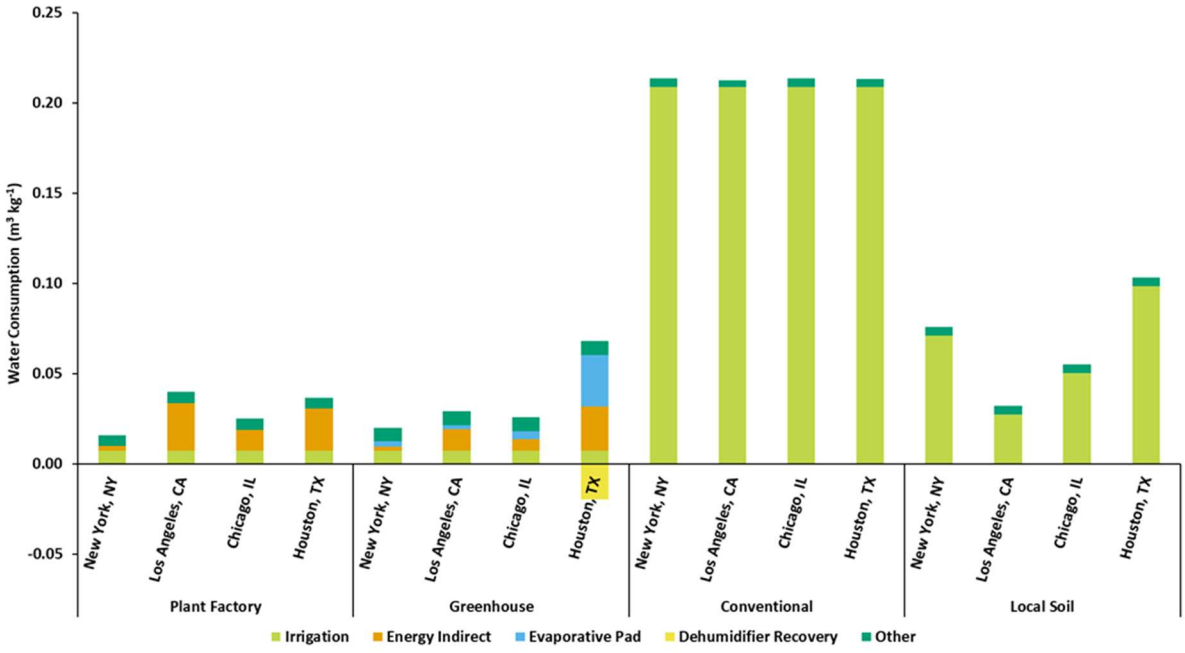

Figure 4. *Cradle-to-shelf water consumption of leaf lettuce production for four system types in the four largest United States cities. Where electric dehumidifiers are the primary dehumidification technology, recovered condensed water has been included.*

These overview results largely align with the range of results observed in the existing literature, as observed in **Appendix A Figure A1 and Figure A2**. Plant factory GWP values fall within the observed literature range (0.89–8.9 kg CO_2e kg^{-1})[16] as do greenhouse GWP values when compared to heated greenhouses in the literature (0.5–26.51 kg CO_2e kg^{-1})[14,40]. This study's conventional model GWP values largely fall within literature values for centralized production with transportation (0.68–0.92 kg CO_2e kg^{-1})[14,16], though the influence of transportation emissions means that locations very close or very far from California start to fall outside the range. This study's local soil lettuce GWP values are somewhat higher than the literature range (0.15–0.25 kg CO_2e kg^{-1})[14,26], but further inspection indicates this discrepancy is due to differences in system boundaries (e.g., previous work has excluded post-harvest inputs). For water consumption, similar considerations apply. This study's plant factory and greenhouse water results compare well to literature values (0.002–0.22 m^3 kg^{-1})[14,16] for hydroponic systems; the available literature varies in its inclusion of indirect water consumption from flows like electricity. For California conventional production, this study compared very well to two studies of lettuce water usage in the region (0.21–0.25 m^3 kg^{-1})[13,26], though a more recent literature value appears to be an outlier (0.09 m^3 kg^{-1})[16]. Finally, for local soil cultivation water footprints, some of this study's locations estimate higher values than others found in the literature (0.01–0.06 m^3 kg^{-1})[16]; however, this discrepancy reflects the difficulty in comparing crop blue water footprints across multiple locations, as irrigation varies significantly with climate patterns. Thus, additional validation of the AquaCrop water consumption outputs was performed in **Appendix A Section A2.3.2** with a focus on the American Southwest. These comparisons for GWP and water are discussed in greater detail in **Appendix A Section A2.4**.

Sensitivity analyses figures are included in **Appendix A Section A4**. For CEA systems, the most sensitive inputs differ depending on the system. In plant factories, yield per head has the highest impact, reflecting the high number of plants in the multi-level vertical farm setup. A significant amount of energy-intensive activity (lights, dehumidification load, etc.) is based on that high number of crops; thus, an increase or decrease in the final produced mass across the facility can cause a significant swing in the impact intensity. Further, the energy-intensity of these facilities is reflected in the sensitivity attributable to electricity and natural gas inputs. While some sensitivity is associated with material flows like fertilizer and supplementary carbon dioxide, energy sensitivity predominates.

The sensitivity analysis of greenhouse facilities differs from plant factories in two significant ways. First, yield per head is not the most significant input for greenhouses. This difference likely corresponds to the lower density of heads in the modeled single-layer greenhouse and that energy inputs were not as directly related to the number of heads present; for example, since greenhouses utilize sunlight in addition to supplementary lamps, not as much lighting demand and radiated heat is associated with a plant as in the artificially lit plant factory. The second difference between greenhouses and plant factories is the variation of energy inputs between some sites. In sites using vent-reheat dehumidification, natural gas dominates the sensitivity of the system; meanwhile, in the electric dehumidification sites along the Gulf Coast, natural gas input has little impact on the model output, with electricity input increasing its relative impact.

The soil systems, both centralized and local, demonstrate less sensitivity to energy inputs than to material inputs. For the conventional system, sensitivity varies by distance from California. For Los Angeles, CA, yield dominates the sensitivity analysis, followed by material

inputs like cardboard packaging and fertilizer. Energy-related inputs like transportation, farm machinery, and irrigation then follow, reflecting the low energy intensity of outdoor cultivation. However, in distant locations like New York City, NY, refrigerated shipping predominates the sensitivity analysis. This change reflects the energy-related impact of "food-miles" and how transportation can become a significant factor in soil systems at a great enough distance. By contrast, in the local soil system, the removal of this significant transportation footprint results in farm-level inputs such as fertilizer usage dominating the sensitivity analysis.

Overall, this sample of locations highlights that CEA systems have higher GWP impacts driven by energy inputs but lower water impacts than California centralized production and local seasonal production. Further exploring regional trends beyond these case studies can illustrate the factors driving these impacts.

2.3.2 Mapped results comparison to conventional

This section discusses the mapped comparisons of different system impacts, particularly the results of EnergyPlus outputs for the plant factory and greenhouse models, highlighting their high energy intensities and low water footprints, and the implications of these factors on the GWP impacts of CEA compared to conventional agriculture. When this energy intensity is translated to climate impact, the CEA GWP impacts are always higher than conventional impacts, as illustrated in **Figure 5**. The plant factory energy footprint stems largely from lighting and from dehumidification via the overcool-reheat process; thus, impacts largely reflect the GHG intensity of eGRID subregions. Greenhouses, meanwhile, are dominated by their heating duties, followed by lighting, and so impacts reflect differences in local climate: the colder the location, the greater the natural gas usage in winter. Breakdowns of building average energy demand by category are included in **Appendix A Figure A7 and Figure A8**, and impact maps for each

production system type are included in **Appendix A Figure A9, Figure A10, Figure A11,** and **Figure A12**.

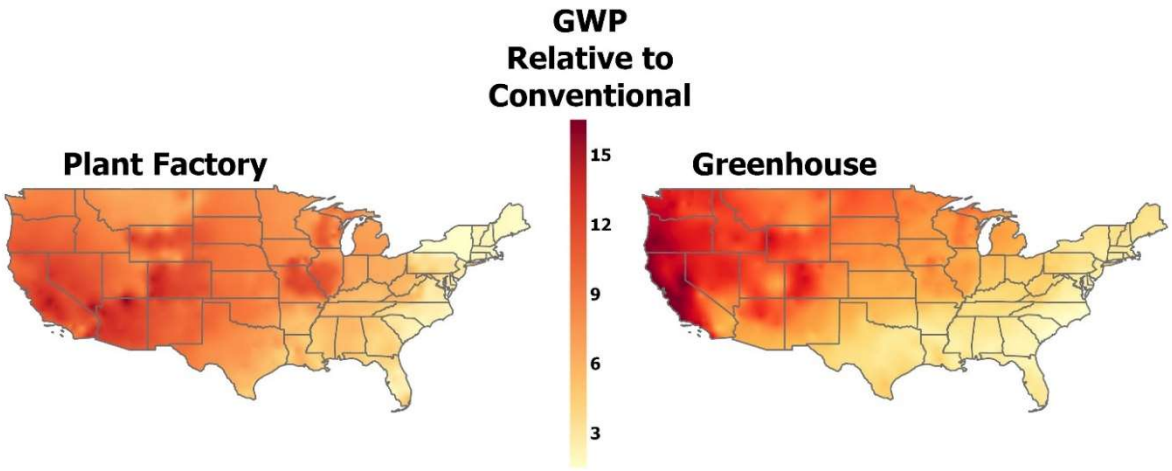

Figure 5. *GHG impacts per kg of lettuce from local CEA systems relative to conventional production and transport:* $\frac{GWP_{CEA}}{GWP_{Conventional}}$*. A value less than one indicates the evaluated technology performs better than the conventional system. Note that no CEA system simulated here results in a ratio less than one.*

Considering water consumption, CEA impacts are universally lower than conventional usage, as seen in **Figure 6**. Even when considering evaporative cooling water usage and indirect water impacts, the simulated facilities used at most half the amount of life cycle water as conventional irrigation methods. Similar to the GWP results, the water impacts of CEA also exhibit regional variations. In the case of the plant factory, the water footprint is mainly influenced by energy consumption, and hence the map for plant factory water impacts reflects the water footprints of electricity generation in different NERC regions. The water usage in greenhouses is affected by both energy consumption and evaporative cooling. As a result, while some patterns in NERC region water footprints can be observed, the water consumption in greenhouses is higher in warmer and drier climates, where the demand for cooling and evaporative pad water usage is high.

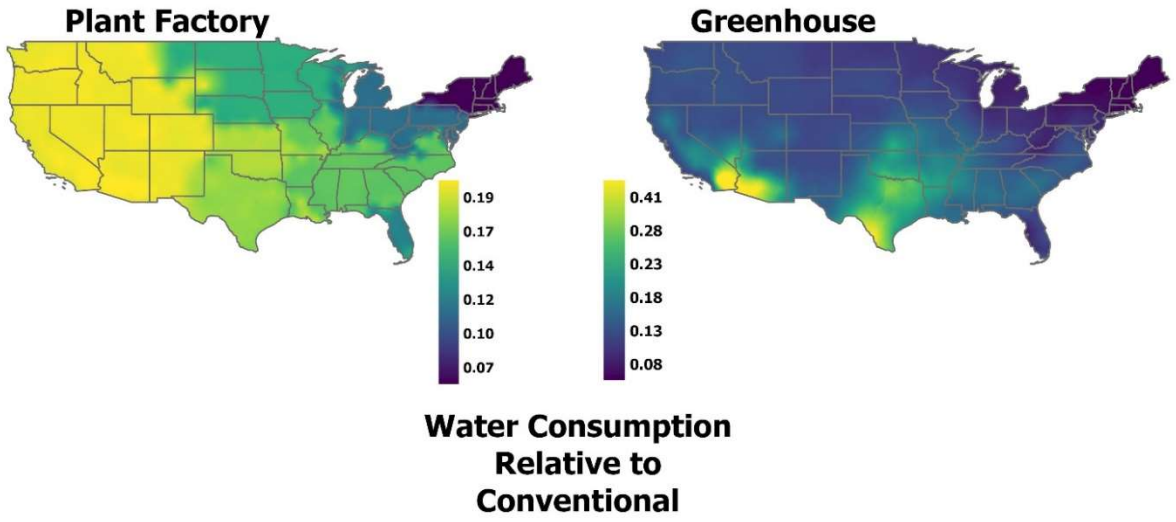

Figure 6. *Water consumption per kg of lettuce from local CEA systems relative to conventional production and transport:* $\frac{Water_{CEA}}{Water_{Conventional}}$ *. A value less than one indicates the evaluated technology performs better than the conventional system. Note that all CEA systems here result in ratios less than one.*

The baseline CEA results show a significantly higher GWP impact than the conventional system, as the emissions resulting from CEA energy inputs far outweigh the food mile impacts of centralized production. These impacts can vary by distance, local grid mix, climate, and system type, but no CEA system GWP simulated in this study outperforms growing lettuce in California and transporting it by refrigerated truck. In contrast, simulated CEA blue water consumption is universally lower than conventional consumption owing to the efficiency of hydroponic systems; even when considering evaporative cooling consumption and upstream water associated with energy production, CEA systems are more water efficient. Consumers and other local stakeholders would need to weigh these trade-offs when considering the value of year-round local food production in their community.

As a comparison to the year-round CEA systems, a mixture of local seasonal soil consumption and conventional soil impacts was created to reflect a consumer pattern of buying local when in-season, mapped in **Appendix A Figure A13 and Figure A14**. Generally, local soil

production represents the most sustainable system when in-season, though some locations whose dry seasons coincide with lettuce growing seasons demand more water than the conventional system. However, even if local produce is more sustainable from a GHG and water perspective, it is not available year-round. Consuming a mix of conventional and local food more accurately represents annual consumption and illustrates the same conclusion: from a climate change perspective, eating locally in-season is generally more sustainable, followed by centralized conventional production. Thus, in most locations, consumers and policymakers can view local outdoor produce as a more environmentally sustainable addition to local markets than CEA systems.

2.3.3 Controlled environment agriculture scenario analyses

This section evaluates the GHG impacts of different CEA facility designs with three scenarios evaluated. First, the vent-reheat greenhouse dehumidification model is associated with high heating loads. The widespread application of electric dehumidification could lower energy consumption and GHG emission profiles. Second, as both CEA models evaluated in this paper utilize natural gas for heating demand, the electrification of heating could reduce emissions depending on heat pump performance and local grid cleanliness. In the third scenario, these dehumidification and electrified heating technologies are combined with low carbon electricity. Each scenario is considered across this study's simulation sites.

2.3.3.1 Greenhouse dehumidification technologies

The baseline simulation models a traditional ventilation with reheat dehumidification system for most sites; the exceptions are humid areas where this system fails to maintain humidity control targets, so electric dehumidification is employed. One scenario to consider is the wider replacement of the older ventilation method with electric dehumidification. These

simulations result in lower energy footprints and thus lower climate impact, as shown compared to the conventional system in **Figure 7**. Notably, the regional patterns more closely resemble the grid-dependency of the plant factory simulation due to the reduction in natural gas usage for reheat and the concurrent increase in dehumidification electricity. For example, in Madison, Wisconsin, the technology change reduces energy intensity by 54%, and at a similar latitude and climate in Rochester, New York, electric dehumidification reduces energy intensity by 58%. However, in Madison the GWP reduces by only 27% while in Rochester it reduces by 59%. The difference stems from the MRO East grid subregion in Wisconsin having one of the highest carbon intensities in the country while the Upstate New York subregion has one of the lowest.

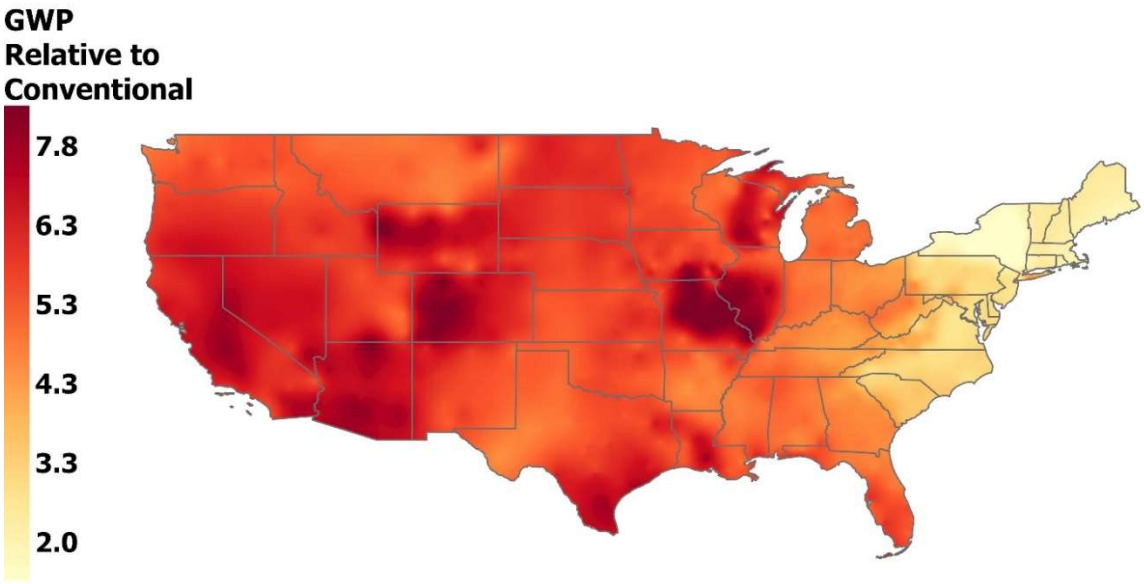

Figure 7. *GHG impacts per kg of lettuce from local greenhouses using electric dehumidification relative to conventional production and transport:* $\frac{GW_{Greenhouse}}{GWP_{Conventional}}$*. A value less than one indicates the evaluated technology performs better than the conventional system. Note that no CEA system simulated here results in a ratio less than one.*

2.3.3.2 Electrification of CEA heat sources

Utilization of natural gas for heating and reheating purposes is another traditional technology in the CEA baseline simulations. Replacing this incumbent technology with a

geothermal heat pump would result in environmental improvements, especially if paired with low-emission electricity generation. The resulting GWP impacts of electrified CEA heat are shown in **Figure 8**. Across regions, the patterns reflect grid cleanliness, and greenhouses broadly perform better than plant factories. Additionally, the electrified systems generally perform better than natural gas systems, even in areas with greater grid carbon intensity (compare to **Figure 5**), reflecting the energy efficiency gains of a reliably efficient heat pump. As in the electric dehumidification scenario, Madison, Wisconsin and Rochester, New York provide a clear example. Energy intensity reduces by about 58% in both cities, but Madison's GWP reduces by only 17% while Rochester's reduces by 66%. Thus, heat pump performance paired with clean electricity can have significant impacts on the sustainability improvements of electrified CEA systems.

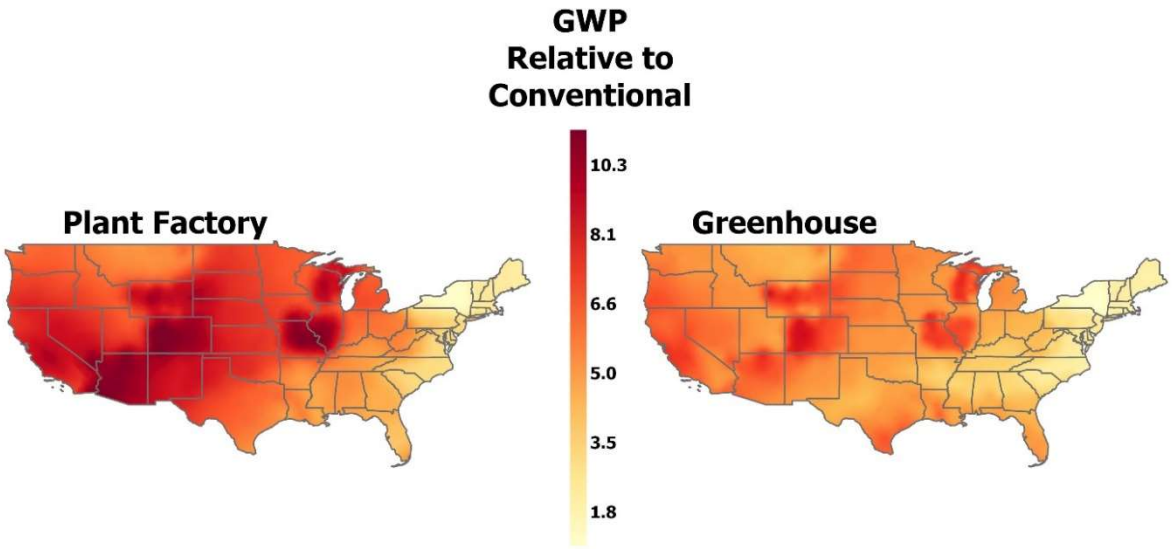

Figure 8. *GHG impacts per kg of lettuce from local CEA systems using electrified heating relative to conventional production and transport. A value less than one indicates the evaluated technology performs better than the conventional system. Note that no CEA system simulated here results in a ratio less than one.*

2.3.3.3 Clean electrification scenario

In addition to energy efficiency and electrification efforts, CEA operators may consider utilizing low carbon energy through purchasing renewable energy credits or siting facilities next

to low carbon generation resources. As a test case, this study considers the energy footprint of CEA facilities with electrified heating and dehumidification combined with low-emissions electricity, shown in **Figure 9**.

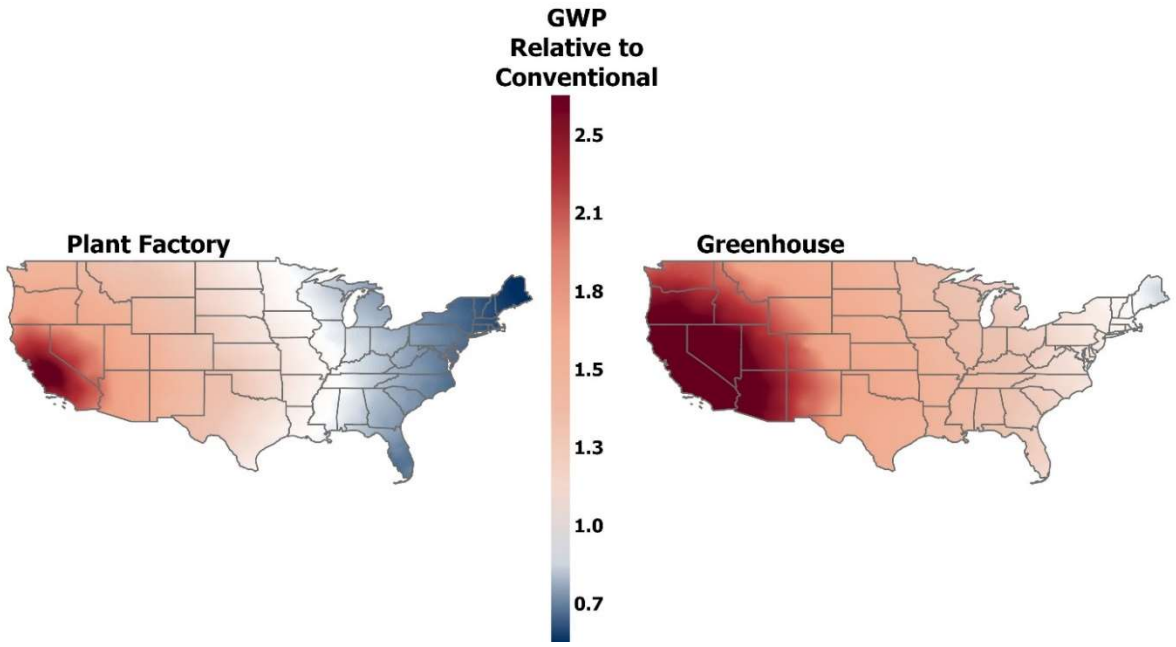

Figure 9. *GHG impacts per kg of lettuce from local CEA systems relative to conventional production and transport. A value less than one indicates the evaluated technology performs better than the conventional system. Note that in this figure, values around one are white and below one are blue.*

Under such a scenario, distance from the conventional production location dominates. For example, the Madison, WI plant factory breaks even with Californian production and transportation, but further east Rochester is 15% less GHG-intensive than the conventional system. Notably, the break-even line for greenhouses is farther east than for plant factories due to higher supplemental CO_2 usage; the Madison greenhouse is 30% more GHG-intensive than the conventional California system, while the Rochester greenhouse is 10% more intensive. Thus, once energy emissions are addressed, other factors become significant in the comparative life cycles; previously negligible inputs like infrastructure could warrant further consideration if an operator successfully addressed their energy emissions. Through such a combination of energy

efficiency and clean energy, CEA operations could begin to perform similarly to the conventional system on greenhouse gas emissions.

2.3.3.4 Scenario analyses implications

This study's scenario analyses suggest that CEA operators have opportunities to improve environmental performance. One analysis indicates that replacing traditional CEA methods with new technologies could improve energy efficiency. For example, this study's greenhouse simulations found that electric dehumidification would halve the national average energy intensity compared to traditional ventilation and reheat dehumidification methods. Additionally, operators could replace incumbent combustion-based technologies like furnaces and unit heaters with heat pumps and see improvements with existing grid mixes, suggesting even greater potential with cleaner energy mixes. Indeed, once full electrification and clean generation are combined, some simulations achieve a lower GWP than the conventional system. Through such efforts, CEA operators could reduce operating costs and environmental impacts.

However, these CEA operational and design changes present trade-offs. Dehumidifiers and heat pumps may reduce environmental impacts, but higher capital costs could present economic challenges for producers and consumers. Further, the crop's energy intensity would remain high, and large-scale production with such electrical demand could burden grid generation and transmission. Stakeholders would need to consider that generation and transmission capacity impacted by CEA may present an opportunity cost for other electrification targets, such as space heating or transportation. Relatedly, adoption of heat pumps could increase refrigerant leak emissions footprints. As electrification of HVAC increases and energy efficiency improves, increased refrigerant leakages could become a prevalent emissions category in CEA. Thus, CEA producers would benefit from considering refrigerant leakage impacts in their system

maintenance and design, including leakage reduction efforts and using refrigerants with low GWP or no GWP. With such tradeoffs, the CEA industry and communities could consider the optimal path to sustainable food production within the local energy and environmental systems.

2.3.4 Limitations and future research

While this study provides insights on the sustainability of agricultural systems, local food production may continue to be an area of future sustainability considerations; therefore, future studies could build upon the energy and life cycle models presented here. This study focuses on the geography of the United States; however, with the necessary inputs, the models could be applied to locations around the world. Such geographic variation would be useful to understand wider food production potential and circumstances. In some regions, an abundance of low-carbon energy could keep energy-related CEA impacts low. Further, in some regions a lack of arable land or nearby conventional sources could incentivize CEA; if the only fresh vegetable supply chains available utilize energy-intensive shipping methods like air freight, CEA may be the more sustainable option. Considering the energy models, future studies could incorporate more complex, advanced systems beyond the baseline models considered in this work. As the CEA field continues to expand and evolve, the adoption of better facility designs, technologies, and operational practices will likely improve sustainability outcomes; the building models created for this study could be adapted to evaluate the effects of such improvements. In addition to these energy considerations, the scope of water footprints could be expanded to consider green water footprints, such as precipitation on crop fields, and gray water footprints, such as the treatment of flushed hydroponic solution. Beyond the energy and water models, the life cycle boundaries of this study could be expanded. This study did not consider food waste, as all food grown was assumed to be delivered to the store. More advanced food spoilage models could

refine the comparison of centralized and local systems, estimating the extent to which greater food mileage results in more waste. Further, this study did not consider land use change effects; CEA facilities were assumed to be built on already-developed land while local seasonal cultivation was assumed to occur on existing cropland. Future work could consider direct land use change effects in terms of biomass carbon and soil carbon stock changes. For example, forest land cleared for a farm or greenhouse would have additional associated emissions; conversely, soil cultivation on previously barren or paved urban land might create soil C stock where little previously existed. Beyond direct land use change, indirect land use change effects could be considered. For example, were local cultivation of vegetables to reach a large enough scale, changes in economic demands could cause changes in land utilization where vegetables are currently cultivated. Through such additions, LCA practitioners could provide even more robust environmental insights to stakeholders.

In addition to environmental considerations, local stakeholders will weigh food production options through an economic lens. Future work could thus leverage technoeconomic assessment and life cycle costing to compare these systems. For example, due to CEA facilities' high energy demands, the CEA lettuce price will be highly dependent on energy prices. Along with the high capitol costs of building materials and HVAC systems, these ongoing operational expenses could drive local CEA produce to a higher price than the conventional supply chain. Future research could also consider whether local outdoor farms would be cost-competitive with centralized supply chains, While the local systems would not have transportation-associated costs, local lettuce production could be less cost-efficient than California due to natural conditions (e.g., colder weather leading to lower yields) and a lack of a scaled-up specialty crop economy (e.g., unexperienced or understaffed labor forces). With such economic considerations,

future life cycle researchers could provide food-energy-water insights to stakeholders around the world.

2.5 Conclusions

This study's production and life cycle models demonstrate that the environmental considerations of food production systems are complex and local is not always more sustainable. Local lettuce CEA systems have a greater GHG impact than California conventional production and truck transport in all simulated United States locations. By comparison, local seasonal soil cultivation of lettuce is associated with the lowest GHG emissions for most simulation sites, and local climate variations can also result in lower water consumption; however, seasonality limits the capacity of such local operations to meet year-round demand. At present, consumers and policymakers can look to a mixture of local seasonal soil systems and conventional systems as the most sustainable option. Thus, this study illustrates the need for local stakeholders to consider all aspects of the food-energy-water sustainability nexus when deciding on sourcing from local compared to centralized food production.

CHAPTER 3: GEOGRAPHIC VARIATION OF ETHANOL FEEDSTOCK LCA

3.1 Background

The aviation sector presents a growing and difficult challenge in the global net-zero effort. Demand for air travel is poised to increase, and alternatives to kerosene jet fuel remain limited in either application, as with electrification and hydrogen, or supply, as with used cooking oil[41]. To accelerate the deployment of sustainable aviation fuel (SAF), the United States federal government announced the SAF Grand Challenge, creating a roadmap to meet 100% of aviation fuel demand by 2050 with an interim target of 3 billion gallons per year in 2030[42]. By cooperating with industry "to reduce cost, enhance sustainability, and expand production," this multiple-agency effort aims to produce fuel with a life cycle GHG impact at least 50% lower than conventional fuel[42]. To ensure technologies and supply chains deliver on this goal, LCA will be a critical tool in this national effort.

One pathway of interest to create SAF leverages an existing biofuel infrastructure in the United States. Through the near-commercialization "alcohol-to-jet" (ATJ) pathway, corn-derived ethanol can be transformed into synthetic paraffinic kerosene which can be blended into jet fuel under current technical standards[42,43]. However, analyses using Argonne National Lab's Greenhouse gases, Regulated Emissions, and Energy use in Technologies Model® (GREET) indicate[44,45] that the corn ATJ pathway exceeds the 50 kg CO_2e $MMBTU^{-1}$ maximum to qualify for federal clean fuel tax credits[46]. In order to qualify for these credits and achieve necessary emissions reductions relative to conventional fuel, corn ATJ producers must improve on existing supply chains and technologies. In addition to industrial measures like clean energy sourcing and fermentation CO_2 capture, farm-level measures will play a role in making corn ATJ a viable SAF

pathway[45]. As part of a United States Department of Agriculture-funded effort, the biofuel producer Gevo has partnered with CSU to examine life cycle emissions in its corn supply chain to determine how local practices compare to national averages and identify eco-efficiency improvements.

In the extensive LCA literature on U.S. corn ethanol, impact results vary based on factors that vary from location to location. Nitrogen fertilizer, for example, accounts for 26% of cradle-to-farm-gate GHG emissions, with the related on-field nitrous oxide emissions accounting for another 27%[47]. These results will vary not only based on the amount of nitrogen fertilizer used but also the type (e.g., ammonia, urea, etc.) due to different upstream production processes. When accounting for such influential factors in large scale studies, LCA practitioners will often utilize top-down methods like back-calculation from GHG emissions inventory data[47] or national-level estimates[48] like the fertilizer mix in GREET[44] and ecoinvent[5]. Additionally, available LCA datasets like ecoinvent[5] and agribalyse[49] provide data for a limited range of fertilizer types (urea, potash, etc.) but do not include process models for many of the diverse fertilizers utilized in actual practice. Further, local climate, soil properties, and land management practices can result in different fluxes of carbon and nitrogen between the soil and atmosphere, representing potential GHG sinks and sources. While some simple estimation methods are available, such as the IPCC Tier 1 methods for fertilizer nitrogen[50], they do not reflect changes in soil organic carbon (SOC) nor do they consider the dynamics of local practices. Thus, studies which do not account for these farm-level variations risk inaccurate carbon intensity estimates that could hinder incentive structures and obfuscate emissions reduction opportunities.

This study utilizes farm-level data resolution to close these gaps and advance the state of corn ATJ life cycle knowledge. A Python-based LCA model, tailored to Gevo's data collection

capabilities, is used to process data from the 2023 harvest for over 400 unique fields in southeast South Dakota and southwest Minnesota. This model incorporates LCA data unique to each field, such as upstream modeling for 15 fertilizers not found in available datasets. Additionally, carbon and nitrogen GHG fluxes are incorporated from field-level Tier 1 calculations and the Daycent biogeochemical soil model[51], reflecting unique chemical application and land management data at each site. Finally, the model utilizes Monte Carlo simulation to estimate uncertainty, validating the significance of these results in comparison to typical biofuel point estimates. Through employing these high-resolution LCA methods, this model enhances the understanding of the production system beyond standard LCA tools that use heuristics, high-level averages, and point estimates, better identifying low-emissions practices and highlighting opportunities for industry practice and data quality improvements.

3.2 Methods

3.2.1 Farm-level data sample

Field-level data were provided for 472 sites across 8 counties in southeastern South Dakota and one county in southwestern Minnesota. The sample available for this analysis was for the 2023 harvest; the continuing project will include 2024 and 2025 data, as well. Within the 2023 harvest sample, farmers provided yield and fertilizer application data for each field. Additionally, Gevo indicated local practices that differed from those described in the GREET model; notably, no fields were irrigated, and no lime was used. Finally, each site indicated the till system applied; all sites in the 2023 harvest utilized either reduced tilling or no tilling.

3.2.2 Field-level LCA model

The inputs and emissions modeled in this study are illustrated in **Figure 10**. As in other corn biofuel modeling literature[47,52,53], the agricultural chemical usage (fertilizer and pesticides), on-farm energy usage, and on-farm fertilizer-related emissions were considered. Further, the annual emission or sequestration of carbon due to SOC changes was calculated. Through incorporating these activities, this LCA inventoried major drivers of corn cultivation emissions, geographically-variant GHG sources, and the critical perspective of soil health and carbon storage.

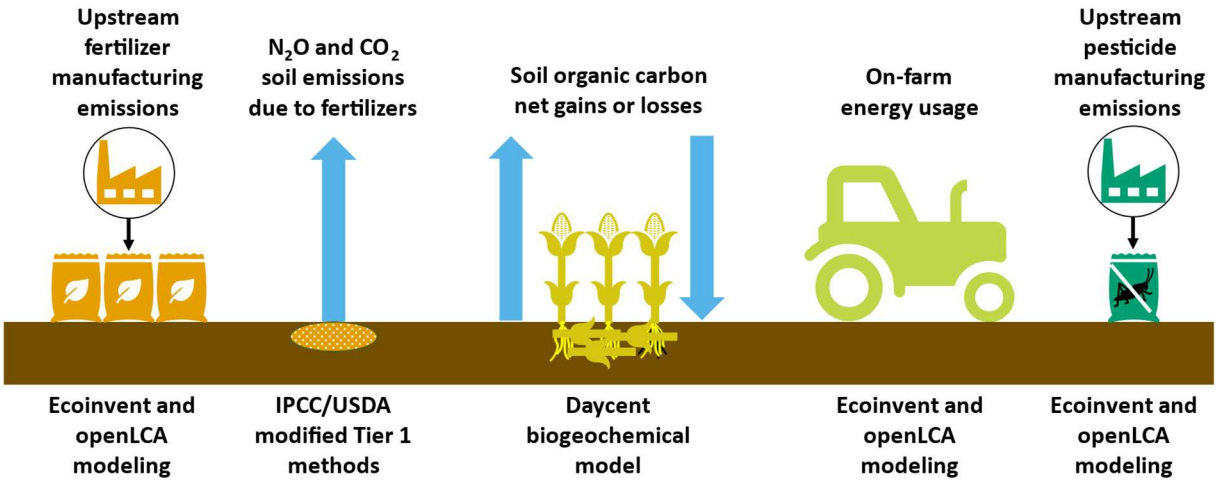

Figure 10. *GHG emission contributors included in the 2023 harvest farm-to-gate LCA model, including brief descriptions of the calculation methods used.*

3.2.2.1 Agricultural chemical upstream modeling

On a field-by-field basis, suppliers provided descriptions and applied amounts of different fertilizers utilized over the 2023 growing season. Among the 22 types of fertilizers applied, 7 were typical fertilizers with existing inventories in the ecoinvent database, such as urea and potash. These inputs required little further modeling except for density considerations for urea ammonium nitrate and ammonium sulfate solution (see **Appendix B Section 1.1**).

Additional analysis was necessary for the other fertilizers. In consultation with a local Gevo agronomist[54], 8 entries were determined to be blends of different dry fertilizers[55] to provide certain relative masses of nitrogen (N), phosphorous (P), potassium (K), and sulfur (S). Based on the rest of the 2023 harvest sample, data from state fertilizer survey data[56], and local expert confirmation with Gevo[54], four standard ingredients were assumed for these blends: urea, monoammonium phosphate (MAP), ammonium sulfate (AS), and potash (KCl). Mass balances for N, P, K, and S were performed to meet the specified amounts for each species. These amounts, summarized in **Appendix B Section 1.2**, were normalized to a per-kg basis with blending equipment energy demand derived from ecoinvent[5]. Finally, 7 fertilizers in this sample were determined to be different compound fertilizers. Some were identified as particular chemical species, others were designated by a particular brand name by the farmers, and still others were identified by nutrient analysis values. In each case, ingredients were determined from corresponding documentation, such as labels and safety data sheets, to perform species balances for each nutrient. Further information about these fertilizer models is included in **Appendix B Sections 1.3-1.5**.

In addition to fertilizer application, this study estimated the application of pesticides and the corresponding upstream emissions. In the 2023 harvest, Gevo was unable to collect field-level pesticide application data. Based on previous literature findings that pesticide contributed less than 5% to corn carbon footprint at the farm gate[47], field-to-field variations were assumed negligible for this GHG-focused study. However, pesticide inputs were implemented in the model to allow future iterations to incorporate non-GWP impact modeling that may be relevant to biofuel feedstock cultivation (e.g., freshwater ecotoxicity). Accordingly, the FDCIC per-bushel value (7.69 g pesticide bu^{-1})[57] and the ecoinvent model for unspecified pesticide[5] were utilized.

3.2.2.2 On-Farm energy usage modeling

In this sample, energy usage within the farm-gate boundary differed from national averages in various respects. First, no field in the sample utilized irrigation, and thus energy consumption for that purpose, like pump electricity, was not included. Additionally, while the GREET model includes energy used to dry harvested corn, Gevo accounts for drying at the fermentation plant. Thus, propane usage found in the GREET model was included in downstream processes instead of the farm-gate system boundary. Finally, while data were unavailable for diesel usage in heavy machinery, each field indicated which form of conservation tillage they had implemented. To reflect fuel savings associated with reduced tilling, USDA data for conservation practices in corn acreage[58] was combined with typical fuel usage factors associated with different tilling practices[59] to estimate average national diesel consumption per corn field acre. By subtracting this value from the GREET corn diesel consumption average[57], diesel usage for non-tilling activities (chemical application, harvesting, etc.) was estimated. Then, for each site, the fuel usage factor[59] for the indicated tilling practice was combined with non-tilling diesel usage and converted to energy per bushel with the GREET yield and diesel lower heating value (LHV) factors, as summarized in **Table 1**.

***Table 1**. Diesel usage values by tillage practice type.*

Tillage Type	Diesel Use (gal ac^{-1})	Diesel Use (gal bu^{-1})	Diesel Energy (MJ bu^{-1})
No till	5.8	0.03	4.7
Reduced till	7.1	0.04	5.8
Conventional	9.4	0.05	7.7
National Mix	7.2	0.04	5.9

3.2.2.3 Soil emissions inventory modeling

Soil emissions due to nitrogen additions were calculated using the modified USDA Tier 1 methods which correspond to the methods found in Daycent[60]. At the site level, fertilizer applications were converted to the mass of nitrogen applied. Additionally, the per-bushel amount of residue left on the field after harvest was estimated to include the nitrogen first incorporated in the leftover plant matter before returning to the soil. From these values, direct and indirect nitrous oxide emissions were estimated using methods described in **Appendix B Section 2.1** Further, CO_2 emissions from urea-containing fertilizers were calculated as described in **Appendix B Section 2.1**.

In addition to fertilizer-related emissions, SOC changes resulting from land management practices were modeled using the Daycent biogeochemical model[51] informed by local geography, typical farming practices, and site-level information. Due to data collection and privacy concerns, the locations of individual sites were not provided; however, counties were provided. Thus, simulations were performed using representative sites from these counties found in COMET-Planner, a Daycent-based USDA database used for high-level modeling of soil conservation measures[61]. Within the Daycent code, these site models were selected and edited to reflect typical corn farming practices in southeast South Dakota and southwest Minnesota; these practices are summarized in **Appendix B Section 2.1**. At the site level, each farm indicated the type of conservation tillage (reduced till and no till) applied; thus, for each county, SOC projection simulations were run for each conservation tillage scenario. Following the 20-year land use change horizon used in GHG accounting methodologies[62] including COMET-Planner[61], the difference between simulated initial year (2022) SOC's and end-year (2042) SOC's were

calculated and divided equally among those 20 years; these annual carbon sequestration values were then applied to the 2023 corn harvests based on indicated locations and till systems.

3.2.3 Downstream process modeling

In order to provide broader context to the cultivation-stage emissions examined in this study, the downstream processes of the ATJ pathway were modeled. The energy and material inputs from Smith et al.'s model were utilized for fermentation, ethanol-to-jet conversion, and transportation stages[53]. Within these unit processes, LHV and density values from GREET[44] were used to convert between fuel mass and energy. Meanwhile, coproducts were handled according to the federal Zero Carbon Fuel (45Z) tax credit guidelines[46]; system expansion was applied to distiller's grains using Xu et al.'s 12.3 g CO_2e MJ^{-1} EtOH factor[63], while energy allocation was utilized in the jet fuel production stage. Finally, impacts at each stage were converted to a basis of kg CO_2e $MMBTU^{-1}$ jet fuel, the units used in the 45Z tax credit calculations[46].

3.2.4 Life cycle impact characterization factors

Aligning with the federal 45Z tax credit guidelines[46], GWP-100 was estimated using the IPCC Fifth Assessment Report (AR5) values. In the cultivation stage model, openLCA was utilized to create characterization factors (CF's) for technosphere flows. In particular, the ecoinvent 3.8 database[5] was utilized to allow for Monte Carlo simulation (described in **Section 3.2.5**). The average value and standard deviations of these simulations were utilized in the Python model to generate CF's which were multiplied by the amount of material or energy indicated at each 2023 sample site.

3.2.5 Uncertainty estimation

Uncertainty estimates were calculated by characterizing the statistical distributions of input and output impacts to run a Monte Carlo stochastic analysis in Python. For inputs such as diesel consumption and fertilizer upstream impacts, 2000-run Monte Carlo analyses were performed in openLCA to generate means and standard deviations which characterized the log-normal distribution of GWP results. With fertilizer blends and other fertilizers not included in ecoinvent, the ecoinvent data pedigree matrix tool was used to estimate flow uncertainties[5]. This tool generated distribution standard deviations for each ingredient in an openLCA model; flows validated by more recent documentation and local expert insight utilized lower uncertainty. As with other inputs, a 2000-run Monte Carlo simulation was performed for each new fertilizer model, characterizing log-normal distributions of GWP impact.

With these statistics for input materials and output soil emissions, a 2000-run Monte Carlo analysis was performed in Python for each of the 472 sites. For each material and energy input in each run, a random value was generated from a log-normal distribution based on the previously-calculated means and standard deviations. Similarly, Tier 1 calculations for nitrous oxide and urea CO_2 emissions were performed with randomized values for different emissions factors (see **Appendix B Section 3.1**). Within the county-level sets of Daycent SOC simulations, the average result, minimum result, and maximum result were utilized in a triangular distribution. These randomized input CF's and soil emissions inventories were then combined with the activity data provided in the 2023 harvest sample to create 2000 estimates of GHG impact per bushel of corn, from which means and standard deviations were calculated for each site.

3.2.6 Standard LCA comparison model

Representing standard LCA with national-level data and heuristics, data from the GREET Feedstock Intensity Calculator (FDCIC) corn cultivation model were utilized[52]. Inputs for energy usage, fertilizer application, and other materials like lime were calculated on a per-bushel basis according to the indicated model yield. Additionally, Tier 1 fertilizer emissions modeling for nitrous oxide and urea CO_2 was performed[60] to reflect different fertilizer application rates between the 2023 Gevo harvest sites and the national estimate. These inputs and direct emissions were then combined in an openLCA process with ecoinvent 3.8 flows[5] to ensure upstream modeling consistency between this comparison model and the 2023 Gevo harvest model. However, reflecting the lack of soil dynamic consideration in the FDCIC, no estimates were made for SOC-related emissions in this default practice comparison. Finally, a 2000-run Monte Carlo simulation was performed in openLCA using the AR5 GWP-100 assessment method.

3.3 Results and Discussion

3.3.1 Harvest 2023 carbon footprints compared to national-level FDCIC tool

At the individual-field-level and on average, corn feedstock in the Gevo supply chain is estimated to have a lower farm gate impact than the value predicted by the FDCIC tool defaults. As seen in **Figure 11**, impacts at 72% of sites were lower than the FDCIC standard while 5% were higher. These field-level values vary widely, and special cases define the extreme ends of the range. For example, poor yields result in outcomes as high as 16.69 +/- 1.73 kg CO_2e bu^{-1} while also causing high sensitivity, and thus uncertainty, in the stochastic model (see **Appendix B Figure B1**). On the opposite end, fields with low fertilizer application rates and increasing SOC can yield negative values as low as -1.10 +/- 0.28 kg CO_2e bu^{-1}. Notably, these fields reflect a special case where the soil already had necessary nutrients for a successful crop; later rotations

on these fields will likely need to replace these nutrients with greater future fertilizer applications.

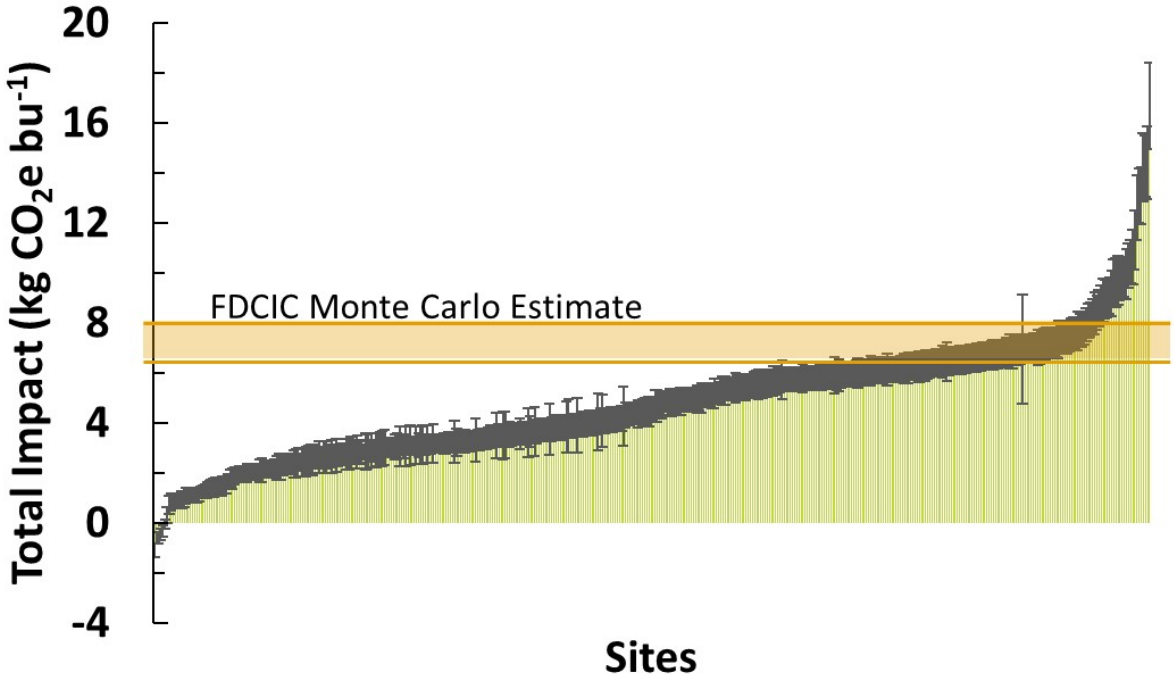

Figure 11. *Average Monte Carlo farm-to-gate GWP estimate of all sites in the 2023 harvest compared to the FDCIC model estimate. The orange box represents the average FDCIC result plus-and-minus the standard deviation. Error bars are standard deviation for that site's Monte Carlo simulation.*

Considering a weighted average of all these fields, as in **Figure 12**, illustrates how emissions in the Gevo supply chain differ from the standard FDCIC approach. These include a 0.50 kg CO_2e bu^{-1} difference in fertilizer upstream emissions, a 0.68 kg CO_2e bu^{-1} difference associated with liming (which was not practiced in the 2023 harvest sample), and a 0.43 kg CO_2e bu^{-1} difference associated with energy resources not used in the 2023 harvest sample (such as irrigation pump energy). Further, SOC buildup associated with local geography and land management practices resulted in an average emissions reduction of 0.74 kg CO_2e bu^{-1}. Thus, consideration of such local factors results in a significantly different estimate from standard assumptions and heuristics.

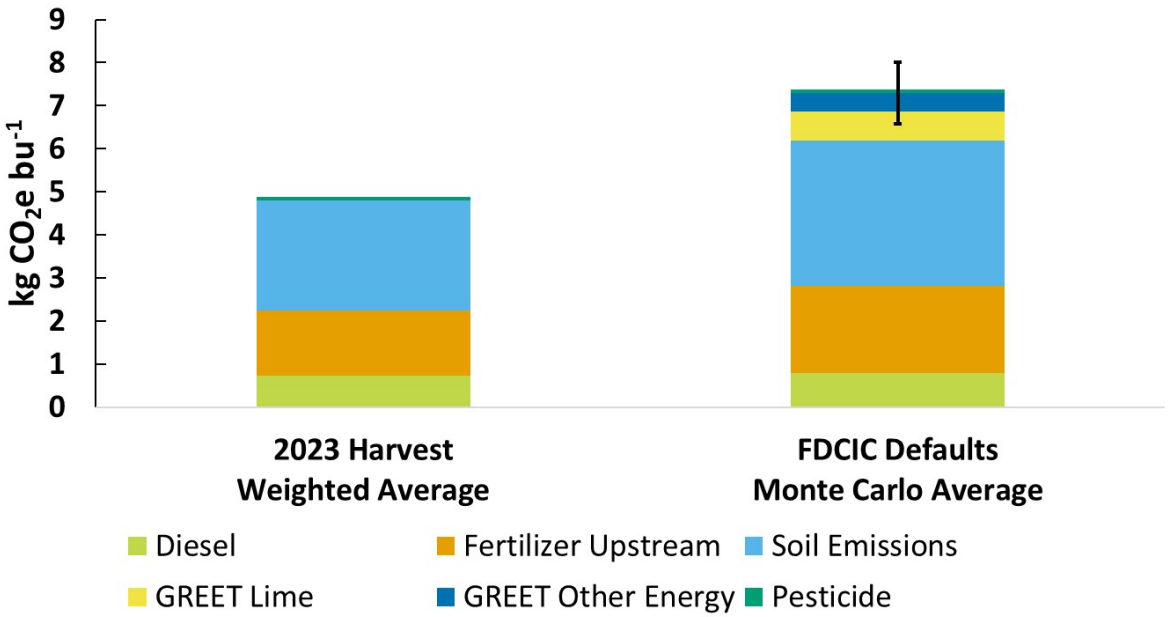

Figure 12. *Contributions of different inputs and direct emissions for the average, weighted by field yields, of the 2023 harvest results compared to the FDCIC default model Monte Carlo simulation. Error bars on the FDCIC model represent the standard deviation of Monte Carlo results. Soil emissions includes fertilizer field emissions and SOC changes.*

3.3.2 Nitrogen application intensity drives GHG outcomes followed by SOC changes

As shown in **Figure 13**, LCA results across the 2023 harvest sample demonstrate that farm-gate results in the Gevo supply chain are driven by nitrogen usage, followed by SOC changes. **12A** differentiates between fields applying reduced tillage and fields applying no tillage; the difference between the two groups corresponds to the greater SOC sequestration occurring on no-till fields. **12B** examines the no-till fields by county, illustrating the variation in SOC change by geography (see also **Appendix B Figure B2** for the Daycent results by acre and the distribution of results in each county). This differentiation between till systems and locations demonstrates the importance of soil conservation measures to feedstock efficiency as well as the need for high-resolution soil modeling, especially on no-till fields.

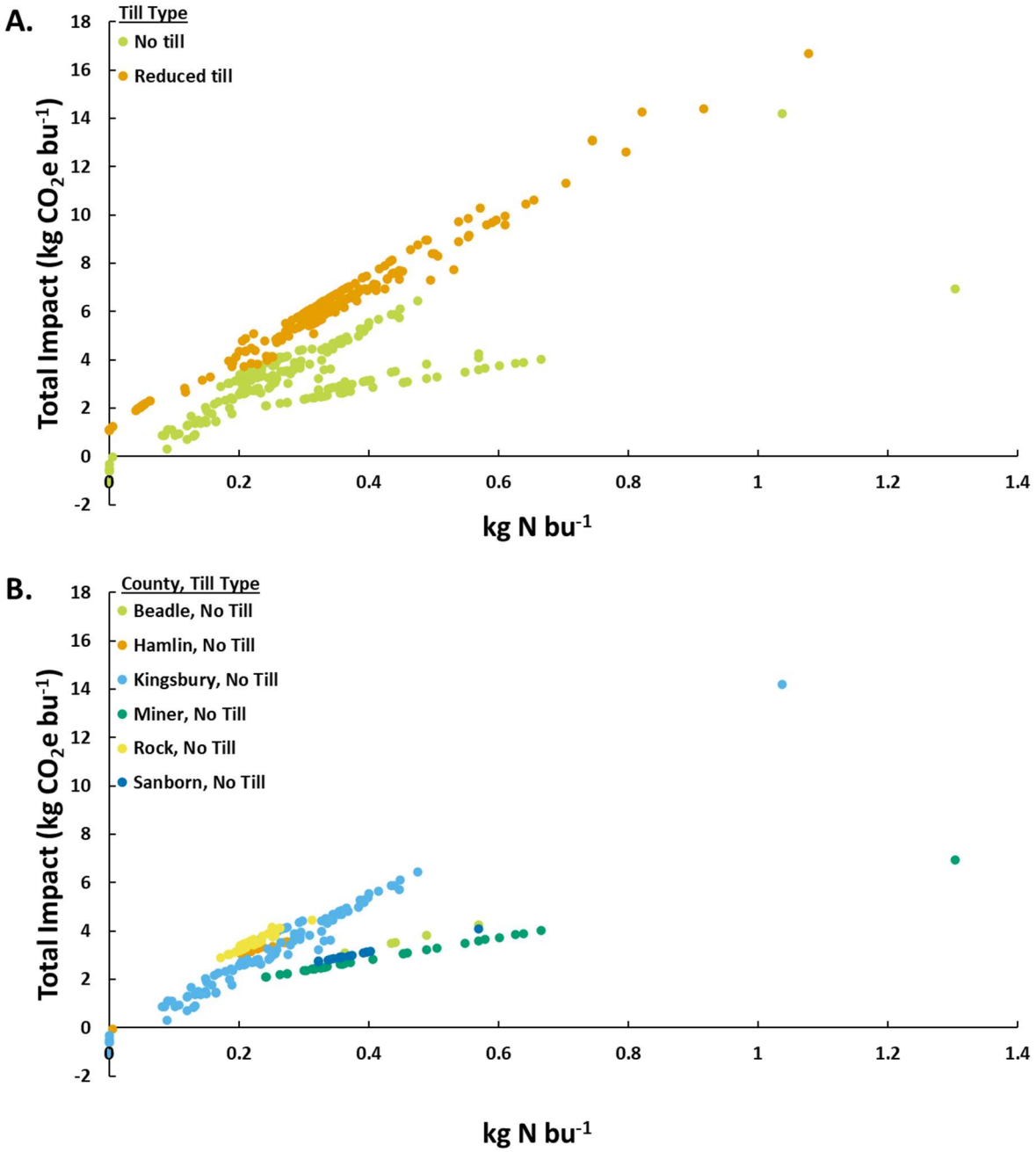

Figure 13. *Scatter plot of 2023 harvest nitrogen usage (kg N applied per bushel produced) vs. GWP impact at the farm gate. a. All site results by till type; b. All no-till sites by county.*

Aside from the effects of conservation tillage, the driving effect of N usage on carbon intensity vis-à-vis upstream emissions and field emissions is observed across all sites. Notably, as illustrated in **Figure 14**, the relationship between nitrogen usage and emissions persists across fields regardless of the fertilizer type that provided the majority of N to each field. Upstream

emissions, shown in **13A**, consistently align among the sites with a small differentiation by primary N source and some variation by non-N fertilizer usage (e.g., potash). **13B** shows an even closer alignment for fertilizer field emissions. Thus, in the context of practices in southeast SD and southwest MN, GWP outcomes depend more on how much nitrogen is utilized rather than the fertilizer used to provide it. However, examining the FDCIC N-related emissions indicates one caveat to this locally-informed finding. The FDCIC default fertilizer mix also aligns with the 2023 harvest sample trend but at a slightly lower impact than sites with similar nitrogen usage (see **Appendix B Figure B3**). This lower emissions result stems from the national model assuming anhydrous ammonia provides 31% of applied N mass while the Gevo sample, and study area farmers in general, tend to use urea and not ammonia (see **Appendix B Figure B4** for breakdowns of 2023 harvest, state-level, and FDCIC nitrogen mixes). Thus, geographically-resolved LCA modeling efforts should examine whether local practices tend to use mostly ammonia, mostly urea, or a mix when weighing the necessity of high-resolution N fertilizer upstream modeling.

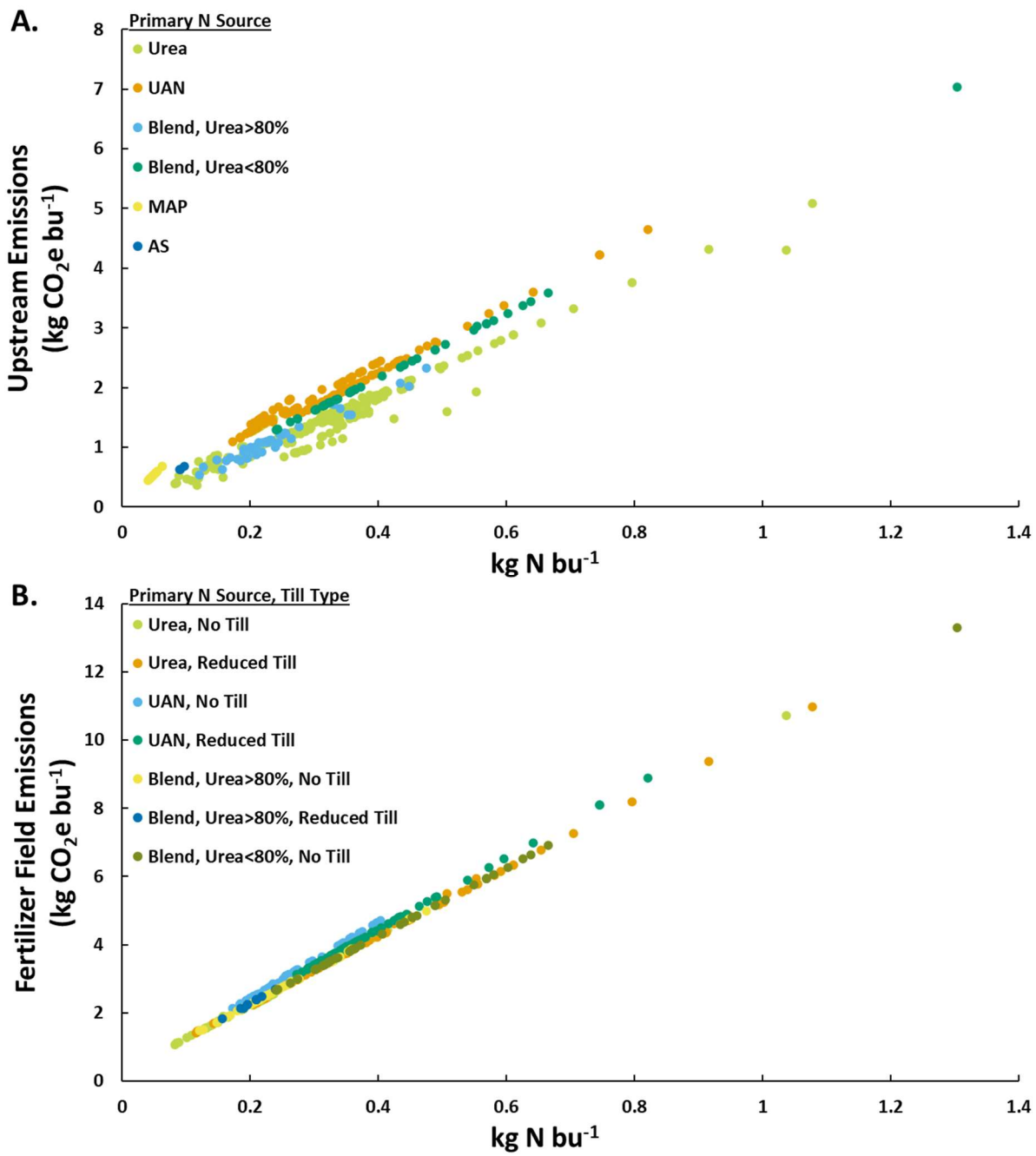

Figure 14*. Scatter plots of 2023 N usage vs. N fertilizer-related emissions grouped by the site's source of the majority of N. a. upstream fertilizer manufacturing emissions, including non-N fertilizers like potash b. Fertilizer direct emissions including direct and indirect N_2O and urea CO_2. Both plots exclude sites which had no N fertilizer applied.*

3.3.3 Recommendations to increase corn cultivation eco-efficiency in study area

Beyond demonstrating that this supply chain has lower GHG emissions than default assumptions would suggest, the harvest 2023 results highlight opportunities for Gevo and its

grower partners to achieve carbon intensity reductions at the cultivation stage. Considering the predominance of N-related emissions (see **Figure 13** and **Figure 14**), efforts to increase N efficiency are particularly important for this area. As multiple years of data are collected, Gevo should monitor which sites consistently demonstrate low N usage to verify what best practices these growers may utilize. For example, cover cropping and enhanced efficiency fertilizers are not yet commonplace in this area's corn operations (see **Appendix B Section 2.2**). The company should track if growers utilize these methods and encourage adoption of successful measures across their grower program. Additionally, Gevo should continue to pursue high-quality field-level evaluation of SOC changes and identify opportunities to boost SOC sequestration. Soil conservation measures can greatly reduce carbon intensity, but soil dynamics can vary greatly by location (see **Figure 13B** and **Appendix B Figure B2**). Capturing these nuances at a field-by-field level will be valuable for carbon reduction efforts and worth the initial logistical investment of data collection. Beyond ensuring GHG flow accuracy, enhanced consideration of field soil dynamics will enable modeling and experimentation of other SOC-building measures in the supply chain, e.g., leaving more residue on the field. By focusing on the drivers of applied nitrogen intensity and SOC change, Gevo can ensure accuracy in its supply chain carbon intensity while exploring innovative, cost-efficient eco-efficiency measures.

3.3.4 Downstream emission reduction stages necessary for low-carbon targets

While the farm-gate LCA results demonstrate the potential for cultivation-stage action, taking a "well-to-wake" view is necessary to consider these efforts in a SAF context. **Figure 15** displays different feedstock corn LCA scenarios in the context of both conventional fossil jet fuel and the 45Z tax credit requirements. Additional context about these SAF results is included in **Appendix B Section B5.**

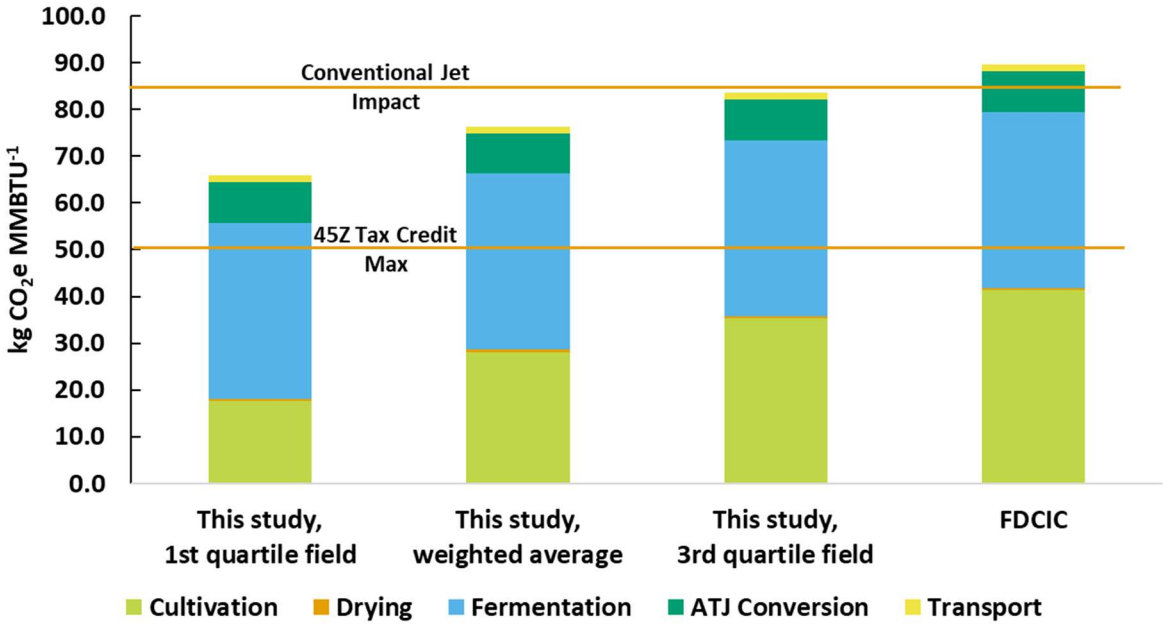

Figure 15. *Well-to-wake GWP of corn-derived ATJ fuel for select results in this study and the FDCIC default model. The 45Z tax credit max is the highest value allowed in the 45Z tax credit; above this value, fuels do not qualify for credits. Drying stage is shown separately here as Gevo accounts for it at the plant while other studies account for it at the farm.*

Notably, compared to FDCIC assumptions, localized cultivation models can result in impacts below that of conventional fossil jet fuel. However, while cultivation measures can make a difference, the threshold set for tax credit qualifications is more stringent. Downstream emissions account for 48.2 kg CO_2e $MMBTU^{-1}$; under these circumstances, only 1% of 2023 harvest fields are eco-efficient enough to qualify. Thus, downstream GHG-reduction initiatives will also be essential to meeting clean fuel targets. Such initiatives range from broader technosphere trends, like renewable electricity sources, to specially-built infrastructure initiatives like carbon capture and sequestration[45,63].

3.3.5 Limitations and future research

While this study provides high-resolution insights and demonstrates the importance of locally-informed agricultural LCA modeling, disruptions in project funding have resulted in data and modeling limitations that future work may address. Notably, funding pauses resulted in SOC

modeling using county-level database information. Compared to the planned field-level simulation plan, this loss in resolution results in a wide distribution of SOC change estimates. When funded work continues in the future, field-specific models will provide more bespoke estimates, reducing the variation associated with county-level estimates. In addition to soil modeling limitations, other measures taken to address data gaps include the usage of local expert opinion to interpret fertilizer reporting and make assumptions necessary for upstream LCA modeling. In future work, collecting additional information from farmers as they report would provide a stronger basis for evaluating local fertilizer usage practices. Further, when funded, the full Gevo study will incorporate three years of data which will provide context to yield and eco-efficiency outcomes, especially for outliers. For example, future crops on fields which used no fertilizer in 2023 may need more nutrient applications to compensate, while fields with poor 2023 yields may return to more average yields and thus lower GWP results. Through addressing these limitations in later stages of the project, the CSU and Gevo collaboration can develop an even more robust model representing the southeast SD and southwest MN area supply chain.

Beyond addressing these data limitations, future research efforts in corn production LCA modeling could identify opportunities for improving biofuel eco-efficiency performance. When project funding resumes, future researchers could cooperate with local farms to implement conservation measures that are currently not common in the Brookings area. For example, practices like leaving more stover on the field to increase SOC or using enhanced efficiency products to decrease nitrogen-related emissions could significantly decrease associated GWP impacts. Further, the corn production model may be expanded to consider relevant non-climate environmental impacts in agricultural production. By considering effects like eutrophication from nitrate leaching and biodiversity impacts from pesticide applications, the model could

identify eco-efficiency co-benefits, tradeoffs, and opportunities as the biofuel production industry evolves. Through such expansions on this present LCA, future researchers will enhance the utility of this high-resolution model and support the continued evolution of the biofuel production field.

Finally, cost modeling may be integrated with the model to consider economic impacts alongside environmental impacts. As SAF production ramps up from multiple feedstocks, the ability to identify life cycle cost opportunities and optimize among multiple objectives will provide invaluable insights for the biofuel production process. One consideration, for example, will be evaluating tradeoffs of conservation tillage. Fuel cost expenses would be reduced and the SOC carbon effects could result in tax credit benefits; however, Gevo and its farmers would benefit from measuring if other expenses go up due to this approach, such as a need for more herbicide volume or more expensive types of herbicides. Another consideration would be the cost efficiency of nitrogen efficiency measures. Ideally, nitrogen efficiency would result in lower fertilizer application costs alongside environmental benefits that could be monetized (e.g., GHG reductions that result in tax credits). However, some measures may actually result in higher costs; for example, enhanced efficiency fertilizers can have higher prices and may not result in significant benefits depending on soil and climate conditions[64]. Downstream mitigation measures will also warrant economic evaluations to ensure corn ethanol ATJ is cost-competitive with other SAF feedstocks. For example, operational expense decisions could be equal-or-lower cost to current sources, e.g., renewable energy vs. fossil-sourced electricity, but other measures will drive costs up, such as low-CI hydrogen sources compared to hydrogen supply chains. Further, capitol expenses for GHG mitigation could pose barriers to cost-competitive corn ATJ SAF. In particular, investments in CO_2 absorption units, pipelines, and injection sites will be important

considerations for fermentation gas carbon capture and sequestration. Thus, future research should integrate geographically-resolved technoeconomic models to aid in evaluating different CI reduction measures in Gevo's supply chain. Through this economic consideration, Gevo and its partners can compare the costs (or savings) of different mitigation measures from the farm to the refinery to help prioritize investments by growers, the company, and policymakers.

3.4 Conclusions

This study's results demonstrate the insights and opportunity of high-resolution modeling in biofuel feedstock crop systems. In the 2023 harvest, Gevo's supply chain average scored below the national-level heuristic model owing to geographically-unique energy usage, agrichemical application, and soil conservation practices. The inclusion of fertilizer field emissions and SOC dynamics is essential to accurately understand farm-gate carbon intensity. Further enhancing the resolution of these data collection and modeling efforts will yield opportunities to achieve eco-efficient production across the grower network. In concert with downstream initiatives, this drive for climate-conscious corn will help the nation's sustainable aviation future take off.

CHAPTER 4: DYNAMIC LCA OF AGRICULTURAL SYSTEMS[2]

4.1 Background

In order to meet climate change mitigation targets, the global community must develop and implement greenhouse gas (GHG) reduction strategies across all economic sectors, including food systems. The food system accounts for one-third of anthropogenic emissions[65,66] and addressing these emissions will be important in the global effort to meet the Paris Agreement goals[10]. To respond to these challenges, food system stakeholders will need to understand opportunities within their product systems to reduce emissions. At the same time, however, the world around them will change. Rapid technology evolutions are expected to mitigate emissions while a transforming climate reality will challenge agricultural systems and require adaptations[1,2].

When preparing for this evolving future, stakeholders will need tools to understand not only how systems perform now, but how they will perform over many years. One such systems-modeling tool, life cycle assessment (LCA), calculates environmental impacts like GHG emissions and water footprints; however, standard LCA is static, capturing a snapshot that reflects the current data available and assumes no change in the life of the product. In order to address this limitation, various forms of forward-looking LCA have been developed[67]. Among these approaches is Dynamic LCA (DLCA), which integrates temporal and spatial variations in the industrial and environmental systems surrounding the modeled process[68], and the related

[2] This chapter was submitted for publication as a peer-reviewed journal article: R. Maynard, J.C. Quinn, "The Future of Sustainable Food: Evaluating the Effect of Dynamic Life Cycle Assessment Methods on Lettuce Production Ecoefficiency," Journal of Cleaner Production, Revision submitted April 2025.

process of Prospective LCA (PLCA) which studies the maturation and diffusion of emerging technologies[69]. By capturing projected transformations in the ecosphere and technosphere, practitioners can use forward-looking LCA methods to inform stakeholders about potential opportunities and risks in their operations.

In the agricultural sector, DLCA and PLCA have been utilized in limited applications to explore climate and technology changes. To capture climate change impacts, Viveros Santos et al. combined historical viticulture and weather data to predict French grape yield changes under different climate scenarios while also considering the effects of extreme events and adaptation strategies on LCA results[70]. Lucas et al. also focused on yield changes for assorted Brazilian crops in different regions by extrapolating from past data into the future to estimate prospective biodiversity impacts[71]. Beyond modeling system inputs and outputs, some DLCA methods capture dynamics in characterization factors, such as Lebailly et al.'s study of zinc fertilizer emission impacts on freshwater ecotoxicity[72]. Other studies have modeled the life cycle impact of specific emerging agricultural technologies with different LCA approaches. For example, Tsoy et al. compared reflective coatings in a greenhouse tomato application, using "anticipatory" LCA to compare a technology currently at laboratory scale to conventional industrial scale alternatives [73]. In another recent study, Fargnoli et al. compared the lifetime impacts of a more mature technology, a hybrid diesel tractor, to incumbent diesel technologies[74]. In addition to agriculture-focused methods, broader dynamic and prospective LCA tools are available that may be applied to agriculture. Sacchi et al.'s premise methodology combines integrated assessment modeling with the ecoinvent database to model certain upstream technosphere transformations and create prospective LCI databases[75]. With continued development of prospective models for different upstream sectors, like Boyce et al.'s ammonia modeling[76], the premise library offers agricultural

LCA practitioners a tool to consider how background decarbonization transitions can affect their product systems.

While these studies provide various insights into the utility of dynamic and prospective LCA methods, they often focus on the effects of specific techniques or technologies without translating these insights to crop LCA impacts. Agricultural DLCA can include everything from modeling yield changes to background PLCI development to projecting emerging technology adoption, each having an effect on eco-efficiency results, yet the limited existing agricultural DLCA literature lacks applications of these techniques. Even where some dynamic methods are applied, they are not considered alongside other techniques. For example, studies which consider future yield trends do not also consider technospheric trends. Thus, this work provides a comparative view of different techniques, allowing insights for practitioners on the relative impact of different DLCA tools. Further, this study contributes to the agricultural DLCA literature by examining a previously-unmodeled product system in DLCA: production of lettuce in the United States. In filling these literature gaps, the objective of this research was to compare static and dynamic agricultural LCA outcomes, evaluate the effects of different DLCA methods, and provide agricultural stakeholders with DLCA-informed eco-efficiency strategies.

Utilizing a previously-published LCA model[77], leaf lettuce was examined as an example crop, including multiple locations and weather sets to account for geographic variations and temporal variations as the climate changes from a baseline year of 2020 up to the year 2050. Based on previous results from that model, DLCA methods were applied to crop yields, nitrogen fertilizer production, and on-farm energy usage. Dynamic process modeling examined how a changing climate would affect yield and irrigation demand in the product system. Additionally, background technosphere transformation of operating expenses was considered through

prospective electrical grid resources, renewable diesel availability, and prospective life cycle inventories (PLCI) of fertilizer production. Foreground technology adoption rates were modeled for on-farm energy capital investments, particularly the electrification of pumps and the electrification of heavy machinery. Scenario analyses were then performed to explore the range of climate mitigation potential associated with each technology transformation. Finally, modern-day implementation costs of technological transformations were considered to compare the marginal abatement cost of the different climate emissions mitigation efforts. Through these analyses, DLCA was utilized to provide practitioners and stakeholders with forward-looking insights into agricultural sustainability.

4.2 Materials and Methods

4.2.1 Life Cycle System Overview

In order to evaluate the environmental impact of lettuce production, this study's life cycle assessments were performed following four phases: goal and scope definition, life cycle inventory analysis, life cycle impact assessment, and interpretation. The goal of the project was to provide stakeholders with insights on potential climate change impact improvements based on evolving technological systems in the agricultural supply chain. The functional unit was defined as 1 kg of fresh lettuce, allowing comparison to previous crop modeling and LCA work[77]. The technological transformations all occur prior to harvesting; thus, the system boundary is "cradle-to-harvest." To provide geographical insights, the geographic scope included two sites representative of current major lettuce production regions (Monterrey County, California and Yuma County, Arizona) as well as local production models in the four largest United States cities: New York City, Los Angeles, Chicago, and Houston. For the temporal scope, dynamic effects were considered in five-year increments from 2020 to 2050.

In the life cycle inventory analysis (LCI) stage, the inputs and outputs of the lettuce production system were determined, and in this stage DLCA methods were implemented. As a basis, the LCI model from previous LCA research was adapted[77], which identified crop yield, nitrogen fertilizer upstream emissions, and on-farm energy usage as significant and sensitive inputs. Thus, this study's DLCA methods focused on understanding dynamic effects on those inputs. In order to model these dynamics, three categories of dynamic methods, based on the framework developed by Collinge et al.[68], were applied (see **Figure 16**): dynamic process modeling, background technosphere transformation, and foreground technology adoption rates.

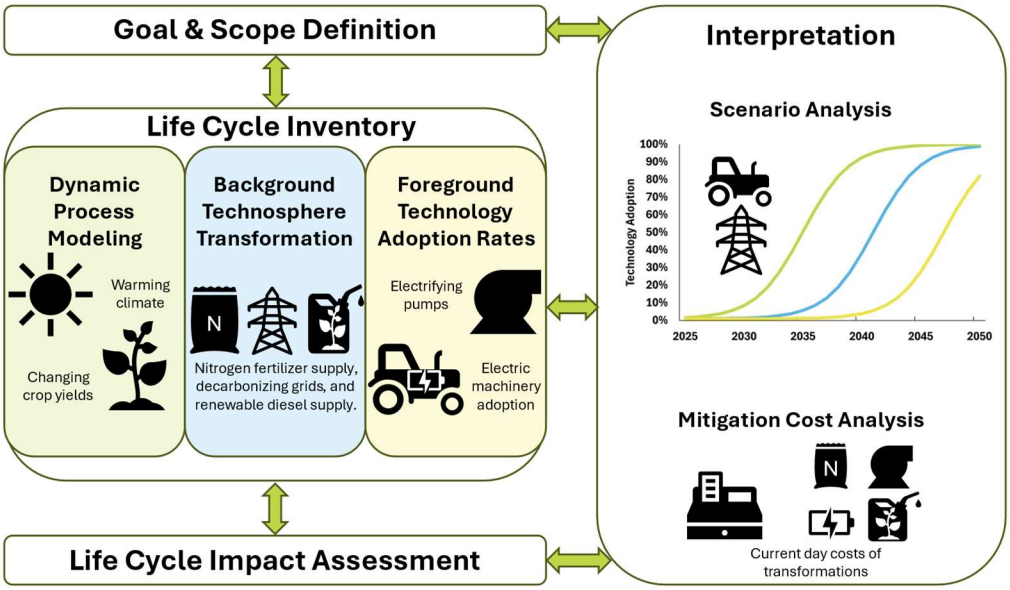

Figure 16. *Diagram illustrating this study's implementation of dynamic methods in the LCA stages. Subcategories of dynamic LCI methods are based on those identified by Collinge et al.[68].*

These three methods were applied to lettuce production in order to capture dynamic aspects particular to the agricultural sector as well as those related to the broader dynamic transformations in the economy. Dynamic process modeling allowed for the simulation of changing yields and irrigation demands due to climate change. Previous studies have shown the

importance of yield to crop eco-efficiency[71,78], including the authors' previous lettuce LCA study[77]. Thus, crop growth was dynamically modeled to reflect oncoming climate changes and the expected effects on yield[79]. Meanwhile, background technosphere transformation allows an examination of how broader decarbonization efforts affect high-impact aspects of lettuce production. Namely, nitrogen fertilizer and on-farm energy usage were identified as major drivers of lettuce system GWP outcomes[77]; expected upstream changes to the production of ammonia[80], electricity[81], and liquid biofuel[82] would thus affect life cycle outcomes in lettuce production. Finally, foreground technology adoption rates were considered to examine emerging technologies in the on-farm energy usage category. To compare the status quo to alternatives in PLCI, the proposed technology should have a high technology readiness level[83]. Accordingly, this study examined the adoption of electric irrigation pumps, which are commercially available, and electric heavy machinery, which recently began entering the market[84]. By considering ecospheric and technospheric transformations through these three methods, the high-Impact inputs and outputs of a lettuce LCA model were examined in a novel dynamic context.

4.2.2 Dynamic Process Modeling

One dynamic method applied to the LCI phase involved modeling crop growth to estimate irrigation demand and yield, affecting system input and output flows. Previous lettuce modeling work[77] was implemented into the AquaCrop-OS Python tool[85]. To account for dynamic changes in climate over the coming decades, weather projections based on the RCP-4.5 CMIP5 pathway were utilized[86]. As with other decisions in this work, RCP-4.5 was selected to align with the two-to-three-degree Celsius estimate of the UNEP Gap Report. In addition to climatology inputs (temperatures and precipitation)[87], hydrology input projections were also obtained[88] for initial soil moisture values and to estimate evapotranspiration using an edited version of the

pyfao56 tool[89]. Combined with the lettuce growth parameters and local soil conditions utilized in the53ubliccation[77], each location and year combination was simulated 32 times; the average yield and irrigation demand were then used as flows in the DLCA model, as illustrated in **Figure 17**. Additional details on this dynamic crop modeling are included in **Appendix C Section C1.1**, and the Python codes utilized are included in the **Appendix C Section C2**.

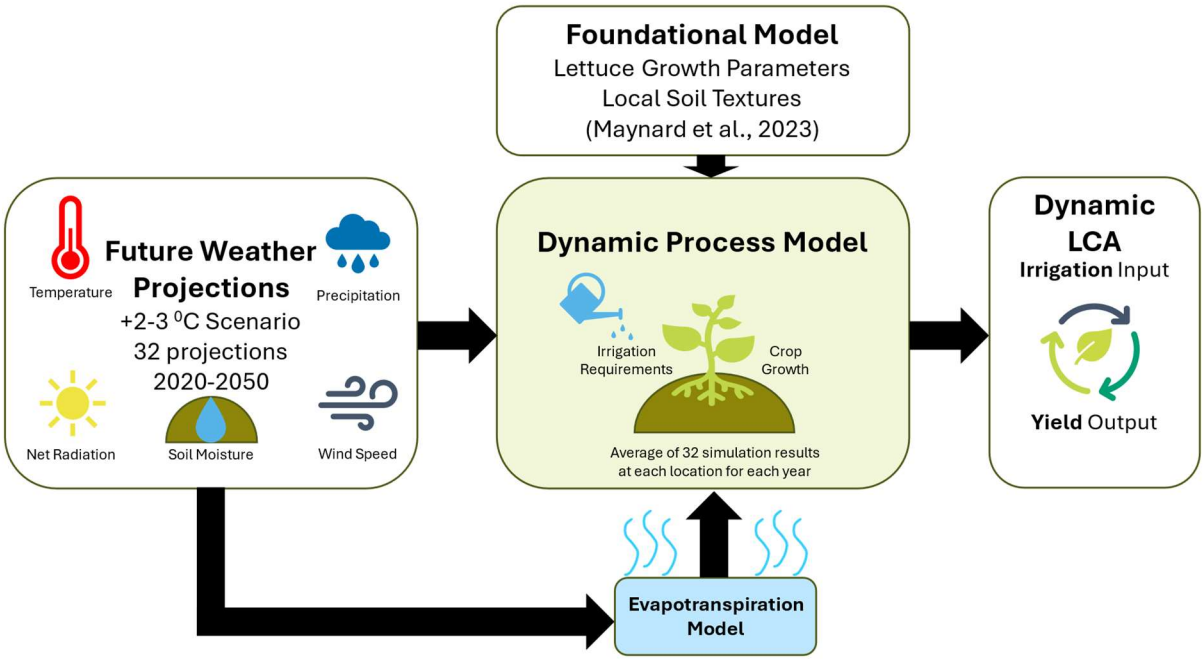

Figure 17. *Process diagram showing how future weather projections were combined with AquaCrop modeling to calculate lettuce cultivation irrigation and yield flows.*

4.2.3 Background Technosphere Transformation

Another DLCA method applied to this lettuce system considered background technosphere transformations related to three high-impact categories: upstream nitrogen fertilizer (N fertilizer) production, upstream generation of electricity used on the farm, and renewable diesel (RD) available from domestic production. For the N fertilizer emissions, the PLCI work of Boyce et al. was utilized to estimate the carbon intensity of ammonia[76] and then combined with the GHG emissions associated with energy and transport as noted in Argonne National

Laboratory's Feedstock Carbon Intensity Calculator (FD-CIC) model for urea fertilizer[57]. Boyce et al.'s SSP2-RCP2.6 model – consistent with a +2 ^{0}C trajectory – was used as a baseline case, while the SSP2-Base model – consistent with a +3 ^{0}C trajectory – was used as a conservative case. For the optimistic nitrogen fertilizer case, the International Energy Agency's projections on low-impact hydrogen[90] were used to construct technology diffusion "S-curves[69]" for green urea adoption. These projections were then combined with the green urea manufacturing emissions estimates found in the FD-CIC tool[57]. Further details on this background modeling are included in **Appendix C Section C1.2.1**. In addition to the fertilizer supply chain, the generation of electricity used on the farm was considered. For these inputs, NREL's Cambium dataset was used to allow for region-specific grid modeling[81] of future grid emissions factors. Of the projection cases available, the Cambium MidCase was utilized in this study as the baseline case. Other cases included in the model were Low Natural Gas Price as a conservative case and Low Renewable Energy Cost as an optimistic case. Finally, upstream transformation for diesel used in heavy machinery was considered. RD was considered as a drop-in replacement fuel option that has seen considerable production growth in recent years[91] and which machinery makers currently consider more viable than electrification for high power agricultural use (John Deere & Company, 2023). Soybean oil has seen the highest growth among US feedstocks[91], so this study modeled soy-derived RD using the LCI developed by Xu et al.[92]. Utilizing the ecoinvent database[5] for these inputs allowed for the application of the premise database[75] to capture technosphere transformations that affected RD GWP in the projected years, such as the declining carbon intensity of bio-refinery energy usage. RD usage as a proportion of heavy machinery energy demand was modeled based on ratios of projected domestic RD production capacity to total diesel capacity. In the baseline case, the US Energy Information Administration's Reference

Case for RD was considered compared to the Reference Case production of conventional diesel, while the conservative case used the Low Oil Price case[93]. This study's optimistic case used the High Oil Price case for RD production but divided this value by the total diesel sold to farm consumers[94]; essentially, this case modeled US domestic RD capacity's theoretical proportion of domestic farm diesel demand, optimistically assuming the farm sector was not outcompeted by other sectors for RD supply. Further details on RD modeling, including upstream input dynamics and indirect land use change considerations, are included in **Appendix C Section C1.2.2**.

4.2.4 Foreground Technology Adoption

Beyond upstream transformations in supply chains, lettuce producers can invest in equipment which reduces onsite emissions; this study examined electric technology adoption rates. One significant input for lettuce, irrigation energy, was considered as a readily-available form of electrification. The energy mix for irrigation has previously been examined on a national level by Driscoll et al. using USDA survey data[95], and those techniques were adapted to the regions and inventories considered in this study, including using Driscoll et al.'s 5%-per-year electrification scenario as a baseline case. Additionally, this study considered transition cases of 2.5% and 7.5% per year as conservative and optimistic cases. Notably, motor-powered irrigation represents a mature electrification technology whose barriers to adoption are usually logistics and costs, i.e., connections to electrical grids and high electricity prices. Additional details on the methods and tools used for irrigation electrification are included in **Appendix C Section C1.2.3**. In addition to the mature technology of irrigation electrification, the more-difficult task of heavy machinery electrification was considered as an alternative to RD usage. Battery electric vehicle (BEV) farm machinery are emerging in the market, but often in lower power applications[84,96,97]. Based on similar equipment sizes in both the ecoinvent product system[5] and California-specific

lettuce farm management data[98], this study modeled lettuce operations as feasibly adopting electric machinery in the near-future. Based upon NREL's different projections for nationwide industrial sector electrification[99] and CALSTART projections for agriculture-specific electrification[84], change cases for conservative, baseline, and optimistic adoption were constructed. Details on these scenarios, as well as details for modeling battery production impacts, are included in **Appendix C Section C1.2.4.**

4.2.5 Marginal Abatement Cost Calculations

In order to further compare the near-term feasibility of potential GHG-reduction measures in the agricultural sector, present-day marginal abatement costs were calculated for four measures: irrigation electrification, heavy machinery RD drop-in, heavy machinery electrification, and green ammonia-based fertilizer adoption. Notably, these costs were estimated as costs to the lettuce producer. For example, the RD costs calculated in this study included subsidies like federal renewable identification number (RIN) credits in the California market[100]. Transition costs were calculated based on available present-day estimates for each technology, with one exception: due to a lack of total cost of ownership data for full-sized farm BEV's, proxy data for other heavy duty vehicle applications were adapted from a recent Argonne National Laboratory study[101]. Mitigation costs for urea were calculated using ammonia price data as in **Equation 1**:

Equation 1. *Mitigation cost calculation for transitioning from "grey" ammonia feedstock to "green" ammonia feedstock in urea fertilizer production.*

$$Cost_{Grey-Green} = \frac{Price_{Green} - Price_{Grey}}{CI_{Grey} - CI_{Green}} * 1000$$

Where:

- $Price_{Green}$ is the price for green ammonia-derived urea $\left(\frac{\$}{kg}\right)$,

- $Price_{Grey}$ is the price for grey ammonia-derived urea $\left(\frac{\$}{kg}\right)$,
- CI_{Grey} is the emissions intensity for grey ammonia-derived urea $\left(\frac{kg\ CO_2e}{kg}\right)$,
- CI_{Green} is the emissions intensity for green ammonia-derived urea $\left(\frac{kg\ CO_2e}{kg}\right)$, and
- $Cost_{Grey-Green\ Machiner}$ is the mitigation cost to switch from grey ammonia-based fertilizer to green ammonia-based fertilizer $\left(\frac{\$}{ton\ CO_2e}\right)$.

For irrigation transition costs, a net present value calculation was performed for both an electric and a natural gas pump as in **Equation 2**:

Equation 2. *Mitigation cost calculation for transition from natural gas-powered irrigation pumps to electricity-powered irrigation pumps.*

$$Cost_{NG-E\ Pump} = \frac{NPV_{electric} - NPV_{natural\ gas}}{CI_{natural\ gas} - CI_{electric}} * 1000$$

Where:

- $NPV_{electric}$ is the net present value for an electric pump $\left(\frac{\$}{m^3}\right)$,
- $NPV_{natural\ gas}$ is the net present value for a natural gas pump $\left(\frac{\$}{m^3}\right)$,
- $CI_{natural\ gas}$ is the emissions intensity for a natural gas pump $\left(\frac{kg\ CO_2e}{m^3}\right)$,
- $CI_{electric}$ is the emissions intensity for an electric pump $\left(\frac{kg\ CO_2e}{m^3}\right)$, and
- $Cost_{NG-E\ Pump}$ is the mitigation cost to switch from natural gas to electric pumps $\left(\frac{\$}{ton\ CO_2e}\right)$.

In the heavy machinery case, total cost of ownership for diesel and BEV machines were used as in **Equation 3**:

***Equation 3**. Mitigation cost calculation for transition from fossil diesel heavy machinery to electric heavy machinery.*

$$Cost_{D-E\ Machinery} = \frac{TCO_{electric} - TCO_{diesel}}{CI_{diesel} - CI_{electric}} * 1000$$

Where:

- $TCO_{electric}$ is the total cost of ownership for electric machinery $\left(\frac{\$}{mi}\right)$,
- TCO_{diesel} is the total cost of ownership for diesel machinery $\left(\frac{\$}{mi}\right)$,
- CI_{diesel} is the emissions intensity for diesel machinery $\left(\frac{kg\ CO_2e}{mi}\right)$,
- $CI_{electric}$ is the emissions intensity for electric machinery $\left(\frac{kg\ CO_2e}{mi}\right)$, and
- $Cost_{D-E\ Machinery}$ is the mitigation cost to switch from diesel to electric machinery $\left(\frac{\$}{ton\ CO_2e}\right)$.

Finally, fossil diesel and RD costs were compared as in **Equation 4**:

***Equation 4.** Mitigation cost calculation for transition from fossil diesel to renewable diesel in heavy machinery.*

$$Cost_{FD-RD\ Machinery} = \frac{Price_{RD} - Price_{FD}}{CI_{FD} - CI_{RD}} * 1000$$

Where:

- $Price_{RD}$ is the price for renewable diesel $\left(\frac{\$}{MJ}\right)$,
- $Price_{FD}$ is the price for fossil diesel $\left(\frac{\$}{MJ}\right)$,
- CI_{FD} is the emissions intensity for fossil diesel $\left(\frac{kg\ CO_2e}{MJ}\right)$,
- CI_{RD} is the emissions intensity for renewable diesel $\left(\frac{kg\ CO_2e}{MJ}\right)$, and
- $Cost_{FD-RD\ Machinery}$ is the mitigation cost to switch from fossil diesel to renewable diesel $\left(\frac{\$}{ton\ CO_2e}\right)$.

Details for costs and avoided emissions estimates in each transition case are provided in **Appendix C Section C1.3**. Finally, a 10,000-trial Monte Carlo simulation was performed for cost data estimates using the Argo Excel plug-in[102] to estimate uncertainty in the range of mitigation costs associated with technologies and supply chains of varying maturity.

4.3 Results and Discussion

4.3.1 Effects of Dynamic Methods on LCA Results

DLCA methodology was combined with a case study of lettuce production in the US to estimate GHG impacts across the six study sites between 2020 and 2050. The DLCA results show a decline in GHG intensity of 26-37% from static modeling between 2020 and 2050 depending on location of study. **Figure 18** illustrates the decline in impacts across modeled sites and years. Notably, while local production sites may demonstrate a greater decline as a percentage of their baseline (e.g., in New York where fossil fuels initially comprise a greater proportion of irrigation energy), the conventional production sites in the American Southwest remain the most GHG-efficient producers of lettuce owing to geographic advantages like high yields and projected low-carbon electricity. In Salinas, CA, for example, static LCA estimates an impact of 0.21 kg CO_2e kg^{-1} lettuce. By 2050, the DLCA estimates an impact of 0.15 kg CO_2e kg^{-1} lettuce. Forty-five percent of this reduction is associated with irrigation, 33% with heavy machinery, and 22% with N fertilizer. Across all scenarios, the consistency of fertilizer field emissions should be noted. When decarbonization strategies like those considered here are implemented in crop product systems, direct non-carbon emissions like N_2O will have a growing relative impact, emphasizing the need for developing additional technologies and techniques for increasing nitrogen efficiency.

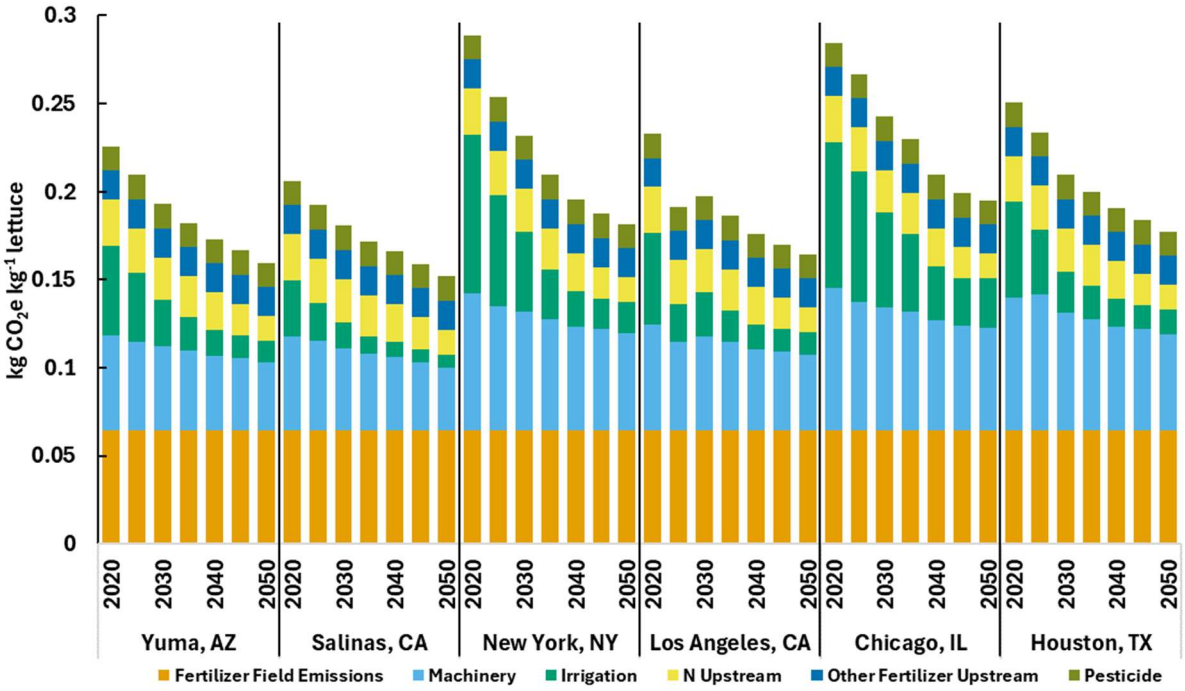

Figure 18. *LCA results across all study locations and years. Results are shown for baseline scenarios of technology adoption and include yield effects from dynamic crop modeling.*

While **Figure 18** displays GHG-intensity by each simulated year, **Figure 19** illustrates the difference in emissions from 2020 to 2050. This comparison demonstrates each DLCA methods' impact on the analysis relative to a 2020 static LCA. In addition to the techniques employed in this study, the effect of a PLCI performed with premise and Cambium data is also presented for comparison to using a PLCI database alone. Technosphere modeling of nitrogen fertilizer embodied GHG results in a 5% decline on average among the sites; notably, this is greater than the 2% decline captured in the premise PLCI database alone. Such a discrepancy shows that DLCA practitioners could benefit from PLCI data that emphasizes upstream modeling for high impact inputs as in the case of Boyce et al.'s ammonia work[76] for this study's agricultural systems. Dynamic modeling of weather accounts for a similar impact of 6%, due to an average 12% increase in simulated yields. While such an increased yield is not guaranteed every year for every site (see **Appendix C Figure C1** and note error bar overlaps), such an

increase is consistent with other work that shows higher ambient temperature can have a positive effect on leafy vegetables[103]. However, this effect is not universal for all crops[79,104,105]; dynamic weather effects for one crop should not be extrapolated to other crops without verifying such differences. Across the sites, on-farm electricity background modeling accounts for the greatest average reduction of 8%, followed by an average reduction of 7% related to electric irrigation adoption. Notably, the DLCA method with the greatest individual effect varied by location, partially due to the differences in initial pump electrical energy mix (see **Appendix C** Error! Reference source not found.). Overall, these baseline results demonstrate that, in addition to PLCI data like premise, DLCA practitioners should consider tools that capture other sources of impact variation.

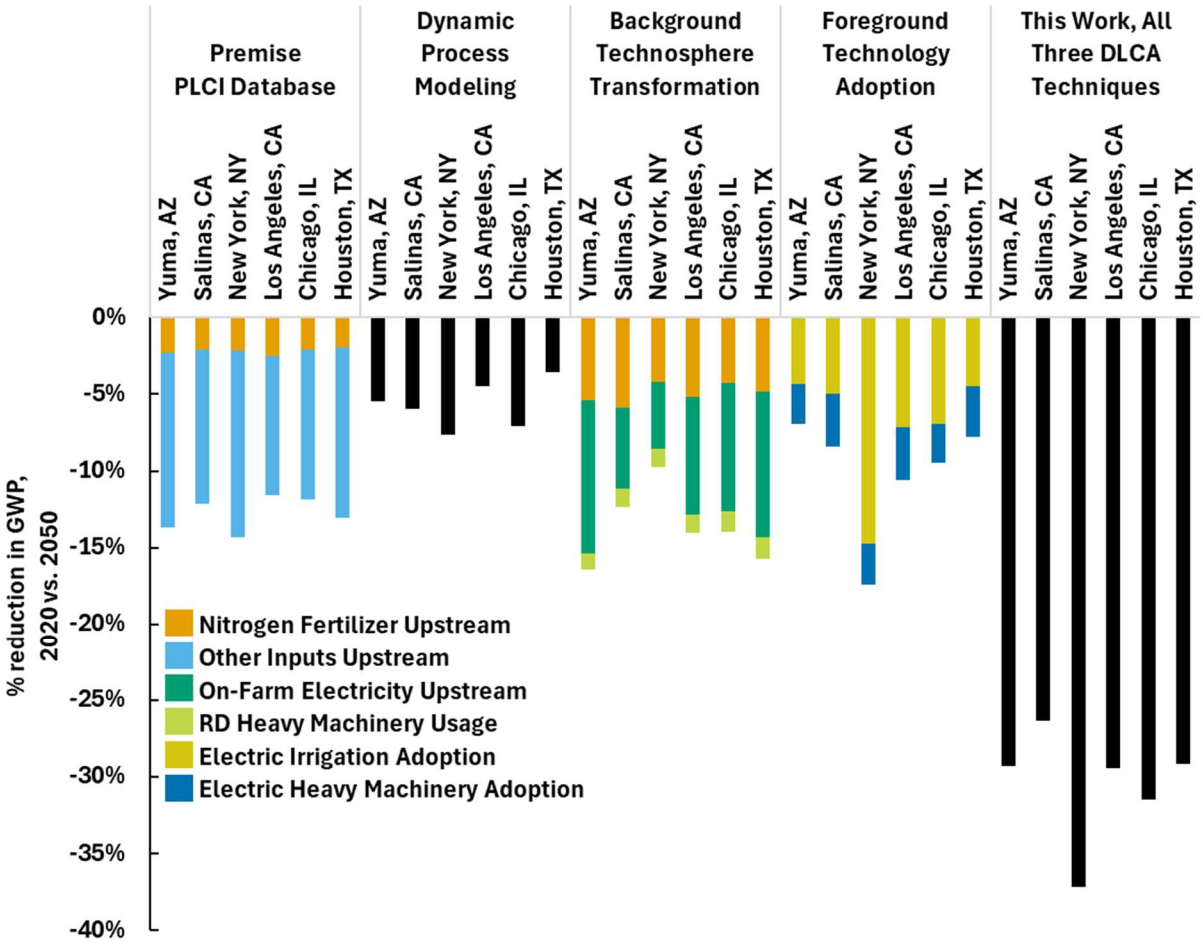

Figure 19. *Percent reduction in impact between 2020 and 2050 of different DLCA methods used in this study compared to a Background PLCI performed with the premise SSP2 Base PLCI.*

4.3.2 Technology Adoption Scenario Analyses

In addition to the baseline technology change case, **Figure 20** displays the impact of conservative and optimistic cases for background N fertilizer upstream transitions, electric pump adoption with decarbonizing electricity, RD usage in heavy machinery, and BEV heavy machinery adoption with decarbonizing electricity. Notably, though varying by location, irrigation electrification has a consistently high impact potential when combined with decarbonizing grids upstream. For agricultural stakeholders, such a result shows how the implementation of a mature technology in the near-term could have significant impact while long-term technology transformations develop. Across the other technologies, the impact can

vary widely based on prospective adoption projections. While such a variety can be useful to envision goals and possibilities for improvement, this variation also demonstrates how DLCA practitioners must take caution with the selection of technology changes in different modeled cases. Selecting a technology change baseline can significantly shift an analysis; further, the accuracy of a selected baseline could shift over time as technological progress accelerates or decelerates. Transparency in these selections should be paramount so that future users of these studies can reevaluate the accuracy of technology change case selection and apply alternative projections if necessary.

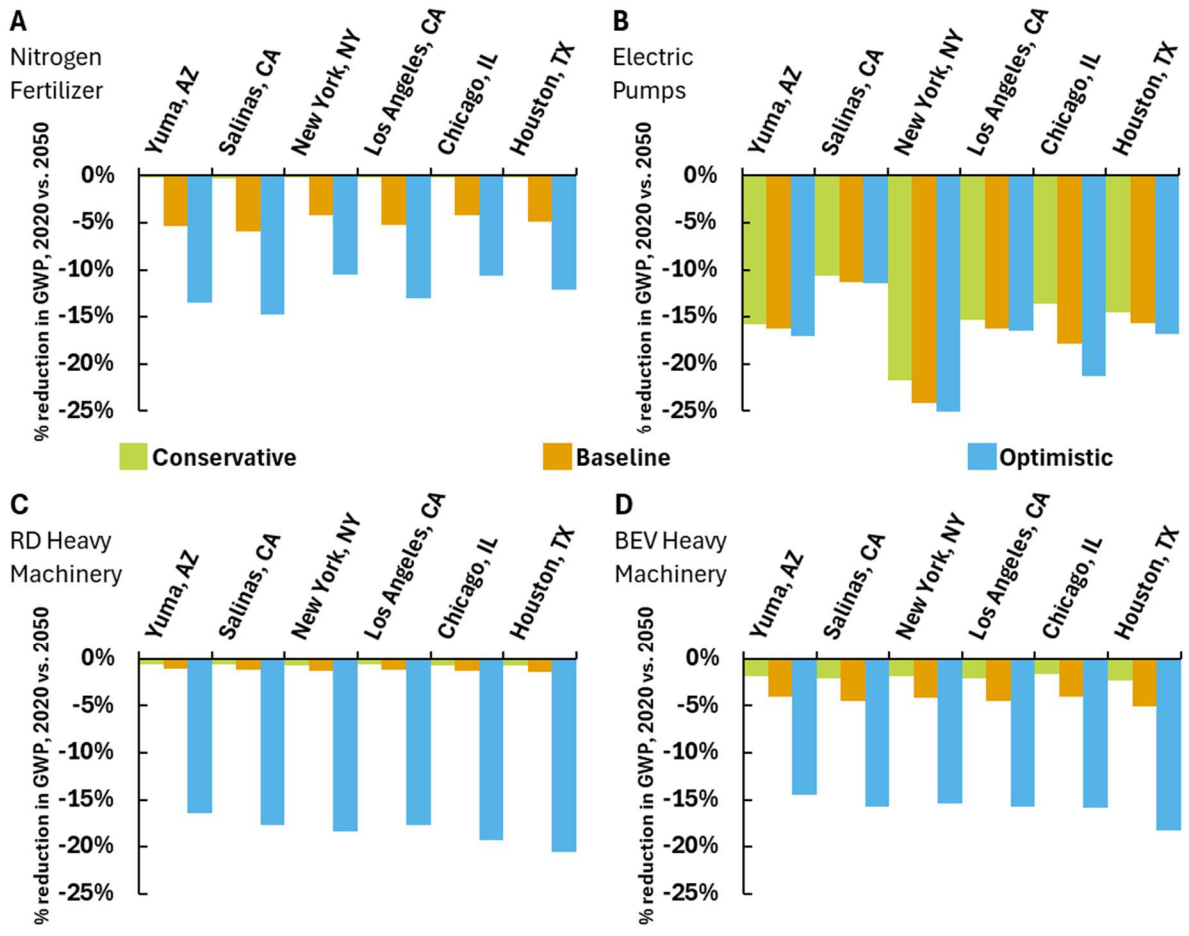

Figure 20. *Relative impacts of conservative, baseline, and optimistic transition cases for:* ***A)*** *N fertilizer background transformation,* ***B)*** *electric pump adoption with upstream grid transformation,* ***C)*** *RD usage in heavy machinery, and D) BEV heavy machinery adoption with upstream grid transformation.*

In addition to the extent of change over time, stakeholders may wish to consider the pace of change. For example, **Figure 21** compares the impacts of two alternatives for heavy machinery energy transitions: RD and BEV's. RD is currently available in some U.S. markets while BEV farm machinery is still a developing technology, especially for high-power applications. If RD is prioritized for the agricultural sector diesel supply (optimistic case), it could make immediate reductions in product impacts. However, if farmers only use RD as a proportional mix of all available diesel (conservative and baseline cases), even limited BEV adoption can exceed renewable diesel's proportional impact by 2050. For DLCA practitioners and agricultural stakeholders, such scenario analyses could shape transition fuel conversations for the sector. Depending on RD production trends, and the availability of RD to farms, stakeholders could invest in a new diesel engine or decide that BEV technology has matured enough for their needs. Thus, when making such comparisons across decades, DLCA practitioners should evaluate all scenarios not just at the start and end points but also at intermediate years to provide a clear view of technology availability and near-term opportunity.

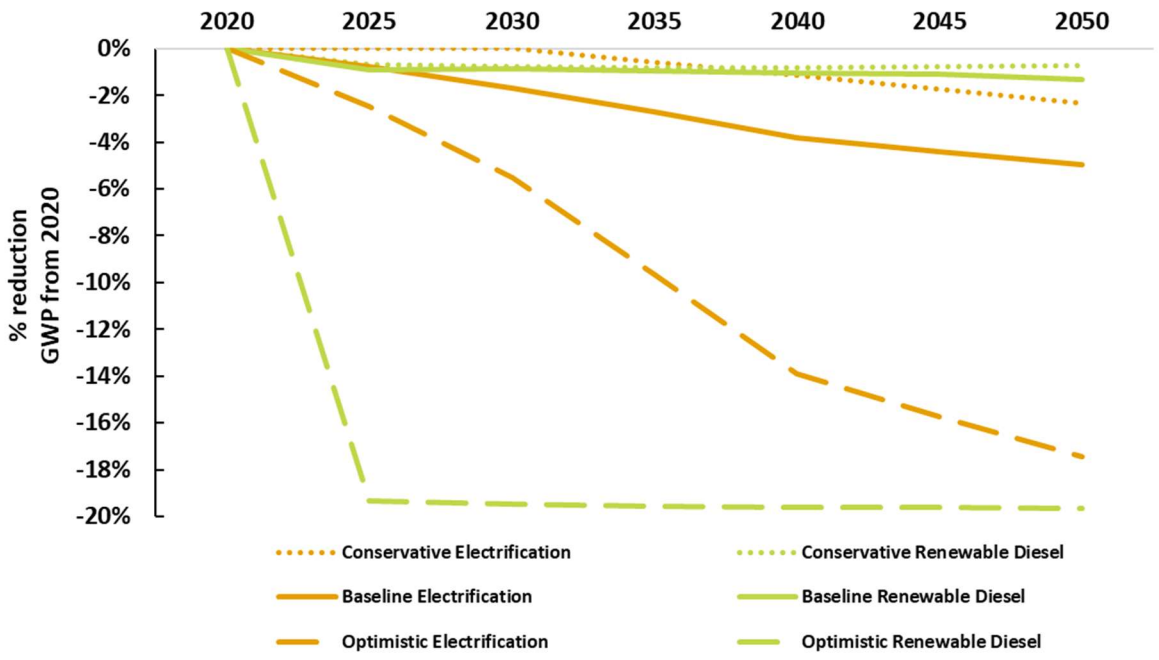

Figure 21. *Impact of heavy machinery alternative energy strategies on GWP results over time using the Salinas, CA simulation as an example. Note impact backsliding in baseline and conservative diesel cases reflects temporary declines in U.S. RD production capacity.*

4.3.3 Marginal Abatement Cost Comparisons

In addition to DLCA scenario analyses, the current costs of available technologies can help inform GHG reduction strategies, and **Figure 22** shows the relative costs of this study's modeled strategies. In most cases, irrigation electrification would save farmers money while also reducing emissions and this is reflected by the negative abatement result. Alternatively, high utility connection costs and high electricity costs relative to natural gas prices could make the cost of abatement positive, which may hinder adoption rates. Implementation of this solution could depend on farmers overcoming these logistical hurdles. RD simulations result in a near-zero or negative cost, reflecting federal RINs and state Low Carbon Fuel Standard (LCFS) incentives in California; with such continued support, farmers could utilize the biofuel in the near-term as an effective GHG reduction strategy. In comparison, electric machinery would likely cost farmers if implemented today, reflecting the high initial cost of this developing

technology. Finally, green ammonia-based fertilizer would be costly to implement in the near-term; while green ammonia can potentially be at a lower price than conventional ammonia, in 75% of simulated cases farmers would pay a high cost to avoid upstream emissions. Thus, widespread adoption of green ammonia-based fertilizer would necessitate subsidies or would be delayed until the green ammonia supply chain becomes more cost-competitive. In combination with the forward-looking insights of DLCA, this modern-day cost analysis can show stakeholders which GHG-reduction measures can be implemented easily in the near-term and which measures warrant reconsideration when emerging supply chains mature.

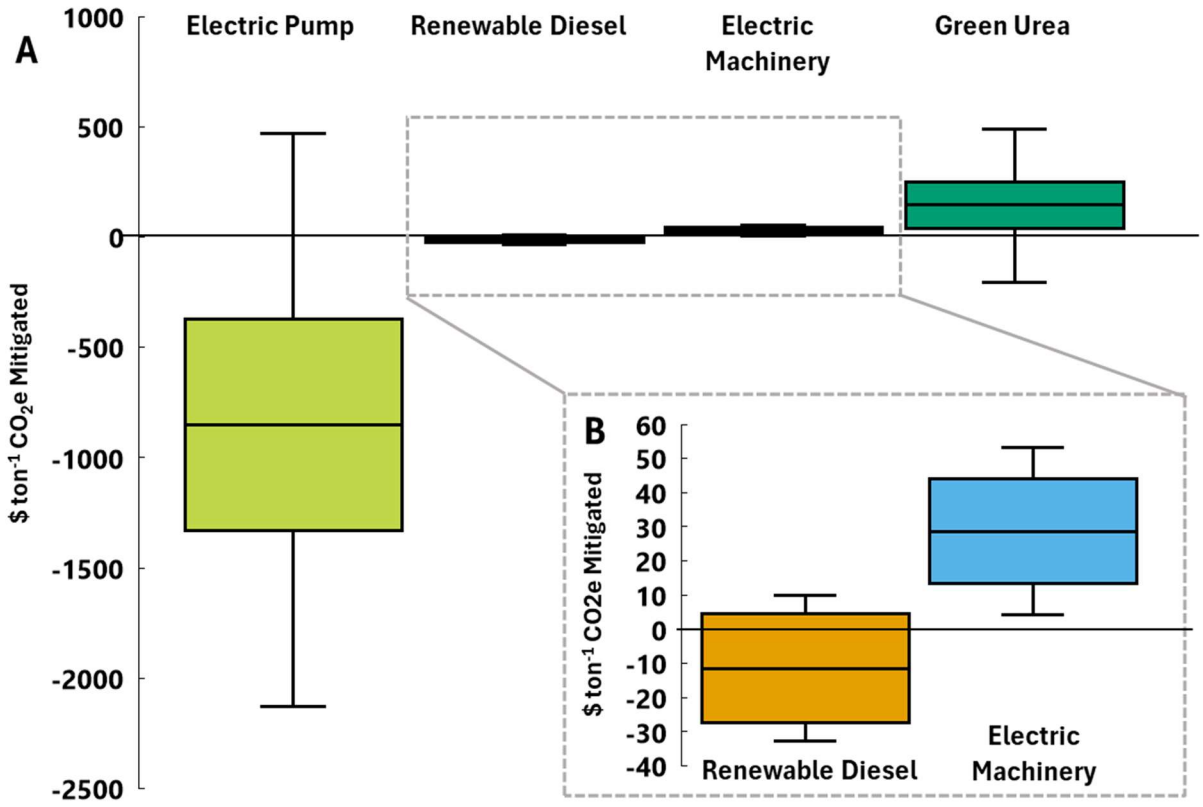

Figure 22. *Box-and-whisker plot of current day costs to California farmers for different GHG-reduction strategies.* ***A)*** *All mitigation measures considered in this analysis.* ***B)*** *Magnified inset of heavy machinery emissions reduction measures. Generated from a 10,000 trial Monte Carlo simulation of costs, showing the minimum and quartile results of that simulation. Note that pump electrification and RD purchases are reflective of California-specific price data while electric machinery and green urea estimates are for the entire United States.*

4.3.4 Recommendations for Stakeholders

In addition to methodology implications for DLCA practitioners, the results of this study illustrate actions that agricultural producers and policymakers can prioritize to reduce emissions. By considering the emissions reduction potential (see **Figure 19**) and associated costs (see **Figure 22**) of different measures, stakeholders can prioritize near-term efforts in foreground technology adoption. Further, comparing different transition cases, as in **Figure 20**, can indicate where investments in technology development and industrial capacity could enable large reductions in agricultural emissions. Finally, using multiple-year DLCA modeling to compare alternative decarbonization methods, as in **Figure 21**, allows stakeholders to weigh relative rates of progress and cumulative emissions reductions in their decision-making. Applying these methods to lettuce indicates a range of decarbonization opportunities for the specific crop and crops with similar cultivation and emissions characteristics.

The first recommendation from these results stems from the large emissions reduction opportunity (see **Figure 19**) and cost efficiency (see **Figure 22**) of electric pumps. For crops like lettuce with a high irrigation emissions footprint, enabling pump electrification is a low-cost, high-reward priority. The barriers to adoption of high utility connection costs and high electricity costs could be addressed by leveraging rural electric infrastructure programs such as those offered by the USDA[106]. Policymakers should continue to support and expand such programs with a priority of supporting clean irrigation in areas with low electric pump shares. Within these efforts, USDA officials could identify and encourage farmers of irrigation-intensive crops to apply for electric infrastructure and distributed generation loans which would enable their fields to use electric pumps powered by low-cost renewable resources.

Considering less-mature emissions reduction measures, this study's results show how stakeholders can reduce emissions associated with heavy machinery. While the baseline GHG reduction potential of BEV machinery is greater than RD usage (see **Figure 20C** and **19D**),), a more optimistic transition case for RD would achieve greater near-term reductions than an optimistic BEV case (see **Figure 21**). To encourage such near-term decarbonization progress, policymakers could subsidize farmer purchases of RD for use in existing diesel equipment, especially in California where lettuce is widely produced and RD is available under state LCFS programs. However, policymakers should view these RD adoption measures as a bridge strategy with BEV adoption as the ultimate goal. Aside from competition for biofuel production capacity from other sectors like aviation and long-haul trucking, some agricultural uses will need to be prioritized for RD capacity. As discussed in **Appendix C Section C1.2.4**, the machinery used for specialty crops like lettuce will be more feasible to electrify than the larger machinery used for field crops. Thus, to achieve long-term emissions reductions while prioritizing limited biofuel capacity, stakeholders should support the electrification of heavy machinery in lettuce and other specialty crop systems. Policymakers should fund the accelerated development and production of electrified farm machinery while also providing support to farmers to purchase these machines and the necessary charging equipment. In the meantime, university Extension offices and partner producers could experiment with deploying smaller existing BEV machinery in innovative ways, such as Lagnelov et al.'s study of replacing one larger machine with two smaller autonomous tractors[107]. Through such investments and investigations, agricultural stakeholders could accelerate the decarbonization of farm machinery in lettuce and similar crops.

4.3.5 Limitations and Future Research

While this study provides insights into DLCA applications in the agricultural sector, some assumptions and scoping decisions have been made which limit the applicability of this research. One limitation is the assumption that all lettuce grown is harvested instead of incorporating decay rates. If decay were incorporated into the model, these losses in production could translate to higher impact estimates than those calculated in this study. Other assumptions in this study included leaving some static values, such as the energy efficiencies of pumps and the per-lettuce-mass demand for macronutrients. Further dynamic work could consider such static values. In the macronutrients example, evolving soil conditions and lettuce cultivars could change applied fertilizer needs, and thus higher or lower fertilizer usage could result in higher or lower life cycle emissions. Additionally, in setting the scope of dynamic work, this study considered a particular set of scenarios which limits its applicability. For example, policy changes to fund or defund emerging technology development could accelerate or decelerate adoption rates and thus accelerate or decelerate emissions reductions. Therefore, stakeholders who reference previous DLCA work must weigh the limitations of these previous assumptions in light of more recent developments. In addition to these temporal limitations, this study had a particular geographic focus on the United States. Future applications of these methods to other geographies would need to consider the projected evolution of local supply chains, the influence of local policies and regulations, and the trajectory of future weather patterns. Similarly, this study's methods could be applied to crops besides lettuce, but model parameters would need to be appropriately adjusted. Horticultural models would need to be developed in tools like AquaCrop to characterize growth and irrigation demand, which may behave drastically differently from lettuce; for example, unlike leafy greens, which benefit from warmer ambient temperatures in

this study, other crop types could suffer and lead to an increase in environmental impacts. Further, crop-specific inventories of energy, fertilizer, and other materials would need to be collected with each of the supply chains for these inputs considered for dynamic transformations. Future DLCA practitioners would benefit from a "hot spot" analysis of static LCA results for different crops, as this information could aid in prioritizing more rigorous dynamic modeling efforts.

Beyond these assumptions and scope limitations, this study examined a limited set of dynamic methods; future studies could iterate upon these methods to expand their utility. In the case of dynamic crop modeling, this study's yield estimates are based on average outcomes and do not account for probabilities of extreme events that may affect lettuce harvests, such as heat events above 32 ^{0}C causing bolting[108]. Future studies might implement more stochastic elements to understand the dynamic effects of climate risk and consider whether mitigation strategies (changing planting schedule, using heat-tolerant varieties, etc.) should be implemented in the model. Other opportunities for future study include more complex and updated models for upstream systems. For example, this study modeled soy renewable diesel due to its high growth in the current market, but future analyses could consider the effects of alternative feedstocks and imports. Similarly, as BEV applications in agriculture mature, more complex inventories could be created reflecting variations like new battery chemistries. Finally, future studies could incorporate prospective inventories for other emerging agricultural technologies. Modeling adoption of precision agriculture methods, for example, could decrease the amount of fuel and chemical inputs while decreasing on-farm air and water emissions[109]. By examining these opportunities for future research, LCA researchers could advance DLCA methods in agriculture while offering insights for greater eco-efficiency in food systems.

4.3 Conclusions

This study's results demonstrate how DLCA methods can have an impact on agricultural environmental impacts compared to a standard static LCA. Crop-and-location-specific methods like dynamic crop modeling, high-impact supply chain modeling, and sector-specific technology adoption projections can affect results more than a simple analysis with PLCI database values alone. DLCA practitioners and sector stakeholders should utilize scenario analysis to understand the opportunities available for eco-efficiency improvements over time. Combined with cost modeling, these analyses can help stakeholders identify near-term priorities, like electrifying irrigation and using RD in heavy machinery, while estimating possible timelines for future supply chain transformations, such as BEV heavy machinery and low-GHG N fertilizer. Through further utilization of the methods illustrated in this study, agricultural actors can plan and invest in a more sustainable food system in the decades to come.

CHAPTER 5: OVERALL CONCLUSIONS AND FUTURE RESEARCH

5.1 Overall Conclusions

The three phases of research within this dissertation have identified and addressed emerging agricultural system sustainability questions. In the first phase, LCA methods were used to compare local and centralized lettuce production impacts in the United States. By modeling building energy demand, crop growth, transportation, and electricity supply chains across hundreds of locations, this phase went beyond the site-specific studies typically found in the literature, providing food-energy-water nexus insights to a diverse array of community stakeholders. In the second phase, geographically-resolved LCA was applied to SAF feedstock corn production in southeast South Dakota and southwest Minnesota, scrutinizing how field-level input inventories and soil dynamics modeling, in comparison to national heuristics, could inform carbon intensity reduction efforts. Reflecting different practices in energy usage, agrichemical usage, and soil conservation, these resources were found to be less carbon-intensive than the default model would predict. While limitations related to funding interruptions and data collection emphasized the need for continued work in this ongoing project, the results highlighted the importance of nitrogen efficiency and accurate SOC modeling as this region seeks to play a role in the emerging SAF market. In the third phase, DLCA was used to consider temporal resolution in agricultural system sustainability, leveraging and comparing advanced techniques to explore how emerging climate conditions, industries, and technologies will affect environmental outcomes. The work in this phase demonstrated that lettuce crop carbon intensity in coming decades will decrease relative to static assumptions. Because of these dynamics, agricultural LCA practitioners should consider impending ecospheric and technospheric changes

to provide better guidance to the sector. Further, the results of this research phase provided sustainability insights to agricultural stakeholders, demonstrating how investments in low-carbon electrification, fuels, and chemicals could be both environmentally and economically efficient. The cumulative result of these three research phases has been a novel exploration of the importance of advanced resolution in agricultural LCA and subsequent decisions. Through applying these methods, agricultural system stakeholders can be better equipped to navigate complexity and deliver a sustainably-farmed future.

5.2 Future Research on LCA of Local and Centralized Food Systems

The first research phase evaluated three different localized lettuce production systems in comparison to centralized conventional production. The energy and crop models developed in this study provide tools to perform geographically-resolved LCA in any location with available weather data to consider food, energy, water, and climate data. Though such insights are a valuable addition to the field, further work could expand the utility of the toolset. Notably, researchers seeking to continue this work could expand the LCI models and integrate more sustainability perspectives to obtain a broader perspective on food production sustainability.

While the tools developed allow for future application to different locations, more substantial changes to system design could be made to future iterations of this model. For example, the CEA facilities evaluated were intended as simple entry-level designs. Various more innovative designs exist to reduce HVAC and lighting demands; future researchers could adapt the EnergyPlus models to compare to the benchmarks provided in this study. Additionally, while the scenario analyses considered future clean energy usage at the CEA sites, the study did not include a full dynamic analysis across all production systems and inputs. Future research could apply the DLCI techniques discussed in Chapter 4 for a more complete understanding of impacts

in future scenarios; for example, the deployment of low-emission cultivation and transportation technologies in the conventional system could change the position of the break-even lines seen in **Figure 9**. Such enhancements to this study's LCI models would provide deeper insights into the food-energy-water nexus tradeoffs posed by local and centralized production.

Beyond improving the tools that model GHG and water impacts, future researchers could integrate more sustainability perspectives through environmental, economic, and social lenses. While climate change and water conservation are pressing issues, this analysis could benefit from considering tradeoffs posed by other relevant environmental impacts. For example, the enclosed nature of CEA could reduce the emission of agrichemicals like fertilizers and pesticides to local ecosystems; subsequent reduction of eutrophication and biodiversity loss could be important context for stakeholders. Additionally, techniques like life cycle costing and technoeconomic assessment would reflect economic sustainability. Considering the energy usage- and subsequent costs- of CEA, future researchers could provide local the stakeholders with context on local food affordability. Similarly, future researchers could evaluate social sustainability measures through methods like social LCA, reflecting the impact of local jobs, fresh food availability, and food system resilience for communities. With such additional life cycle insights, future researchers could provide a broader context for local food sustainability conversations.

5.3 Future Research on Geographic Variation of Ethanol Feedstock LCA

The second research phase evaluated SAF feedstock corn production in southeast South Dakota and southwest Minnesota. The study provided geographically-resolved results by considering local practices and incorporating soil carbon dynamic modeling which lower-resolution approaches do not capture. While the work performed so far provides valuable

insights, future work in this ongoing project and other research initiatives should build on this foundation to enhance modeling resolution and evaluate sustainability measures within the region's supply chain.

Limitations in this study's models stemming from funding interruption and scoping decisions should be addressed in future data gathering and LCA work. Primarily, the planned field-level Daycent modeling should be performed with as much detail as possible. The emissions reductions associated with soil conservation measures are a promising avenue for farm-gate carbon intensity reductions; however, the variations apparent in this study's county-level resolution indicate that location-by-location nuances will be essential to ensure reliable and useful SOC estimates. Further, data collection efforts should invest in accurately capturing nitrogen application and efficiency activity at the farm level. The upstream and on-field emissions associated with nitrogen application drives corn carbon intensity in the southeast SD and southwest MN region; understanding the presence and efficacy of efficiency measures in the area will be essential to rationalizing field-by-field variations in GWP outcomes.

Leveraging these soil modeling and data collection enhancements, future research can apply the model developed in this study to identify eco-efficiency and cost efficiency opportunities. Within the SOC models, different soil conservation measures could be simulated to evaluate their carbon sequestration potential in relation to other goals like cost. For example, users could simulate leaving more crop residue on the field, evaluating which fields could most benefit from this practice instead of using the stover for grazing, baling, and bedding. Similarly, the model could evaluate and simulate nitrogen efficiency measures. If fields which utilize technology like slow-release fertilizers offset higher initial investments through efficiency gains and end-product tax credit value, the practice can be encouraged and supported across the

participating farms. Finally, the model can be expanded to include environmental impacts beyond GWP. By considering eutrophication with the enhancement of Daycent nitrate leaching estimates and ecotoxicity related to agrichemical application, future research can broaden biofuel stakeholder perspectives to weigh co-benefits and tradeoffs in carbon intensity reduction efforts. Through these applications of this study's base model, future research can help the biofuel sector to meet the demands of an emerging market while remaining environmentally and economically sustainable.

5.4 Future Research on Dynamic LCA of Agricultural Systems

The third research phase examined U.S. lettuce cultivation systems utilizing DLCA methodology. Applying multiple methods to a crop system that had not previously been considered in a DLCA study, these results represent a significant contribution to the field; however, some limitations exist due to different assumptions and scoping decisions. Future research could build on this study's foundation by exploring these assumptions and expanding the scope of dynamic methods themselves.

In addressing various assumptions and scope limitations, future research could improve study and expand its findings to other crop systems. Notably, some values in the model which are static could prove to be dynamic due to technosphere and ecosphere changes. With more dynamic modeling, the energy efficiencies of motors may change with improving technology while fertilizer demand may change with evolving soil conditions and lettuce cultivars. Additionally, future research could expand dynamic considerations beyond the trios of technology change cases considered in this work. For example, funding support for emerging technologies could grow or shrink based on shifting policy developments. Continued efforts to reflect these changes in technology diffusion curves would provide updated insights to DLCA

practitioners. Finally, the scope decision of lettuce in the United States opens the opportunity to consider different crops in different geographies using this study's methods. Future research on different crop systems could develop horticultural models in AquaCrop and identify crop-specific inventories for energy, water, and fertilizers, while examining different global geographies would reflect different supply chains, policy environments, and climate trajectories. Improving these assumptions and limitations would provide further validation of this study while expanding the DLCA literature to reflect more of the global agricultural sector.

Future research could also iterate upon the three dynamic methods considered in this work. Within dynamic crop models, researchers could move beyond the averages considered in this study to incorporate the effects of extreme events, such as heat or flooding events. DLCA practitioners could leverage stochastic models to consider yield losses and their effects on attributional eco-efficiency results. Further, these modeling efforts could examine the need for and LCA effects of climate adaptation measures, providing more complex agricultural sustainability perspectives. Concerning background technology transformation, additional studies could expand upon modeled inputs to the lettuce production system. By considering upstream systems like non-soy biofuel feedstocks and emerging BEV battery chemistries, researchers would account for supply chain complexities while expanding the body of industrial sector DLCA work. Finally, future research could examine the foreground adoption of other emerging agricultural technologies. For example, the use of autonomous machinery, drones, and enhanced efficiency fertilizers could impact the energy demands, chemical usage, and direct emissions inventories of farm operations. Life cycle modeling of farms using these emerging technologies while modeling their adoption within the agricultural sector would characterize their environmental and economic implications in the present and future. Expanding on the

methods found in this study represents a large opportunity for agricultural DLCA research that will help practitioners, farmers, and policymakers understand the evolving technological landscape while identifying opportunities for more sustainable production.

REFERENCES

(1) Climate Change 2022 - Mitigation of Climate Change: Working Group III Contribution to the Sixth Assessment Report of the Intergovernmental Panel on Climate Change, 1st ed.; IPCC, Ed.; Cambridge University Press, 2023. https://doi.org/10.1017/9781009157926.

(2) IPCC. Climate Change 2022 – Impacts, Adaptation and Vulnerability: Working Group II Contribution to the Sixth Assessment Report of the Intergovernmental Panel on Climate Change, 1st ed.; Cambridge University Press, 2023. https://doi.org/10.1017/9781009325844.

(3) ISO. ISO 14040: Environmental Management – Life Cycle Assessment – Principles and Framework, 2006.

(4) Matthews, H. S.; Hendrickson, C. T.; Matthews, D. Life Cycle Assessment: Quantitative Approaches for Decisions That Matter; Open access textbook: Carnegie Mellon University, 2014.

(5) Wernet, G.; Bauer, C.; Steubing, B.; Reinhard, J.; Moreno-Ruiz, E.; Weidema, B. The Ecoinvent Database Version 3 (Part I): Overview and Methodology. Int. J. Life Cycle Assess. 2016, 21 (9), 1218–1230. https://doi.org/10.1007/s11367-016-1087-8.

(6) Barreiros, T.; Ciroth, A.; Zipfel, E. IPCC 2021 AR6 Impact Assessment Method, 2022. https://nexus.openlca.org/database/openLCA%20LCIA%20methods (accessed 2023-02-16).

(7) Nabuurs, G.-J.; Hatab, A. A.; Bustamante, M.; Clark, H.; Havlík, P.; Ninan, K. N.; Popp, A.; Roe, S.; Aoki, L.; Angers, D.; Ravindranath, N. H.; Ayala-Niño, F.; Emmet-Booth, J. P. Agriculture, Forestry and Other Land Uses (AFOLU). In IPCC, 2022: Climate Change 2022: Mitigation of Climate Change. Contribution of Working Group III to the Sixth Assessment Report of the Intergovernmental Panel on Climate Change; Cambridge University Press: Cambridge, UK and New York, NY, US, 2022.

(8) Poore, J.; Nemecek, T. Reducing Food's Environmental Impacts through Producers and Consumers. Science 2018, 360 (6392), 987–992. https://doi.org/10.1126/science.aaq0216.

(9) Ritchie, H.; Rosado, P.; Roser, M. Environmental Impacts of Food Production. Our World Data 2022.

(10) Clark, M. A.; Domingo, N. G. G.; Colgan, K.; Thakrar, S. K.; Tilman, D.; Lynch, J.; Azevedo, I. L.; Hill, J. D. Global Food System Emissions Could Preclude Achieving the 1.5° and 2°C Climate Change Targets. Science 2020, 370 (6517), 705–708. https://doi.org/10.1126/science.aba7357.

(11) Milan Urban Food Policy Pact, 2015. https://www.milanurbanfoodpolicypact.org/.

(12) Gómez, C.; Currey, C. J.; Dickson, R. W.; Kim, H.-J.; Hernández, R.; Sabeh, N. C.; Raudales, R. E.; Brumfield, R. G.; Laury-Shaw, A.; Wilke, A. K.; Lopez, R. G.; Burnett, S. E. Controlled Environment Food Production for Urban Agriculture. HortScience 2019, 54 (9), 1448–1458. https://doi.org/10.21273/HORTSCI14073-19.

(13) Barbosa, G.; Gadelha, F.; Kublik, N.; Proctor, A.; Reichelm, L.; Weissinger, E.; Wohlleb, G.; Halden, R. Comparison of Land, Water, and Energy Requirements of Lettuce Grown Using Hydroponic vs. Conventional Agricultural Methods. Int. J. Environ. Res. Public. Health 2015, 12 (6), 6879–6891. https://doi.org/10.3390/ijerph120606879.

(14) Goldstein, B.; Hauschild, M.; Fernández, J.; Birkved, M. Testing the Environmental Performance of Urban Agriculture as a Food Supply in Northern Climates. J. Clean. Prod. 2016, 135, 984–994. https://doi.org/10.1016/j.jclepro.2016.07.004.

(15) Martin, M.; Molin, E. Environmental Assessment of an Urban Vertical Hydroponic Farming System in Sweden. Sustainability 2019, 11 (15), 4124. https://doi.org/10.3390/su11154124.
(16) Casey, L.; Freeman, B.; Francis, K.; Brychkova, G.; McKeown, P.; Spillane, C.; Bezrukov, A.; Zaworotko, M.; Styles, D. Comparative Environmental Footprints of Lettuce Supplied by Hydroponic Controlled-Environment Agriculture and Field-Based Supply Chains. J. Clean. Prod. 2022, 369, 133214. https://doi.org/10.1016/j.jclepro.2022.133214.
(17) USDA National Agricultural Statistics Service. Vegetables 2021 Summary; United States Department of Agriculture, 2022. https://release.nass.usda.gov/reports/vegean22.pdf (accessed 2023-01-10).
(18) Smith, R.; Cahn, M.; Daugovish, O.; Koike, S.; Natwick, E.; Smith, H.; Subbarao, K.; Takele, E.; Turini, T. Leaf Lettuce Production in California; University of California, Agriculture and Natural Resources, 2011. https://doi.org/10.3733/ucanr.7216.
(19) United States Department of Energy. EnergyPlus™ Version 9.5.0 Documentation, 2021. https://energyplus.net/ (accessed 2021-06-17).
(20) Zhang, Y.; Kacira, M. Comparison of Energy Use Efficiency of Greenhouse and Indoor Plant Factory System. Eur. J. Hortic. Sci. **2020**, 85 (5), 310–320. https://doi.org/10.17660/eJHS.2020/85.5.2.
(21) Rufí-Salís, M.; Petit-Boix, A.; Villalba, G.; Ercilla-Montserrat, M.; Sanjuan-Delmás, D.; Parada, F.; Arcas, V.; Muñoz-Liesa, J.; Gabarrell, X. Identifying Eco-Efficient Year-Round Crop Combinations for Rooftop Greenhouse Agriculture. Int. J. Life Cycle Assess. 2020, 25 (3), 564–576. https://doi.org/10.1007/s11367-019-01724-5.
(22) Kozai, T. Resource Use Efficiency of Closed Plant Production System with Artificial Light: Concept, Estimation and Application to Plant Factory. Proc. Jpn. Acad. Ser. B 2013, 89 (10), 447–461. https://doi.org/10.2183/pjab.89.447.
(23) Stranghellini, C.; van 't Ooster, B.; Heuvelink, E. Greenhouse Horticulture; Wageningen Academic Publishers: Wageningen, 2019.
(24) USDA National Agricultural Statistics Service. (Dataset) NASS - Quick Stats., 2017. https://quickstats.nass.usda.gov/ (accessed 2023-01-09).
(25) Plawecki, R.; Pirog, R.; Montri, A.; Hamm, M. W. Comparative Carbon Footprint Assessment of Winter Lettuce Production in Two Climatic Zones for Midwestern Market. Renew. Agric. Food Syst. 2014, 29 (4), 310–318. https://doi.org/10.1017/S1742170513000161.
(26) Venkat, K. Comparison of Twelve Organic and Conventional Farming Systems: A Life Cycle Greenhouse Gas Emissions Perspective. J. Sustain. Agric. 2012, 36 (6), 620–649. https://doi.org/10.1080/10440046.2012.672378.
(27) Vanuytrecht, E.; Raes, D.; Steduto, P.; Hsiao, T. C.; Fereres, E.; Heng, L. K.; Garcia Vila, M.; Mejias Moreno, P. AquaCrop: FAO's Crop Water Productivity and Yield Response Model. Environ. Model. Softw. 2014, 62, 351–360. https://doi.org/10.1016/j.envsoft.2014.08.005.
(28) Stoessel, F.; Juraske, R.; Pfister, S.; Hellweg, S. Life Cycle Inventory and Carbon and Water FoodPrint of Fruits and Vegetables: Application to a Swiss Retailer. Environ. Sci. Technol. 2012, 46 (6), 3253–3262. https://doi.org/10.1021/es2030577.
(29) Tourte, L.; Smith, R.; Murdock, J.; Sumner, D. A. Sample Costs to Produce and Harvest Romaine Hearts, 2019. https://coststudyfiles.ucdavis.edu/uploads/cs_public/7a/c9/7ac93a02-6ad3-439a-a74d-2bcf9e40180c/2019romainehearts-final-7-8-2019.pdf (accessed 2023-01-19).
(30) Morgan, B.; Broadfoot, C.; Holmes, D.; Mahe, L.; McDonald, M.; Thorogood, S.; Wohltman, S.; McDonald, S. Google Maps Services for Python, 2022. https://github.com/googlemaps/google-maps-services-python (accessed 2022-04-28).

(31) The Water Footprint Assessment Manual: Setting the Global Standard; Hoekstra, A. Y., Ed.; Earthscan: London; Washington, DC, 2011.
(32) Rodríguez, C.; di Noi, C.; Srocka, M.; Ciroth, A. openLCA LCIA Methods 2.1.3, 2017. https://nexus.openlca.org/database/openLCA%20LCIA%20methods (accessed 2023-02-28).
(33) Huijbregts, M.; Steinmann, Z.; Elshout, P.; Stam, G.; Verones, F.; Vieira, M.; Hollander, A.; Van Zelm, R. ReCiPe2016: A Harmonized Life Cycle Impact Assessment Method at Midpoint and Endpoint Level; 2016–0104; RIVM: Bilthoven, The Netherlands., 2016. https://www.rivm.nl/en/life-cycle-assessment-lca/downloads (accessed 2021-12-01).
(34) United States Environmental Protection Agency (EPA). Emissions & Generation Resource Integrated Database (eGRID), 2020.; Office of Atmospheric Protection, Clean Air Markets Division: Washington DC, 2022. https://www.epa.gov/egrid (accessed 2024-05-01).
(35) Lee, U.; Han, J.; Elgowainy, A.; Wang, M. Regional Water Consumption for Hydro and Thermal Electricity Generation in the United States. Appl. Energy 2018, 210, 661–672. https://doi.org/10.1016/j.apenergy.2017.05.025.
(36) ESRI. ArcGIS Pro, 2023. https://pro.arcgis.com/en/pro-app/latest/get-started/download-arcgis-pro.htm (accessed 2023-05-01).
(37) U.S. Census Bureau. 2018 Cartographic Boundary Files. United States Census Bureau. https://www.census.gov/geographies/mapping-files/time-series/geo/carto-boundary-file.html (accessed 2023-03-28).
(38) EnergyStar. ENERGY STAR Program Requirements Product Specification for Geothermal Heat Pumps Version 3.2, 2012. https://www.energystar.gov/products/geothermal_heat_pumps/partners (accessed 2023-01-24).
(39) National Renewable Energy Laboratory. Life Cycle Greenhouse Gas Emissions from Electricity Generation: Update, 2021. https://www.nrel.gov/docs/fy21osti/80580.pdf (accessed 2022-10-17).
(40) Körner, O.; Bisbis, M. B.; Baganz, G. F. M.; Baganz, D.; Staaks, G. B. O.; Monsees, H.; Goddek, S.; Keesman, K. J. Environmental Impact Assessment of Local Decoupled Multi-Loop Aquaponics in an Urban Context. J. Clean. Prod. 2021, 313, 127735. https://doi.org/10.1016/j.jclepro.2021.127735.
(41) IEA. Aviation; IEA: Paris, 2022. https://www.iea.org/reports/aviation.
(42) U.S. Department of Energy; U.S. Department of Transportation; U.S. Department of Agriculture; U.S. Environmental Protection Agency. SAF Grand Challenge Roadmap; 2022. https://www.energy.gov/sites/default/files/2022-09/beto-saf-gc-roadmap-report-sept-2022.pdf (accessed 2023-05-04).
(43) Office of Energy Efficiency and Renewable Energy. Sustainable Aviation Fuel Review of Technical Pathways, 2020. https://www.energy.gov/sites/default/files/2020/09/f78/beto-sust-aviation-fuel-sep-2020.pdf (accessed 2024-03-28).
(44) Wang, M.; Elgowainy, A.; Lee, U.; Baek, K.; Balchandani, S.; Benavides, P.; Burnham, A.; Cai, H.; Chen, P.; Gan, Y.; Gracida-Alvarez, U.; Hawkins, T.; Huang, T.-Y.; Iyer, R.; Kar, S.; Kelly, J.; Kim, T.; Kolodziej, C.; Lee, K.; Liu, X.; Lu, Z.; Masum, F.; Morales, M.; Ng, C.; Ou, L.; Poddar, T.; Reddi, K.; Shukla, S.; Singh, U.; Sun, L.; Sun, P.; Sykora, T.; Vyawahare, P.; Zhang, J. Greenhouse Gases, Regulated Emissions, and Energy Use in Technologies Model ® (2023 Excel), 2023. https://doi.org/10.11578/GREET-EXCEL-2023/DC.20230907.1.
(45) Yoo, E.; Lee, U.; Wang, M. Life-Cycle Greenhouse Gas Emissions of Sustainable Aviation Fuel through a Net-Zero Carbon Biofuel Plant Design. ACS Sustain. Chem. Eng. 2022, 10 (27), 8725–8732. https://doi.org/10.1021/acssuschemeng.2c00977.

(46) Office of Energy Efficiency and Renewable Energy. Guidelines To Determine Life Cycle Greenhouse Gas Emissions of Clean Transportation Fuel Production Pathways Using 45ZCF-GREET, 2025. https://www.energy.gov/eere/greet (accessed 2025-01-24).
(47) Pelton, R. Spatial Greenhouse Gas Emissions from US County Corn Production. Int. J. Life Cycle Assess. 2019, 24 (1), 12–25. https://doi.org/10.1007/s11367-018-1506-0.
(48) Scully, M. J.; Norris, G. A.; Alarcon Falconi, T. M.; MacIntosh, D. L. Carbon Intensity of Corn Ethanol in the United States: State of the Science. Environ. Res. Lett. 2021, 16 (4), 043001. https://doi.org/10.1088/1748-9326/abde08.
(49) Koch, P.; Salou, T.; Colomb, V.; Payen, S.; Perret, S.; Tailleu, A.; Willmann, S. AGRIBALYSE®: METHODOLOGY Version 1.3, 2016. https://nexus.openlca.org/database/Agribalyse (accessed 2025-01-27).
(50) IPCC. 2019 Refinement to the 2006 IPCC Guidelines for National Greenhouse Gas Inventories; Buendia, E. C., Tanabe, K., Kranjc, A., Jamsranjav, B., Fukuda, M., Ngarize, S., Osako, A., Pyrozhenko, Y., Shermanau, P., Federici, S., Eds.; IPCC: Switzerland, 2019.
(51) Hartman, M. D.; Parton, W. J.; Gurung, R.; Grosso, S. J. D.; Easter, M.; Hendryx, J.; Hilinski, T.; Kelly, R.; Keough, C. A.; Killian, K.; Lutz, S.; Marx, E.; McKeown, R.; Ogle, S.; Ojima, D. S.; Paustian, K.; Swan, A.; Thompson, V.; Williams, S. The Daily Century Ecosystem, Soil Organic Matter, Nutrient Cycling, Nitrogen Trace Gas, and Methane Model User Manual, Scientific Basis, and Technical Documentation, 2023.
(52) Liu, X.; Cai, H.; Kwon, H.; Wang, M. Feedstock Carbon Intensity Calculator (Fd-Cic): Users' Manual and Technical Documentation; ANL/ESD--21/12 Rev. 2, 2205308, 185916; 2023; p ANL/ESD--21/12 Rev. 2, 2205308, 185916. https://doi.org/10.2172/2205308.
(53) Smith, J. P.; Limb, B. J.; Beal, C. M.; Banta, K. R.; Field, J. L.; Simske, S. J.; Quinn, J. C. Evaluating the Sustainability of the 2017 US Biofuel Industry with an Integrated Techno-Economic Analysis and Life Cycle Assessment. J. Clean. Prod. 2023, 413, 137364. https://doi.org/10.1016/j.jclepro.2023.137364.
(54) Jordan Keltgen. Confirming Dry Blend Ingredients in Brookings Area, 2025.
(55) Carlson, G.; Clay, D.; Reese, C. L. Common Fertilizers Used in Corn Production, 2019. https://extension.sdstate.edu/sites/default/files/2019-09/S-0003-28-Corn.pdf (accessed 2024-01-28).
(56) South Dakota Department of Agriculture. Fertilizer Annual Report; Pierre, SD, 2023. https://danr.sd.gov/Agriculture/Inspection/FertilizerSoilAmendments/FertilizerProgram/default.aspx (accessed 2025-01-24).
(57) Liu, X.; Cai, H.; Kwon, H.; Wang, M. FEEDSTOCK CARBON INTENSITY CALCULATOR (FD-CIC) Model, 2023. https://greet.anl.gov/tool_fd_cic.
(58) Rosenburg, A.; Wallander, S. Adoption of Conservation Tillage Has Increased over the Past Two Decades on Acreage Planted to Major U.S. Cash Crops, 2022.
(59) Conservation Effects Assessment Project; United States Natural Resources Conservation Service. Reduction in Annual Fuel Use from Conservation Tillage; Natural Resources Conservation Service, U.S. Department of Agriculture: [Washington, D.C.], 2022. https://doi.org/10.32747/2022.8135356.nrcs.
(60) Ogle, S. M.; Adler, P. R.; Bentrup, G.; Derner, J.; Domke, G.; Grosso, S. D.; Lehmann, J.; Reba, M.; Woolf, D. Chapter 3: Quantifying Greenhouse Gas Sources and Sinks in Cropland and Grazing Land Systems. In Quantifying greenhouse gas fluxes in agriculture and forestry: Methods for entity-scale inventory; U.S. Department of Agriculture, Office of the Chief Economist.: Washington, DC, 2024.
(61) USDA NRCS; Colorado State University. COMET-Planner, 2024. https://comet-planner-domestic.uc.r.appspot.com/ (accessed 2025-02-07).

(62) EPA. Inventory of U.S. Greenhouse Gas Emissions and Sinks: 1990-2022. U.S. Environmental Protection Agency, EPA 430-R-24-004; 2024. https://www.epa.gov/ghgemissions/inventory-us-greenhouse-gas-emissions-and- sinks-1990-2022 (accessed 2025-03-03).
(63) Xu, H.; Lee, U.; Wang, M. Life-cycle Greenhouse Gas Emissions Reduction Potential for Corn Ethanol Refining in the USA. Biofuels Bioprod. Biorefining 2022, 16 (3), 671–681. https://doi.org/10.1002/bbb.2348.
(64) Hergert, G.; Ferguson, R.; Wortmann, C.; Shapiro, C.; Shaver, T. Enhanced Efficiency Fertilizers:, 2016. https://efotg.sc.egov.usda.gov/#/state/UT/search (accessed 2025-04-17).
(65) Crippa, M.; Solazzo, E.; Guizzardi, D.; Monforti-Ferrario, F.; Tubiello, F. N.; Leip, A. Food Systems Are Responsible for a Third of Global Anthropogenic GHG Emissions. Nat. Food 2021, 2 (3), 198–209. https://doi.org/10.1038/s43016-021-00225-9.
(66) Rosenzweig, C.; Mbow, C.; Barioni, L. G.; Benton, T. G.; Herrero, M.; Krishnapillai, M.; Liwenga, E. T.; Pradhan, P.; Rivera-Ferre, M. G.; Sapkota, T.; Tubiello, F. N.; Xu, Y.; Mencos Contreras, E.; Portugal-Pereira, J. Climate Change Responses Benefit from a Global Food System Approach. Nat. Food 2020, 1 (2), 94–97. https://doi.org/10.1038/s43016-020-0031-z.
(67) Van Der Giesen, C.; Cucurachi, S.; Guinée, J.; Kramer, G. J.; Tukker, A. A Critical View on the Current Application of LCA for New Technologies and Recommendations for Improved Practice. J. Clean. Prod. **2020**, 259, 120904. https://doi.org/10.1016/j.jclepro.2020.120904.
(68) Collinge, W. O.; Landis, A. E.; Jones, A. K.; Schaefer, L. A.; Bilec, M. M. Dynamic Life Cycle Assessment: Framework and Application to an Institutional Building. Int. J. Life Cycle Assess. 2013, 18 (3), 538–552. https://doi.org/10.1007/s11367-012-0528-2.
(69) Arvidsson, R.; Tillman, A.; Sandén, B. A.; Janssen, M.; Nordelöf, A.; Kushnir, D.; Molander, S. Environmental Assessment of Emerging Technologies: Recommendations for Prospective LCA. J. Ind. Ecol. 2018, 22 (6), 1286–1294. https://doi.org/10.1111/jiec.12690.
(70) Viveros Santos, I.; Renaud-Gentié, C.; Roux, P.; Levasseur, A.; Bulle, C.; Deschênes, L.; Boulay, A.-M. Prospective Life Cycle Assessment of Viticulture under Climate Change Scenarios, Application on Two Case Studies in France. Sci. Total Environ. 2023, 880, 163288. https://doi.org/10.1016/j.scitotenv.2023.163288.
(71) Lucas, K. R. G.; Caldarelli, C. E.; Ventura, M. U. Agriculture and Biodiversity Damage: A Prospective Evaluation of the Impact of Brazilian Agriculture on Its Ecoregions through Life Cycle Assessment Methodology. Sci. Total Environ. 2023, 899, 165762. https://doi.org/10.1016/j.scitotenv.2023.165762.
(72) Lebailly, F.; Levasseur, A.; Samson, R.; Deschênes, L. Development of a Dynamic LCA Approach for the Freshwater Ecotoxicity Impact of Metals and Application to a Case Study Regarding Zinc Fertilization. Int. J. Life Cycle Assess. 2014, 19 (10), 1745–1754. https://doi.org/10.1007/s11367-014-0779-1.
(73) Tsoy, N.; Prado, V.; Wypkema, A.; Quist, J.; Mourad, M. Anticipatory Life Cycle Assessment of Sol-Gel Derived Anti-Reflective Coating for Greenhouse Glass. J. Clean. Prod. 2019, 221, 365–376. https://doi.org/10.1016/j.jclepro.2019.02.246.
(74) Fargnoli, M.; Parrella, E.; Costantino, F.; Tronci, M. Hybrid Solutions for Agricultural Vehicles: A Comparative Life Cycle Analysis from the Users' Standpoint. J. Clean. Prod. **2024**, 485, 144406. https://doi.org/10.1016/j.jclepro.2024.144406.
(75) Sacchi, R.; Terlouw, T.; Siala, K.; Dirnaichner, A.; Bauer, C.; Cox, B.; Mutel, C.; Daioglou, V.; Luderer, G. PRospective EnvironMental Impact asSEment (Premise): A Streamlined Approach to Producing Databases for Prospective Life Cycle Assessment Using Integrated Assessment Models. Renew. Sustain. Energy Rev. 2022, 160, 112311. https://doi.org/10.1016/j.rser.2022.112311.

(76) Boyce, J.; Sacchi, R.; Goetheer, E.; Steubing, B. A Prospective Life Cycle Assessment of Global Ammonia Decarbonisation Scenarios. Heliyon 2024, 10 (6), e27547. https://doi.org/10.1016/j.heliyon.2024.e27547.
(77) Maynard, R.; Burkhardt, J.; Quinn, J. C. Sustainability of Lettuce Production: A Comparison of Local and Centralized Food Production. J. Clean. Prod. 2023, 428, 139224. https://doi.org/10.1016/j.jclepro.2023.139224.
(78) Fan, J.; Guo, D.; Han, L.; Liu, C.; Zhang, C.; Xie, J.; Niu, J.; Yin, L. Spatiotemporal Dynamics of Carbon Footprint of Main Crop Production in China. Int. J. Environ. Res. Public. Health 2022, 19 (21), 13896. https://doi.org/10.3390/ijerph192113896.
(79) Dumitru, E. A.; Berevoianu, R. L.; Tudor, V. C.; Teodorescu, F.-R.; Stoica, D.; Giucă, A.; Ilie, D.; Sterie, C. M. Climate Change Impacts on Vegetable Crops: A Systematic Review. Agriculture **2023**, 13 (10), 1891. https://doi.org/10.3390/agriculture13101891.
(80) Nabera, A.; José Martín, A.; Istrate, R.; Pérez-Ramírez, J.; Guillén-Gosálbez, G. Integrating Climate Policies in the Sustainability Analysis of Green Chemicals. Green Chem. 2024, 26 (11), 6461–6469. https://doi.org/10.1039/D4GC00392F.
(81) Gagnon, P.; Cowiestoll, B.; Schwarz, M. Cambium 2022 Scenario Descriptions and Documentation; NREL/TP-6A40-84916, 1915250, MainId:85689; 2023; p NREL/TP-6A40-84916, 1915250, MainId:85689. https://doi.org/10.2172/1915250.
(82) Van Den Oever, A. E. M.; Costa, D.; Messagie, M. Prospective Life Cycle Assessment of Alternatively Fueled Heavy-Duty Trucks. Appl. Energy **2023**, 336, 120834. https://doi.org/10.1016/j.apenergy.2023.120834.
(83) Thonemann, N.; Schulte, A.; Maga, D. How to Conduct Prospective Life Cycle Assessment for Emerging Technologies? A Systematic Review and Methodological Guidance. Sustainability **2020**, 12 (3), 1192. https://doi.org/10.3390/su12031192.
(84) Lund, J.; Slosky, J.; Whitson, J.; McLane, R. Technology and Market Assessment of Zero-Emission Off-Road Equipment; CALSTART, 2022. https://calstart.org/off-road-assessment/ (accessed 2024-09-03).
(85) Foster, T.; Brozović, N.; Butler, A. P.; Neale, C. M. U.; Raes, D.; Steduto, P.; Fereres, E.; Hsiao, T. C. AquaCrop-OS: An Open Source Version of FAO's Crop Water Productivity Model. Agric. Water Manag. **2017**, 181, 18–22. https://doi.org/10.1016/j.agwat.2016.11.015.
(86) Maurer, E. P.; Brekke, L.; Pruitt, T.; Duffy, P. B. Fine-resolution Climate Projections Enhance Regional Climate Change Impact Studies. Eos Trans. Am. Geophys. Union 2007, 88 (47), 504–504. https://doi.org/10.1029/2007EO470006.
(87) Pierce, D. W.; Cayan, D. R.; Thrasher, B. L. Statistical Downscaling Using Localized Constructed Analogs (LOCA)*. J. Hydrometeorol. 2014, 15 (6), 2558–2585. https://doi.org/10.1175/JHM-D-14-0082.1.
(88) Vano, J.; Hamman, J.; Gutmann, E.; Wood, A.; Mizukami, N.; Clark, M.; Pierce, D. W.; Cayan, D. R.; Wobus, C.; Nowak, K.; Arnold, J. Comparing Downscaled LOCA and BCSD CMIP5 Climate and Hydrology Projections - Release of Downscaled LOCA CMIP5 Hydrology; 2020. https://gdo-dcp.ucllnl.org/downscaled_cmip_projections/techmemo/LOCA_BCSD_hydrology_tech_memo.pdf (accessed 2024-01-11).
(89) Thorp, K. R.; Brekel, J.; DeJonge, K. C. Version 1.2.0 — Pyfao56: FAO-56 Evapotranspiration in Python. SoftwareX 2023, 24, 101518. https://doi.org/10.1016/j.softx.2023.101518.
(90) IEA. Hydrogen; IEA: Paris, 2023. https://www.iea.org/reports/hydrogen-2156 (accessed 2024-02-12).

(91) Gerveni, M.; Irwin, S. Renewable Diesel Feedstock Trends over 2011-2022. farmdoc daily; Department of Agricultural and Consumer Economics, University of Illinois at Urbana-Champaign, 2023.
(92) Xu, H.; Ou, L.; Li, Y.; Hawkins, T. R.; Wang, M. Life Cycle Greenhouse Gas Emissions of Biodiesel and Renewable Diesel Production in the United States. Environ. Sci. Technol. 2022, 56 (12), 7512–7521. https://doi.org/10.1021/acs.est.2c00289.
(93) U.S. Energy Information Administration. Annual Energy Outlook 2023 Table 11. Petroleum and Other Liquids Supply and Disposition, 2023. https://www.eia.gov/outlooks/aeo/data/browser/#/?id=11-AEO2023&region=0-0&cases=ref2023&start=2021&end=2050&f=A&linechart=~~ref2023-d020623a.27-11-AEO2023~ref2023-d020623a.53-11-AEO2023&map=&ctype=linechart&sourcekey=0 (accessed 2024-08-07).
(94) U.S. Energy Information Administration. U.S. No 2 Diesel Adj Sales/Deliveries to Farm Consumers, 2022. https://www.eia.gov/dnav/pet/hist/LeafHandler.ashx?n=PET&s=K2DVAFNUS1&f=A (accessed 2024-08-07).
(95) Driscoll, A. W.; Conant, R. T.; Marston, L. T.; Choi, E.; Mueller, N. D. Greenhouse Gas Emissions from US Irrigation Pumping and Implications for Climate-Smart Irrigation Policy. Nat. Commun. 2024, 15 (1), 675. https://doi.org/10.1038/s41467-024-44920-0.
(96) Gray, A. Case IH's New All-Electric Farmall Tractor. Successful Farming. September 11, 2023. https://www.agriculture.com/case-ih-s-new-all-electric-farmall-tractor-7968311 (accessed 2024-08-05).
(97) John Deere & Company. 2023 Business Impact Report, 2023. https://about.deere.com/en-us/sustainability#download-reports (accessed 2024-07-30).
(98) Tourte, L.; Smith, R.; Murdock, J.; Goodrich, B. Sample Costs to Produce and Harvest Romaine Hearts Lettuce, 2023. https://coststudies.ucdavis.edu/current/commodities/lettuce (accessed 2024-08-27).
(99) Mai, T. T.; Jadun, P.; Logan, J. S.; McMillan, C. A.; Muratori, M.; Steinberg, D. C.; Vimmerstedt, L. J.; Haley, B.; Jones, R.; Nelson, B. Electrification Futures Study: Scenarios of Electric Technology Adoption and Power Consumption for the United States; NREL/TP--6A20-71500, 1459351; 2018; p NREL/TP--6A20-71500, 1459351. https://doi.org/10.2172/1459351.
(100) Gerveni, M.; Irwin, S. Overview of the U.S. Renewable Fuel Standard. farmdoc daily; Department of Agricultural and Consumer Economics, University of Illinois at Urbana-Champaign, 2023.
(101) Burnham, A.; Gohlke, D.; Rush, L.; Stephens, T.; Zhou, Y.; Delucchi, M.; Birky, A.; Hunter, C.; Lin, Z.; Ou, S.; Xie, F.; Proctor, C.; Wiryadinata, S.; Liu, N.; Boloor, M. Comprehensive Total Cost of Ownership Quantification for Vehicles with Different Size Classes and Powertrains; ANL/ESD-21/4, 1780970, 167399; 2021; p ANL/ESD-21/4, 1780970, 167399. https://doi.org/10.2172/1780970.
(102) Booz Allen Hamilton. Argo, 2021. https://boozallen.github.io/argo/ (accessed 2024-09-01).
(103) Scheelbeek, P. F. D.; Bird, F. A.; Tuomisto, H. L.; Green, R.; Harris, F. B.; Joy, E. J. M.; Chalabi, Z.; Allen, E.; Haines, A.; Dangour, A. D. Effect of Environmental Changes on Vegetable and Legume Yields and Nutritional Quality. Proc. Natl. Acad. Sci. 2018, 115 (26), 6804–6809. https://doi.org/10.1073/pnas.1800442115.
(104) Rezaei, E. E.; Webber, H.; Asseng, S.; Boote, K.; Durand, J. L.; Ewert, F.; Martre, P.; MacCarthy, D. S. Climate Change Impacts on Crop Yields. Nat. Rev. Earth Environ. 2023, 4 (12), 831–846. https://doi.org/10.1038/s43017-023-00491-0.

(105) Zhu, P.; Burney, J.; Chang, J.; Jin, Z.; Mueller, N. D.; Xin, Q.; Xu, J.; Yu, L.; Makowski, D.; Ciais, P. Warming Reduces Global Agricultural Production by Decreasing Cropping Frequency and Yields. Nat. Clim. Change 2022, 12 (11), 1016–1023. https://doi.org/10.1038/s41558-022-01492-5.
(106) USDA Rural Development. Electric Programs. USDA Rural Development. https://www.rd.usda.gov/programs-services/electric-programs (accessed 2025-03-26).
(107) Lagnelöv, O.; Larsson, G.; Larsolle, A.; Hansson, P.-A. Life Cycle Assessment of Autonomous Electric Field Tractors in Swedish Agriculture. Sustainability 2021, 13 (20), 11285. https://doi.org/10.3390/su132011285.
(108) Kerr, A.; Dialesandro, J.; Steenwerth, K.; Lopez-Brody, N.; Elias, E. Vulnerability of California Specialty Crops to Projected Mid-Century Temperature Changes. Clim. Change 2018, 148 (3), 419–436. https://doi.org/10.1007/s10584-017-2011-3.
(109) United States Government Accountability Office. Precision Agriculture : Benefits and Challenges for Technology Adoption and Use; United States Government Accountability Office Report to Congressional Committees TECHNOLOGY ASSESSMENT Precision Agriculture Benefits and Challenges for Technology Adoption and Use January 2024 GAO-24-105962; United States Government Accountability Office: Washington, DC, 2024. https://catalog.gpo.gov/F/?func=direct&doc_number=001255481&format=999 (accessed 2024-10-01).

APPENDIX A

A1. Materials and Methods LCIA Supplementary Information

A1.1 Controlled Environment Agriculture Simulation Overview

In this study, two different types of CEA facilities were modeled: an indoor plant factory model and a greenhouse model. To understand the impacts of CEA production stages, this study focused on energy usage along with operational material inputs. The production stage did not include capitol inputs such as construction, as previous CEA work has found that infrastructure inputs have little carbon impact compared to operational impacts[1,2]. Further validation of this assumption was performed and included in **Appendix A Section A2.1**. To simulate the energy usage of CEA facilities, the United States Department of Energy's EnergyPlus software v9.5.0 was utilized[3]. To allow for the execution of large numbers of site simulations, Dostal and Baumelt's MATLAB-based cosimulation tool[4] was combined with EnergyPlus. Further, the cosimulation tool allowed for the simulation of ventilation control based on relative humidity setpoints in greenhouses, a functionality which EnergyPlus v9.5.0 does not have. With some of the model design considerations, the two CEA systems shared design parameters, such as HVAC setpoints, the model of the lettuce, and the hydroponic system.

For the cultivation environment setpoints, a recent review of CEA energy efficiency was utilized[5]. The dry bulb temperature was 25^0C in the day and 22^0C at night, and the relative humidity limit was 70%. Similar to Pennisi et al.'s work, a range of allowable temperature was included[6], in this case plus-or-minus 1^0C from the target. Additionally, photoperiods were 16 hours long for 30 days. To capture regional variation, 2005-2015 Typical Meteorological Year

(TMY) datasets accessed through the European Commission's PVGIS v5.2 tool were utilized for weather inputs[7], with some exceptions listed in **Table A1**.

***Table A1**. TMY stations where the climate data utilized in EnergyPlus models came from a manually adjusted nearby latitude-longitude pair. These TMY station latitude-longitude pairs elicited errors from the PVGIS database. On inspection, errors tended to correspond to pairs near bodies of water; if the PVGIS dataset designates a coordinate as in water, it does not have TMY data.*

TMY Station	TMY Latitude, Longitude	Adjusted Latitude, Longitude
722016	24.733, -81.050	24.726, -81.052
722315	30.050, -90.033	30.042, -90.028
724040	38.300, -76.417	38.292, -76.417
726480	45.750, -87.033	45.746, -87.062
722010	24.550, -81.750	24.555, -81.755
723096	34.700, -77.383	34.709, -77.440
725030	40.783, -73.883	40.777, -73.875
727934	47.483, -122.217	47.480, -122.204
727935	47.680, -122.250	47.680, -122.266
723085	36.950, -76.283	36.946, -76.283
724035	38.500, -77.300	38.521, -77.293

In addition to setpoints directly reflected in the EnergyPlus models, the LCA model included CO_2 injection to prevent growth inhibition, targeting 50 kg per photoperiod hour per ha of cultivated area[8]; different leakage rates between the models affected actual injection rates and are described in later sections for each CEA type. Through these environmental targets, the CEA models reflected ideal growing conditions for the modeled lettuce.

In addition to HVAC system design considerations, the lettuce model reflected CEA cultivation practice. As an EnergyPlus input, the evapotranspiration of lettuce was considered. The lettuce was modeled at a density[9] of 48 head m^{-2}, and based on the heuristic provided by Aldrich and Bartok[10], 69% of the floor area was available for cultivation. From each of these plants, evapotranspiration was modeled based on Zhang & Kacira's value[11] of 43 mL $head^{-1}$ day^{-}

[1]. Using a heat of vaporization of 2439.3 J g^{-1} for water at 26^0C[12], this translated to 1.21 W $plant^{-1}$[1], reflecting a sensible heat sink and a latent heat source in EnergyPlus.

Beyond the EnergyPlus models, the lettuce impacted the LCA through its production and its hydroponic inputs, including water, pump energy, and fertilizers. For the production estimate, the average daily growth rate was derived from Rufí-Salís, et al.'s experiments[13] and then multiplied by a 30-day cycle for a fresh weight of 192 g $head^{-1}$. To sustain this growth, the system modeled a hydroponic nutrient film technique (NFT) setup, which is common for leaf vegetables[14]. Water consumption was based on evapotranspiration plus 10% accounting for solution tank flushing[14]. Average solution pump power was estimated from previous NFT hydroponic lettuce studies[14,15] as 0.175 W $head^{-1}$, corresponding to the 0.6 m height in Majid et al.'s experiment[15]. For the plant factory's two additional layers above this height, the factor was increased by a ratio of the new height divided by 0.6 m to estimate additional power needs from greater head and additional friction. These power factors were then multiplied by respective numbers of plants and assumed to run continuously to determine annual energy needs. Finally, fertilizer use was derived from Rufí-Salís, et al.'s experimental inventory[13]; these inputs are summarized in **Table A2**, along with the other CEA inputs.

Table A2. *Production stage input data per kg lettuce produced by CEA systems. Input values are the same for plant factory and greenhouse models unless specified otherwise.*

Process	Unit	Quantity	Note
Heat	MJ kg^{-1}	Plant Factory: 3.5 - 24.8 Greenhouse: 0 - 58.2	Range of observed values from EnergyPlus simulations.
Electricity	kWh kg^{-1}	Plant Factory: 7.2 – 9.9 Greenhouse: 2.9 - 13.0	Range of observed values from EnergyPlus simulations.
KPO_4H_2	kg kg^{-1}	1.6e-02	Derived from Rufi-Salis, et al.[13].
KNO_3	kg kg^{-1}	3.1e-02	Derived from Rufi-Salis, et al.[13].
K_2SO_4	kg kg^{-1}	3.5e-02	Derived from Rufi-Salis, et al.[13].
$Ca(NO_3)_2$	kg kg^{-1}	4.2e-02	Derived from Rufi-Salis, et al.[13].
$CaCl_2$	kg kg^{-1}	1.1e-02	Derived from Rufi-Salis, et al.[13].
$Mg(NO_3)_2$	kg kg^{-1}	2.5e-02	Derived from Rufi-Salis, et al.[13].
Irrigation Water	kg kg^{-1}	7.4	From Zhang & Kacira's average daily ET[11], plus 10% tank flushing factor[14].
Supplemental CO_2	kg kg^{-1}	Plant Factory: 0.30 Greenhouse: 0.66	Varies by air exchange with environment. Further detail in description of each CEA simulation type.

While the plant factory and greenhouse models shared these CEA design parameters, their models differed to reflect baseline "off-the-shelf" designs similar to previously-modeled examples in the literature[9] and widely-available resources like textbooks[8,10,16] and university extension publications. Each system is described in greater detail below.

A1.2 Plant Factory Production Model

In the first CEA model, the plant factory was designed as a converted warehouse space similar to Harbick and Albright's study[9]. Reference EnergyPlus building models from the U.S. DOE[17] were converted to 58.5 m x 29.3 m growing spaces with a ceiling height of 3.4 m, with insulation thickness varying by IECC region[18]. Within this space, three layers of plants were modeled at heights of 0.6, 1.0, and 1.4 m. Beyond the previously described CEA inputs, relevant design considerations for the plant factory included its HVAC system, lighting system, and CO_2 supplementation.

For the plant factory HVAC system, the model utilizes and expands the unitary HVAC system included in the reference models[17], representing a converted existing building. Heating was provided by natural gas furnaces with an efficiency of 0.8, while cooling was provided by packaged air conditioning units using direct expansion cooling coils with a Coefficient of Performance (COP) of 3.5. Meanwhile, dehumidification was modeled with an overcool-reheat setup with backup electric dehumidification reflecting units an operator might introduce to supplement the main system. These backup dehumidification units were modeled based on an energy factor of 3.7 L kWh^{-1} and performance curves evaluated by the National Renewable Energy Laboratory[19]. Concerning the cooling systems in this model, this study did not examine direct emissions of refrigerants, focusing instead on the energy impacts associated with HVAC systems. A sample calculation validating this assumption is included in **Appendix A Section A2.2**.

Within the plant factory model, LED lighting was modeled to cover each layer of cultivated area. The lighting targeted the 200 μmol m^{-2} s^{-1} PPFD used by Engler & Krarti[5] with an efficacy[20,21] of 2.7 μmol J^{-1}. Based on these values and a cultivation area of 3548 m^2, the

lighting capacity was 263 kW, with heat sourced to the room based on a visible fraction of 0.52 and a thermal fraction of 0.48[20]. As in Graamans, et al.'s work, the plant factory photoperiod was scheduled for natural nighttime, 18:00-10:00, to maximize heat transfer out of the building[20].

In addition to these HVAC and lighting considerations, the plant factory was modeled with a unique CO_2 supplementation input. As mentioned previously, a CO_2 supplementation target of 50 kg ha^{-1} h^{-1} was used. However, in exchanging the CO_2-enriched air with outdoor air, some modeled supplemental CO_2 was lost, requiring a higher injection rate to compensate. Considering the lower outdoor air exchange rate of plant factories[22], a loss of 12% was used for a total supply of 56.8 kg ha^{-1} h^{-1}.

A1.3 Greenhouse Production Model

While sharing some CEA design inputs with the plant factory model, the greenhouse model differed significantly in other design aspects. The greenhouse design utilized a four peak, gutter-connected construction, similar to that considered by Harbick and Albright[9] from design principles described by Aldrich and Bartok[10]. The glazing modeled for this study was 16 mm clear polycarbonate based on an average of industry data sheet values[23,24]. The floor area was 58.5 m by 29.32 m, with a floor-to-gable height of 2.43 m and a gable-to-peak height of 1.83 m. In this space, a single layer of crops at 0.6 m was modeled. As in the plant factory model, the greenhouse model includes unique design considerations for the HVAC system, lighting system, and CO_2 supplementation.

HVAC systems were designed based on greenhouse textbook and Extension guidance. Forced air unit heaters are noted to be a common greenhouse heat source[25,26] with low capital costs[16]; thus, this study modelled natural gas unit heaters as a baseline technology. For cooling,

fan-and-pad evaporative coolers are common[8,16] and have a lower initial cost than fog coolers[16,27]. This study utilized direct evaporative coolers with draw through fan placement to simulate this baseline technology. Further, the model included an internal window shader, a passive cooling technique[16]. The shader was deployed at an internal temperature of 25^0C, and material properties used the medium reflectivity, medium transmission shade in the EnergyPlus dataset. Along with these greenhouse heating and cooling systems, dehumidification was simulated in two alternative models: ventilation and electric dehumidification. Ventilation of humid air, including winter ventilation where cold outside air is reheated, is a common, traditional method noted in greenhouse texts[8,16], Extension guidance[28,29], and other greenhouse simulation tools[21,30]. Thus, as a baseline technology, an exhaust fan ventilation system plus reheat was utilized. In humid climate simulations, however, this method was insufficient to control humidity; thus, another model was created using electric dehumidification units like the backup units deployed in the plant factory model. If the outside relative humidity was greater than 70%, then these electric dehumidifiers were used instead of ventilation. Results from these two models were then integrated into one based on climate; locations in the Building America Hot-Humid region[18] utilized the electric dehumidification system while all other regions utilized vent-reheat.

Within the greenhouse model, supplementary lighting was modeled using high pressure sodium (HPS) lamps which are common in the greenhouse sector[8,16]. Using the Daylighting function in EnergyPlus, the illuminance within the greenhouse was estimated. Using Stranghellini et al.'s conversion factors[8], sunlight illuminance was converted to PAR radiation. The model considered a daily light integral[31] of 18 mol m^{-2} day^{-1}, which in a 16-hour photoperiod equates to a PPFD of 312.5 μmol m^{-1} s^{-1}; if sunlight did not meet this value

(converted to 13875 lux for the Daylighting tool), then supplementary lights were turned on. The total capacity of the lighting system was 139 kW, based on Engler & Krarti's[5] review value of 200 μmol m^{-1} s^{-1}, an efficacy[9,21] of 1.7 μmol s^{-1}, and a total cultivated area of 1184 m^2. The heat source provided to the room from HPS lamps was modeled by taking an average efficacy[32] of 117.5 lumen W^{-1} and dividing[33] by 683 lumen W^{-1} to yield a visible fraction of 0.17 and a thermal fraction of 0.83.

As in the plant factory model, some supplementary CO_2 was assumed lost, requiring a higher injection rate. Considering the high infiltration rates typical of greenhouses[16], a CO_2 loss of 60% was assumed as an average of Kozai's estimate[22] of 50% for a closed greenhouse and Stranghellini et al.'s estimate[8] of 70% in a high ventilation greenhouse. Thus, the model estimated a supply of 125 kg ha^{-1} h^{-1}, which was also in line with Stranghellini et al.'s capacity guidance range[8].

A1.4 Conventional Production Model

As a comparison to local models, the conventional centralized production model reflected leaf lettuce production in California, which produced 83% of leaf lettuce in the United States in 2019-2021[34] and can produce lettuce year-round[35]. Average yield data used in the model were for state-level leaf lettuce data in USDA surveys[34] for years 2019, 2020, and 2021, leading to a value of 28245 kg ha^{-1}. Meanwhile, irrigation was based on typical California leaf lettuce depths of 18 inches for Central Coast sites and 36 inches for southern desert sites[35]. These two values were then weighted according to acreage for 2012 and 2017 by Agricultural district – 69% for Central Coast and 30% for Southern California- leading to a weighted average of 23.2 inches[34]. Further, irrigation was modeled as a mixture of technologies with 30% drip irrigation[35] and 70% sprinkler irrigation. Previous lettuce cultivation literature was also referenced for inputs like farm

machinery practice[36] and pesticide application[37]. Additionally, urea application field emissions included estimates of nitrous oxide[38] and carbon dioxide[39]. Inputs are summarized in **Table A3.**

Table A3*. Production stage input data per kg lettuce produced by California conventional soil system.*

Process	Unit	Quantity	Note
Planting	ha kg^{-1}	1.06e-04	Based on California Yields, NASS 2019-2021 data, 3 harvests per year.
Sprinkler Irrigation	m^3 kg^{-1}	0.15	Based on typical California irrigation depths[35] and NASS yield data. 70% for sprinkler irrigation.
Drip Irrigation	m^3 kg^{-1}	0.06	Based on typical California irrigation depths[35] and NASS yield data. 30% for drip irrigation[35].
Tilling	ha kg^{-1}	4.25e-04	Area from NASS yield data. 4 times each season[36].
Nitrogen fertilizer	kg kg^{-1}	1.01e-02	Per ha value from Smith et al.[35], weighted for regional production, converted to per mass using NASS yield data.
Phosphorous Fertilizer	kg kg^{-1}	4.6e-03	Per ha value from Smith et al.[35], weighted for regional production, converted to per mass using NASS yield data.
Potassium Fertilizer	kg kg^{-1}	4.78e-03	Per ha value from Smith et al.[35], converted to per mass using NASS yield data.
Fertilizer Application	ha kg^{-1}	1.06e-04	Area from NASS yield data.
Pesticide	kg kg^{-1}	1.40e-03	Per mass rate from Venkat[37], for iceberg lettuce but conventional and in California.
Pesticide Application	ha kg^{-1}	1.06e-04	Area from NASS yield data.
Field Emissions			
N_2O from fertilizer application	kg N_2O kg^{-1}	1.12e-04	IPCC Tier 1 Methods.
CO_2 from fertilizer application	kg CO_2 kg^{-1}	1.6e-02	IPCC Tier 1 Methods.

A1.5 Local Seasonal Farm Production Model

As an additional comparison, outdoor lettuce cultivation was simulated using the UN Food and Agriculture Organization's AquaCrop model[40] with the open source AquaCrop-OS[41]

tool to enable large-scale simulation of multiple sites. Across all locations, crop model inputs from previous AquaCrop studies[42–44] were utilized. One adjustment was made to these models: recognizing that previous studies were based in a greenhouse or in warm climates, the base temperature below which growth would not progress was changed to 4.4 ^{0}C, reflecting guidance on lettuce planting from multiple university Extensions, including Cornell University, Utah State University, Oregon State University, and North Carolina Cooperative Extension[45–48]. To represent large-scale food production, the life cycle model utilized the same inputs as described for the conventional case; thus, impact variations stemmed from yield and irrigation inputs affecting irrigation energy and the intensity of per-hectare activities. With this framework reflecting a baseline soil system, the model needed geographically resolved inputs to determine yield and irrigation.

Geographic variations in AquaCrop inputs included climate data, soil data, and planting dates. For daily weather data inputs, 15-year mean values (2006-2020) were calculated from the Daymet dataset[49] accessed with the daymetpy Python library[50]. Additionally, evapotranspiration values were used from USGS data[51]. For local soil variations, soil texture data were matched to each location using the North American Land Data Assimilation System dataset[52] with three exceptions noted in **Table A4**.

Table A4*. TMY stations where the soil texture was missing and manually set to "loam." In the NLDAS soil texture data, these locations on the Florida Keys returned no data. The nearest mainland locations (722026, 722029, 722020) were all loam or loam-mix texture; thus, the locations were assigned a loam texture.*

TMY Station	TMY Station Name	State	Soil Texture Assigned
722010	KEY WEST INTL ARPT	FL	Loam
722015	KEY WEST NAS	FL	Loam
722016	MARATHON AIRPORT	FL	Loam

Additionally, initial soil moisture at planting was set to the "Wilting Point" default to provide a consistent estimate of irrigation. Beyond climate and soil inputs, the model required simulation dates for planting. Lettuce is a cool weather crop, and cultivation at high temperatures risks "bolting," in which the leaves become bitter[46,48]. Thus, while the model could show growth above 30 ^{0}C, a corresponding real-world crop could be ruined for sale. To account for this limitation, in most locations the model was run for two periods, representing "spring" and "autumn" seasons, using frost data from the Midwestern Regional Climate Center[53]. Based on Extension guidance[46,48], spring plantings occurred on the median last spring date and autumn plantings occurred 80 days prior to the median first autumn date. In some colder climates with shorter growing seasons, only a single spring season could be simulated. In warmer climates without freeze dates, University of Arizona Cooperative Extension guidance for two successive winter crops in Yuma, Arizona was used[54], planting on September 15th for the first crop then planting the second crop the day after the harvest. While most locations thus were simulated and normalized for two harvests, California Central Coast locations were simulated for three successive crops to reflect year-round production, with the first planted on December 15th [35].

Through these geographic variations, yield and irrigation outputs were created and combined with the conventional inventory to make local seasonal inventories across the United States, shown in **Table A5**. For local soil cultivation, 924 locations were simulated, and their yields and irrigation demands were averaged across growing seasons. As in the CEA simulations, TMY location 726130 (Mount Washington, NH) was excluded since it failed to produce a crop. Furthermore, 40 locations with "Clay" soil texture were excluded from analysis. AquaCrop yields for clay locations averaged 1.59 tons ha^{-1}, much lower than non-clay locations at 7.98 tons ha^{-1}. These outputs reflected guidance that lettuce grows better in silt and sand soils, while clay

soils require additional effort to improve structure and drainage[35]. Thus, these locations were excluded from the local seasonal soil analysis, as they would not reflect real-world decisions and methods.

Table A5*. Production input data per kg of lettuce produced by local seasonal soil system. Ranges shown correspond to variations in AquaCrop yield and irrigation outputs; other inputs are the same values as in the California conventional system. Note that ranges shown are for all 924 simulated sites; as explained, some low-performing sites with poor soil conditions are excluded from the results analysis.*

Process	Unit	Quantity	Note
Planting	ha kg^{-1}	8.19e-05 – 2.67e-03	Varies by AquaCrop yield output.
Sprinkler irrigation	m^3 kg^{-1}	0.01 – 1.25	Varies by AquaCrop yield and irrigation outputs. Assumed 70% for sprinkler irrigation as in California conventional system.
Drip irrigation	m^3 kg^{-1}	0.01 – 0.54	Varies by AquaCrop yield and irrigation outputs. Assumed 30% for drip irrigation as in California conventional system.
Tilling	ha kg^{-1}	3.27e-04 – 1.07e-02	Varies by AquaCrop yield output. Assumed 4 times each season as in California conventional system.
Nitrogen fertilizer	kg kg^{-1}	1.01e-02	Same per mass demand as in California conventional system.
Phosphorous fertilizer	kg kg^{-1}	4.6e-03	Same per mass demand as in California conventional system.
Potassium fertilizer	kg kg^{-1}	4.78e-03	Same per mass demand as in California conventional system.
Fertilizer application	ha kg^{-1}	8.19e-05 – 2.67e-03	Varies by AquaCrop yield output.
Pesticide	kg kg^{-1}	1.40e-03	Same per mass demand as in California conventional system.
Pesticide application	ha kg^{-1}	8.19e-05 – 2.67e-03	Varies by AquaCrop yield output.
Field Emissions			
N_2O from fertilizer application	kg N_2O kg^{-1}	1.12e-04	IPCC Tier 1 Methods, as in California conventional system.
CO_2 from fertilizer application	kg CO_2 kg^{-1}	1.6e-02	IPCC Tier 1 Methods, as in California conventional system..

A1.6 Post-Harvest Processing and Packaging Model

For all systems, the same post-harvest processing and packaging was based on conventional lettuce information. At harvest, the model included cleaning with chlorinated water[55]. Next, packaging was modeled as loose leaves in an LDPE bag, packed at the same lettuce-weight-to-bag ratio as documented for Romaine lettuce[56] and a bag mass of based on packaging provider data[57]. Additionally, a carton for field packing was included[35]. Finally, post-harvest initial cooling was included[36]. With these considerations, an inventory for post-harvest processing is included in **Table A6.**

Table A6*. Post-harvest processing input data per kg of lettuce for all four production systems.*

Process	Unit	Quantity	Note
Washing Water	kg kg^{-1}	0.40	Stoessel et al.[58]
Washing Water Chlorination	kg kg^{-1}	4e-05	100 mg L^{-1} [55].
Initial cooling	MJ kg^{-1}	8.6e-02	Plawecki et al.[36]
Cardboard Packaging	kg kg^{-1}	7.1e-02	0.807 kg cardboard carton from Abejon et al.[59], 11.3 kg lettuce per carton from Tourte et al.[60]
LDPE Film Packaging	kg kg^{-1}	3.8e-03	Tourte et al.[56] The Webstaurant Store[57]

A1.7 Transportation Model

For the last unit process prior to delivery at the store, transportation was modeled as a large lorry with refrigeration. The transportation distance varied between the centralized and local systems. In the conventional system, transportation was modeled from San Joaquin, California, and route distance was calculated using Morgan et al.'s Google Maps API Python tool[61]. Some locations could not be accessed through the API; these were manually adjusted in

the Google Maps website[62] to nearby communities listed in **Table A7**. For the three local systems, transport distance was modeled as 10 km[1].

Table A7*. TMY stations where the location used for transportation distance was manually adjusted to a nearby community. On inspection, these stations were connected to military installations to which access is restricted.*

TMY Station	TMY Station Name	State	Manual Input for Nearby Point:	Distance [km]
723066	GOLDSBORO SEYMOUR JOHNSON AFB	NC	Goldsboro, NC	4405
723870	MERCURY DESERT ROCK AP [SURFRAD]	NV	Indian Springs, NV	732
723910	POINT MUGU NF	CA	NAS Pt. Mugu, CA	381
747320	HOLLOMAN AFB	NM	Alamogordo, NM	1696

A2. Validations of Assumptions and Models

A2.1 Infrastructure Impact Estimates

Estimates for construction carbon impacts were compared to operational emissions to validate not including infrastructure impacts. For greenhouses, the ecoinvent "market for greenhouse, glass walls and roof" was utilized[63]. The glass greenhouse was chosen over the plastic greenhouse as a more conservative estimate of carbon impact. Combining this inventory with total floor area and annual production, the impact was estimated at 0.054 kg CO_2e kg^{-1}. Comparing this impact to the range of electrical dehumidifier model GWP's, construction impacts would be 0.69% - 2.1% the magnitude of operational impacts. Similarly, for plant factories, the per-area embodied carbon estimates of Iancu and Moga for warehouses were averaged and divided by that study's 50-year lifespan[64]. Combined with the plant factory total floor area and annual production, the impact was estimated at 0.048 kg CO_2e kg^{-1}. Comparing this impact to the range of modeled plant factory GWP's, construction impacts would be 0.63% - 1.6% the magnitude of operational impacts.

A2.2 Refrigerant Leak Impact Calculation

Considering refrigerant impact for plant factory air conditioning, data from the UNEP Ozone Secretariat were utilized to conservatively estimate emissions[65]. Assuming two 200 kW packaged rooftop units with 100 kg charges and an annual leakage rate of 6%, 12 kg would be leaked per year. Using a GWP of 2088 for the common refrigerant R-410A, the global warming impact for the whole facility would be 25056 kg CO_2e. Using the modeled annual plant factory production of lettuce, the per-kg-lettuce impact would be 0.06 kg CO_2e kg^{-1}; for comparison, this amount is 0.8% - 2.1% of the modeled GWP range for baseline plant factories.

A2.3 System Model Validations

A2.3.1 Controlled Environment Agriculture Model Validation

As a validation of CEA model outputs, the energy and water footprints of the model were compared to recent CEA industry data. Horomia and Gordon-Smith's survey[66] found that respondents of 1000-5000 m^2 facilities reported an average energy footprint of 14.9 kwh kg^{-1}; this intensity is similar to the average footprint of 13.1 +/- 1.2 kWh kg^{-1} for plant factories and 13.3 +/- 3.3 kWh kg^{-1} for greenhouses in the similarly-sized model facilities in this study. Further, the energy footprints of this study aligned with the Cumulative Energy Demand of 16.2 kWh kg^{-1} of the ecoinvent data for lettuce in a heated greenhouse[58]. These validations indicated that this study's baseline models reflect real-world CEA energy usage, though some details within the industry data suggested additional considerations. Notably, there was some discrepancy in this study's results when compared to industry facility-type statistics. Horomia and Gorgon-Smith's[66] respondent greenhouse footprints were an average of 5.4 kWh kg^{-1}; this lower value may reflect larger scale, more efficient greenhouse facilities (>5000 m^2) in the survey sample or the location of greenhouse facilities in warmer climates. For example, the

greenhouse model with venting dehumidification in the Building America Hot-Dry climate zone was 9.8 +/- 2.1 kWh kg^{-1}. Another possibility was that survey respondents utilized alternatives to vent-reheat dehumidification control; in this study, the national energy intensity of greenhouses with electric dehumidification was on average 6.8 +/- 1.2 kWh kg^{-1}. Horomia and Gordon-Smith's vertical farm survey respondents averaged 38.8 kWh kg^{-1}, higher than the average in this study; the discrepancy likely reflected smaller scale vertical farms (<1000 m^2) like shipping container modules, which Horomia and Gordon-Smith noted had higher energy intensities[66].

Water footprint data also corroborated the model evapotranspiration inputs and evaporative cooling results. The simulated water footprint associated with evapotranspiration and tank flushing (7.4 L kg^{-1}) was within a range reported by 25% of Horomia and Gordon-Smith's respondents; adding an average greenhouse evaporative pad consumption of 9.7 L kg^{-1} placed this study's model near their median value of 20 L kg^{-1} product[66]. For lettuce specifically, Horomia and Gordon-Smith[66] compared respondents' consumption to field lettuce consumption, indicating 66% use 2.5 to 25 L kg^{-1}. Overall, while the industry survey data were not necessarily a one-to-one comparison with the modeled facilities and may have indicated some differences in practice, the proximity of industry averages to simulated results provided validation of this study's CEA models.

A2.3.2 Local Seasonal Soil Result Validation

The AquaCrop model was validated by comparing modeled California yield outputs to California NASS yields. Model outputs varied significantly across locations while NASS yield data were only available at a state level; therefore, a weighted average was created from local AquaCrop outputs based on real-world California lettuce acreage. The top 5 California counties by 2012 and 2017 leaf lettuce acreage[34] were selected, representing 96% of acreage. The

proportion of state acreage for each county was combined with the average AquaCrop yield for each county to create a weighted average of 26.0 tons ha^{-1} $year^{-1}$, which is comparable to yield data from all available survey[34] years in California, 2016-2021, averaging 26.0 +/- 4.3 tons ha^{-1}.

For water footprint validation, the local seasonal soil model results for California locations were compared to literature values for lettuce water consumption. As with the yield validation, the top 5 California counties were utilized to create a weighted average of 0.12 m^3 kg^{-1} for water consumption. Notably, this value differed from previous water estimates in the Southwestern United States of 0.205 m^3 kg^{-1} [37] and 0.250 m^3 kg^{-1} [14]. The lower value in this study likely reflected the assumption of 90% application efficiency in AquaCrop, which represented the upper range of efficiencies for sprinkler and drip systems[67]. As Smith et al. note[35], furrow irrigation is still prevalent in some areas of California, such as the southern desert. Considering Imperial County as an example southern desert county and using a furrow application efficiency of 73%[67], the AquaCrop simulation average of 0.16 m^3 kg^{-1} would then adjust to 0.20 m^3 kg^{-1}, similar to the Southwestern United States literature range. Thus, the water consumption modeled in this study was reasonable for the high-efficiency irrigation system considered.

A2.4 Comparison of LCA Results to literature

LCA GWP results were compared to existing literature values as additional verification of the four models, as shown in **Figure A1**. Plant factory results (**Figure A1A**) were compared to existing LCA's of hydroponic modules[1,68]. Notably, while this study falls in the range of observed values, the breadth of the literature range reflects the heavy influence that grid carbon intensity can have on plant factory GWP outcomes. Greenhouse results (**Figure A1B**) were

compared to the ecoinvent heated greenhouse lettuce value, based on a Swiss study[58] and to two literature values for heated greenhouses[1,69]. Note that technology assumptions can play a significant role in greenhouse outcomes; for example, Körner et al.'s low emissions may be connected to the assumption of biogas and co-generator exhaust heat[69], while Goldstein et al.'s soil-based greenhouse might rely on older technology and techniques that lead to its higher emissions[1]. Considering the climate-reliance of these greenhouses, variation between locations is expected, but proximity of the colder locations (New York and Chicago) to the Swiss global inventory offers further validation of the results. Conventional cultivation and transportation results (**Figure A1C**) also align with previous studies except for Los Angeles, whose proximity to California production makes its results more reflective of local cultivation. Finally, the local soil cultivation results (**Figure A1D**) appear more conservative than literature values. This discrepancy may reflect variations between a large-scale farm based on California farm practice compared to smaller scale farms, as in Goldstein et al.[1], or farms in other countries, as in Casey et al.[68]. Notably, Venkat's analysis[37] for California cultivation is fairly close to this study's results; the difference likely reflects Venkat's system boundary not including post-harvest activity like cooling and packaging. Accounting for this study's post-harvest activity adds 0.095 kg CO_2e kg^{-1}, which accounts for the discrepancy in results. Though variations in results are to be expected due to geographical variability in grids, climates, and agricultural practices, this study's GWP results prove reasonable when compared to the literature.

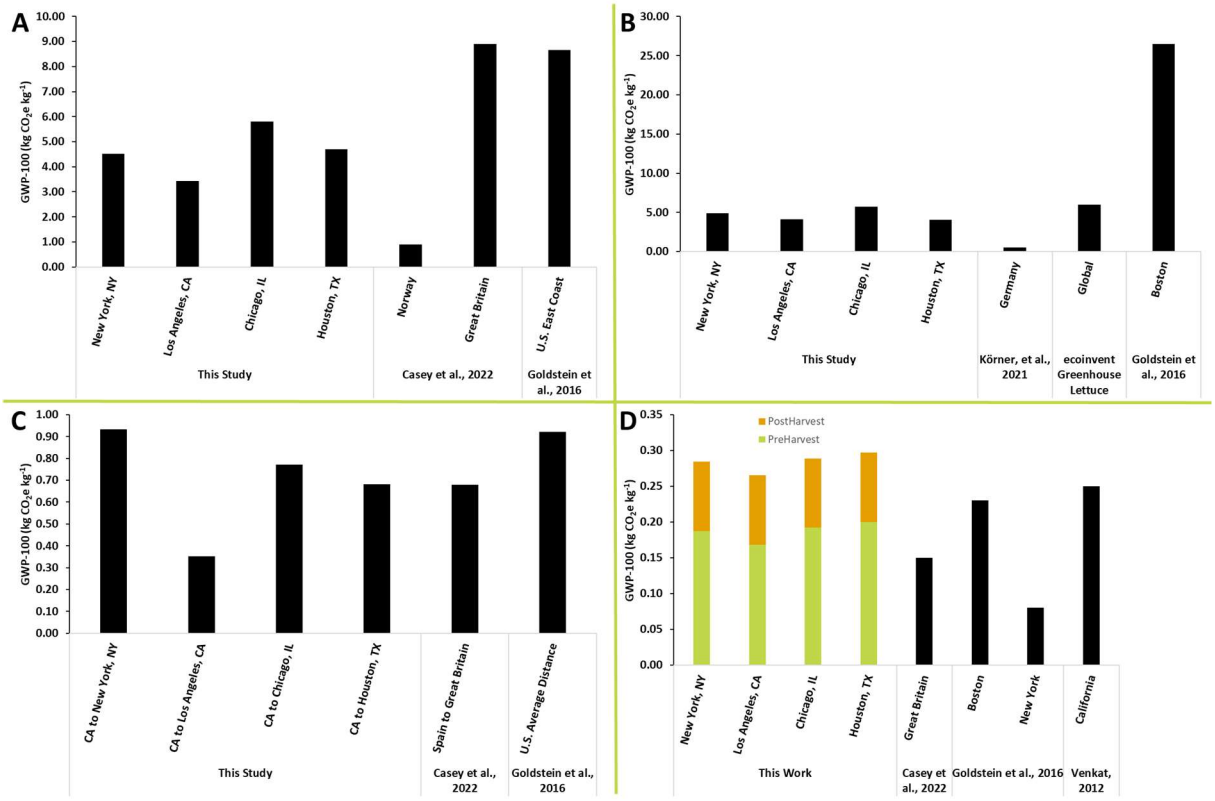

***Figure A1**. Comparison of this study's GWP-100 results to literature values for: **A.** plant factory facilities **B.** greenhouses **C.** conventional cultivation and transportation **D.** local soil cultivation.*

LCA water consumption results were also compared to existing literature values as additional verification of the four models, as shown in **Figure A2**. Plant factories and greenhouses in this study were compared in **Figure A2A** to reported hydroponic system values in ecoinvent, literature values[1,68] and industry survey data[66]. Notably, values fall within the range for those values that consider both direct and indirect water consumption (ecoinvent and Goldstein); additionally, Casey et al. reported a "water scarcity" value of 23 m^3 kg^{-1} in a British hydroponic module, but this value was excluded here as is it adjusted by a localized scarcity coefficient[68]. To account for regional variations in precipitation, this study's conventional cultivation and transportation water results were compared to other studies based in the Southwestern United States[14,37,68] shown in **Figure A2B**. This study aligns very well with two of the three studies, but Casey et al.'s study appears to be an outlier with the other literature values.

Finally, the local farm water consumption results were compared to a variety of literature values from Casey, et al.[68] and the ecoinvent dataset[58], shown in **Figure A2C**. The literature establishes a broad variability, for example between Switzerland[58] and the California desert[14]; the variation of irrigation demand with local seasonal precipitation patterns makes direct comparison of local systems difficult without direct comparisons at the same location. Thus, more localized validation where data are available (like that performed in **Appendix A Section A2.3.2**) proves more valuable in the case of this system. While there are variations, examining this study's results in the context of the literature validates the water footprint estimates.

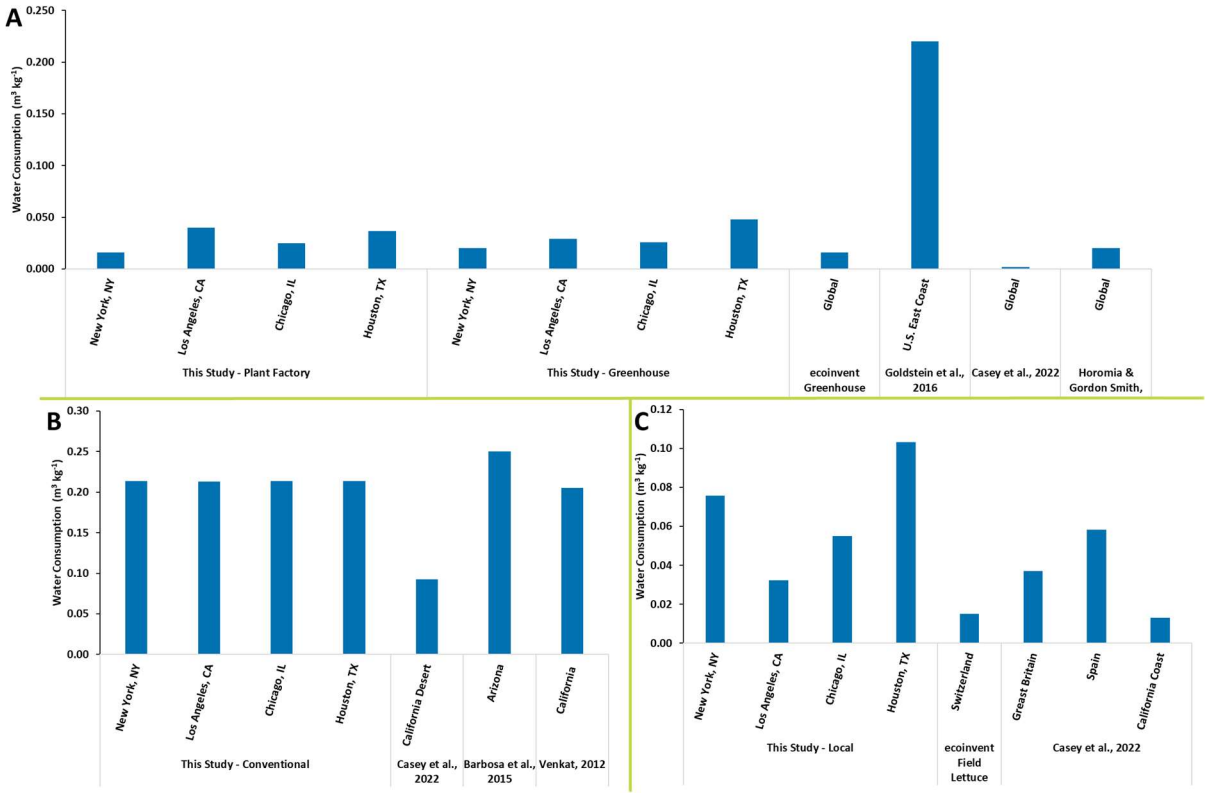

***Figure A2**. Comparison of this study's water consumption results to literature values for: **A.** indoor hydroponic facilities, note that values from Casey et al., and Horomia & Gordon-Smith are direct usage only (irrigation and evaporative cooling) **B.** conventional California cultivation and transportation **C.** local soil cultivation.*

A3. Ecoinvent 3.7.1 Processes

Table A8. *Ecoinvent processes and geographies used in this study.*

CEA Production	
MJ	heat production, natural gas, at industrial furnace low-NOx >100kW | heat, district or industrial, natural gas | Cutoff, S - ROW
kg	market for tap water | tap water | Cutoff, S - ROW
kg	market for carbon dioxide, liquid | carbon dioxide, liquid | Cutoff, S - ROW
kg	market for potassium nitrate, agricultural grade | potassium nitrate, agricultural grade | Cutoff, S - GLO
kg	market for potassium sulfate | potassium sulfate | Cutoff, S - ROW
kg	market for calcium nitrate | calcium nitrate | Cutoff, S - ROW
kg	market for calcium chloride | calcium chloride | Cutoff, S - ROW
kg	market for magnesium sulfate | magnesium sulfate | Cutoff, S - GLO
kg	market for inorganic phosphorus fertiliser, as P2O5 | inorganic phosphorus fertiliser, as P2O5 | Cutoff, S - US
kg	market for inorganic potassium fertiliser, as K2O | inorganic potassium fertiliser, as K2O | Cutoff, S - US
Soil Production	
ha	market for planting | planting | Cutoff, S - GLO
m3	irrigation, sprinkler | irrigation | Cutoff, S - US
m3	irrigation, drip | irrigation | Cutoff, S - US
ha	market for tillage, rotary cultivator | tillage, rotary cultivator | Cutoff, S - GLO
kg	market for urea | urea | Cutoff, S - RNA
kg	market for inorganic phosphorus fertiliser, as P2O5 | inorganic phosphorus fertiliser, as P2O5 | Cutoff, S - US
kg	market for potassium chloride | potassium chloride | Cutoff, S - RoW
ha	market for fertilising, by broadcaster | fertilising, by broadcaster | Cutoff, S - GLO
kg	market for pesticide, unspecified | pesticide, unspecified | Cutoff, S - GLO
ha	market for application of plant protection product, by field sprayer | Cutoff, S - GLO
Post Processing and Packaging	
kg	market for tap water | tap water | Cutoff, S - ROW
kg	market for chlorine, liquid | chlorine, liquid | Cutoff, S - ROW
MJ	cooling energy, from natural gas, at cogen unit with absorption chiller 100kW | cooling energy | Cutoff, S - ROW
kg	corrugated board box production | corrugated board box | Cutoff, S - ROW
kg	market for packaging film, low density polyethylene | packaging film, low density polyethylene | Cutoff, S - GLO
Transportation	
t km	market for transport, freight, lorry with reefer, cooling | transport, freight, lorry with reefer, cooling | Cutoff, S – GLO

A4. Additional Figures

Sensitivity Analyses Plots

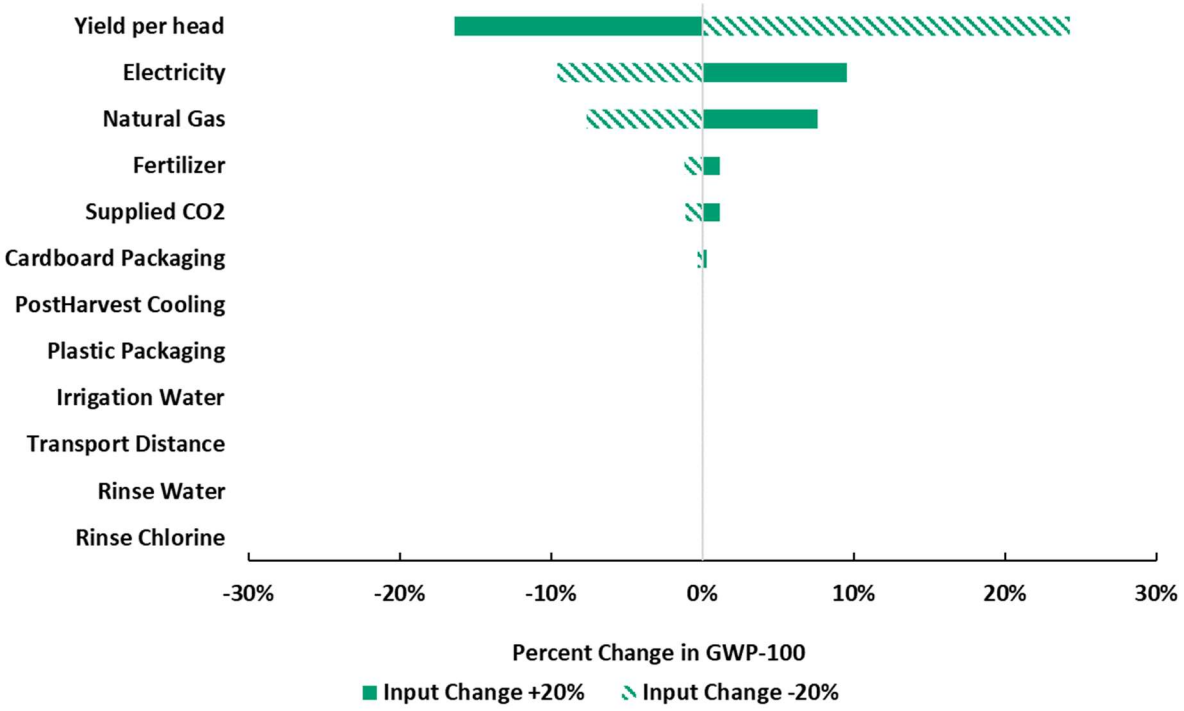

Figure A3. *Sensitivity of relevant inputs to the plant factory system. Note this figure shows results for New York City, NY; sensitivity results did not vary significantly among the four largest cities.*

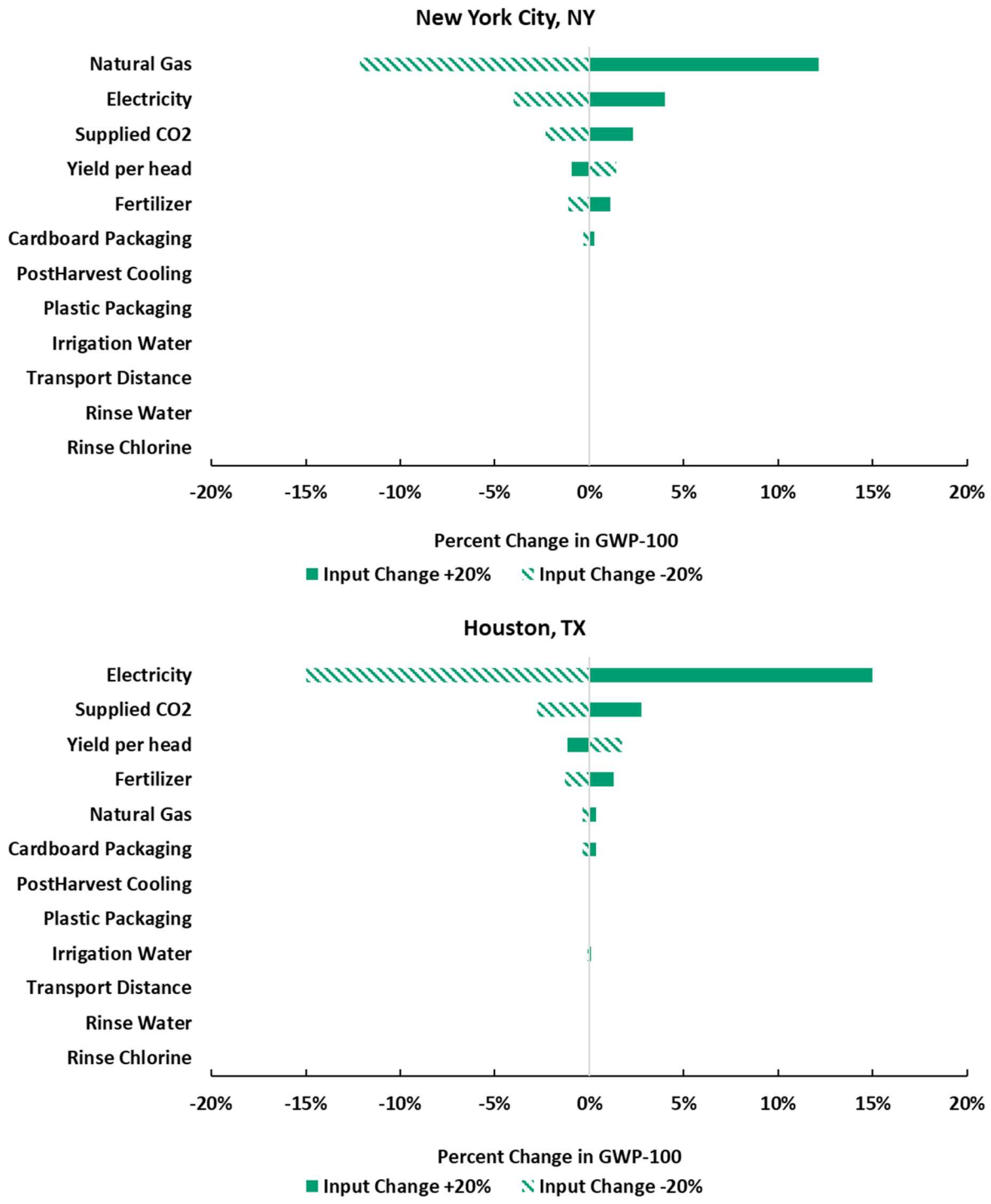

Figure A4. *Sensitivity of relevant inputs to the greenhouse system. Note that New York City, NY is representative of other sites (Los Angeles, CA and Chicago, IL) with vent/reheat dehumidification, while the electric dehumidification system in Houston differs.*

Figure A5. *Sensitivity of relevant inputs to the California production and transport system. Note that Los Angeles, CA and New York City, NY were selected to demonstrate the east-to-west trend of transportation impacts becoming more dominant in the model.*

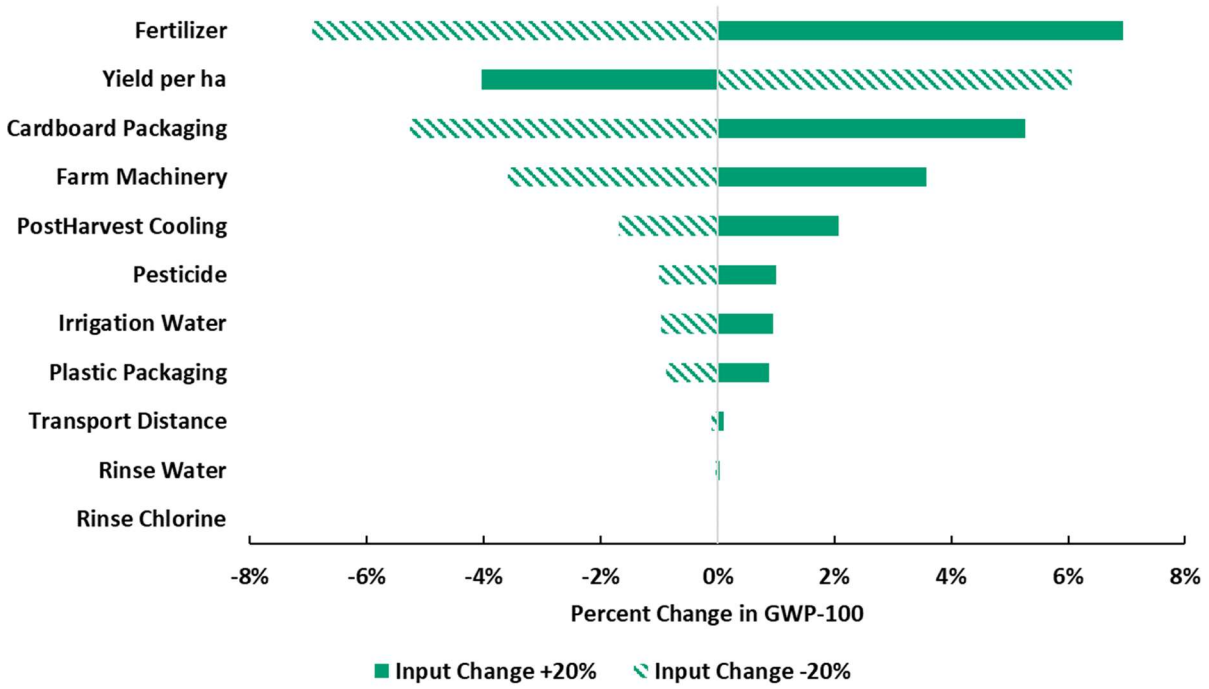

***Figure A6**. Sensitivity of relevant inputs to the local soil cultivation system. Note this figure shows results for New York City, NY; sensitivity results did not vary significantly among the four largest cities.*

Controlled Environment Agriculture Energy Demand Breakdown

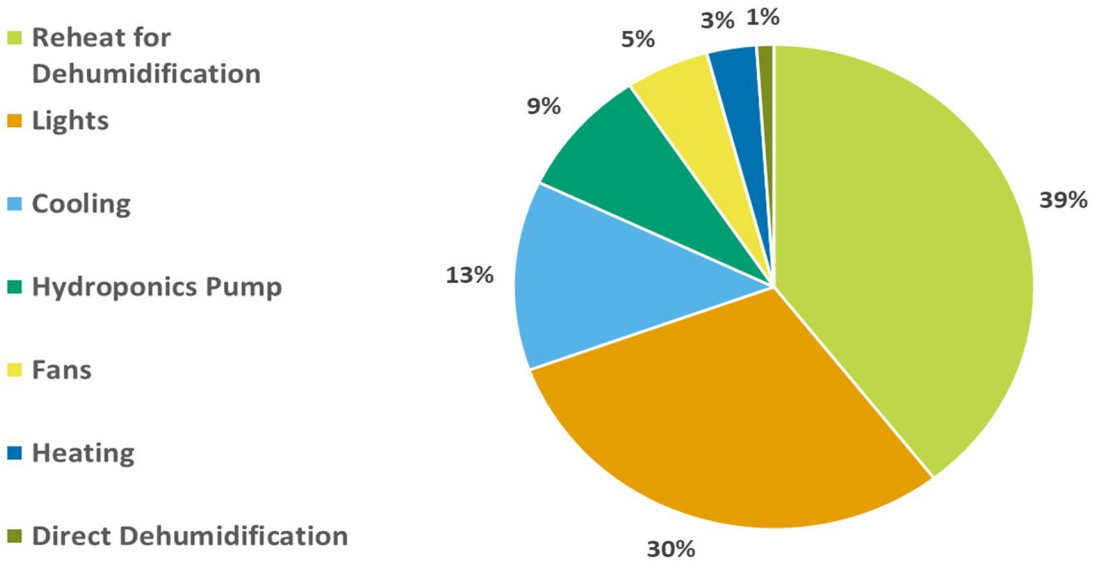

***Figure A7**. Contribution by category to the energy footprint of plant factory lettuce averaged across all simulated sites.*

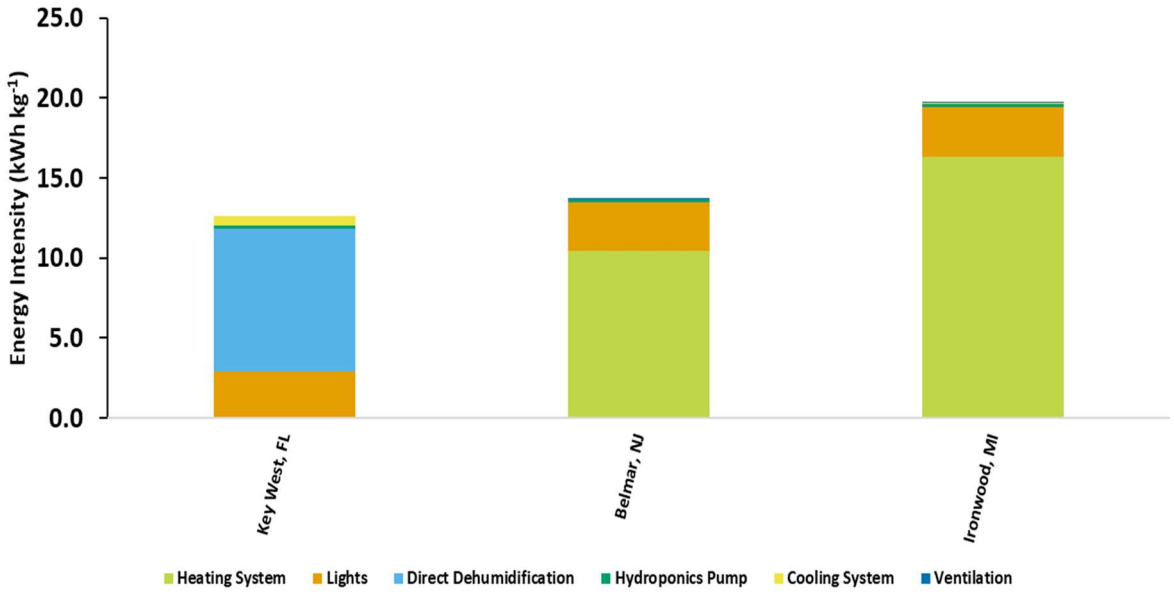

Figure A8*. Contribution by category to the energy footprint of greenhouse lettuce across selected sites, representing the minimum (Key West), median (Belmar), and maximum (Ironwood) natural gas usage to illustrate the geographic variation of heating demand and its effect on energy intensity. "Heating System" includes unit heater gas and fans. "Cooling System" includes evaporative pad pumps and fans.*

Individual System GWP Variations

All maps included in the main text are comparative maps, showing the ratio between a particular local production system and the conventional centralized system. While that format provides insights for local decision making, the effect of transportation distance from California can mask the regional variations within each production system. Thus, this section presents each system's GWP values for additional illustration of regional trends without the effects of transportation. For example, in **Figure A9**, the relatively low carbon intensity of the Californian grid is more apparent than in **Figure 4.** Water consumption maps are not included because transportation does not have a significant effect on water usage; thus, the regional trends would be the same as the comparative maps in the main text.

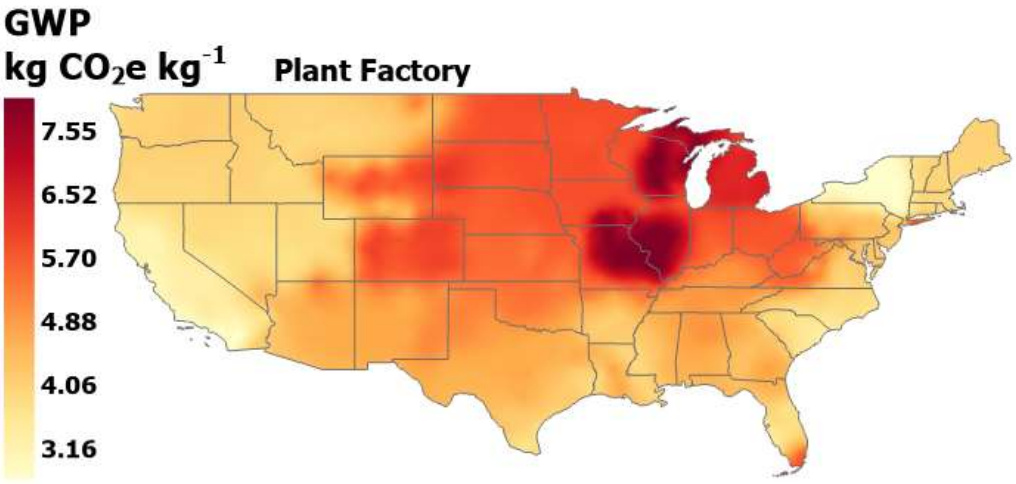

Figure A9. *GHG impacts per kg of lettuce from local plant factory systems. Note the patterns corresponding to NERC subregions, see EPA eGRID.*

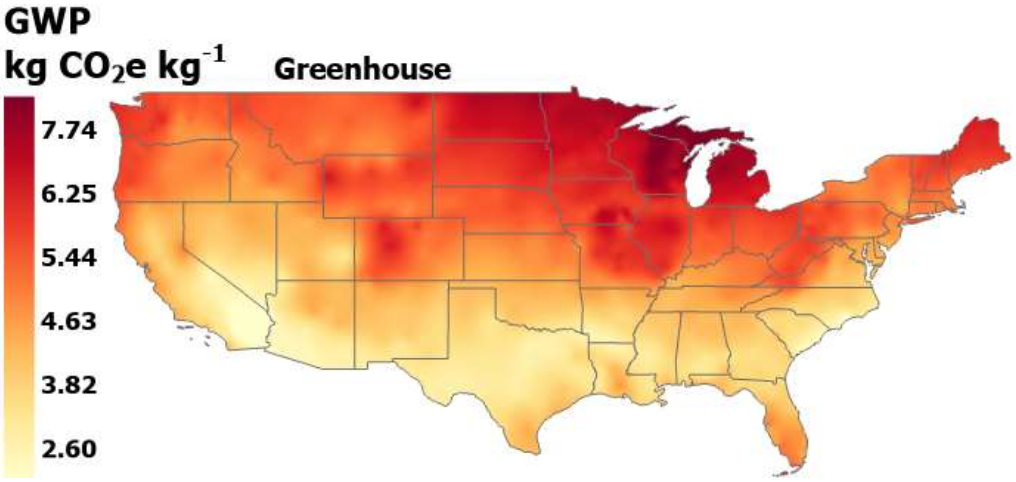

Figure A10*. GHG impacts per kg of lettuce from local greenhouse systems. Note how impact tends to increase with latitude, reflecting the effect of heating demand on emissions.*

***Figure A11**. GHG impacts per kg of lettuce from conventional production and shipping from California system.*

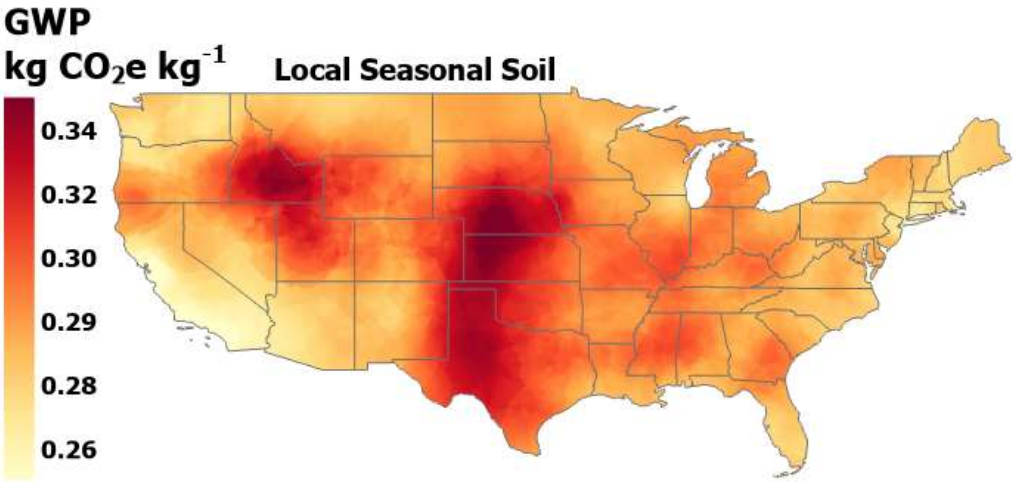

***Figure A12**. GHG impacts per kg of lettuce from local seasonal soil production system for 884 non-clay locations. Note that while results do not vary much with a standard deviation of 0.02 kg CO_2e kg^{-1}, what variation exists largely reflects water consumption per kg of lettuce and the energy required to provide that irrigation.*

Mixed Local Soil and Conventional Model Impacts Maps

Since the local soil model was seasonal in most locations, a mixture of local seasonal soil consumption and conventional soil impacts was created to reflect a consumer pattern of buying local when in-season. To estimate this mixed-model impact, a weighted average of impacts was created based on local yields, as shown in **Equation A1**:

***Equation A1**. Yield-weighted impact of a mixture of local seasonal production and conventional production.*

$$I_{Mix,i} = \frac{I_{C,i} * AY_{CA} + I_{LS,i} * AY_i}{AY_{CA} + AY_i}$$

Where I_{Mix} is the impact (greenhouse gas emitted or water consumed) per kilogram of a conventional and local soil lettuce mixture at location i while $I_{C,i}$ and $I_{L,i}$ are the impacts per kilogram for location i of the conventional and local soil systems, respectively. AY_{CA} and AY_i are the annual yields in tons per hectare of conventional California cultivation and the AquaCrop yield outputs for location i, respectively.

Across all locations, the lack of significant transport footprint from local production results in less lower impacts than for the conventional systems, as shown in **Figure A13**. The production impacts of local seasonal harvests are consistent, with some variation by average yield and irrigation (see **Figure A12).** In some locations, low local annual yields result in impacts closer to parity with the conventional system than other locations at a similar distance from California. For example, in the Northeast, two spots appear related to silty-clay soil texture in Burlington, Vermont and related to a single growing season in Berlin, New Hampshire. Thus, local conditions can play a significant role, but in general the principle of a local community garden or farm providing lower-carbon produce stands.

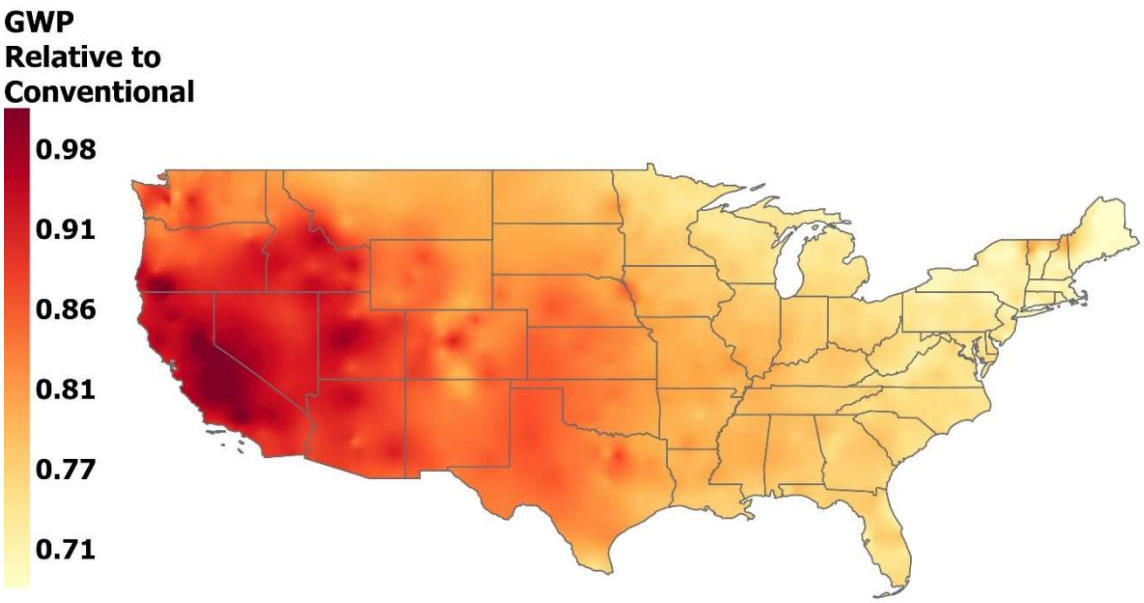

***Figure A13**. GHG emissions per kg of lettuce from a yield-weighted mix of local seasonal soil production and conventional production and transport, relative to conventional production and transport.*

In contrast to the clear GWP reductions, the water implications of local seasonal produce are more mixed. The water consumption of local seasonal production can be lower than conventional production; however, as shown in **Figure A14**, impact relative to conventional production can vary greatly. Climatic variations, such as precipitation during the simulated growing months, can result in higher or lower irrigation demand relative to the conditions in California. For example, the aridity of the Great Plains during the lettuce growing seasons is apparent in the high impacts stretching from West Texas to South Dakota. In contrast to the positive water tradeoff of CEA systems, stakeholders in some climates would need to weigh the community desire for local seasonal soil lettuce production against the high water demand it would pose to the community.

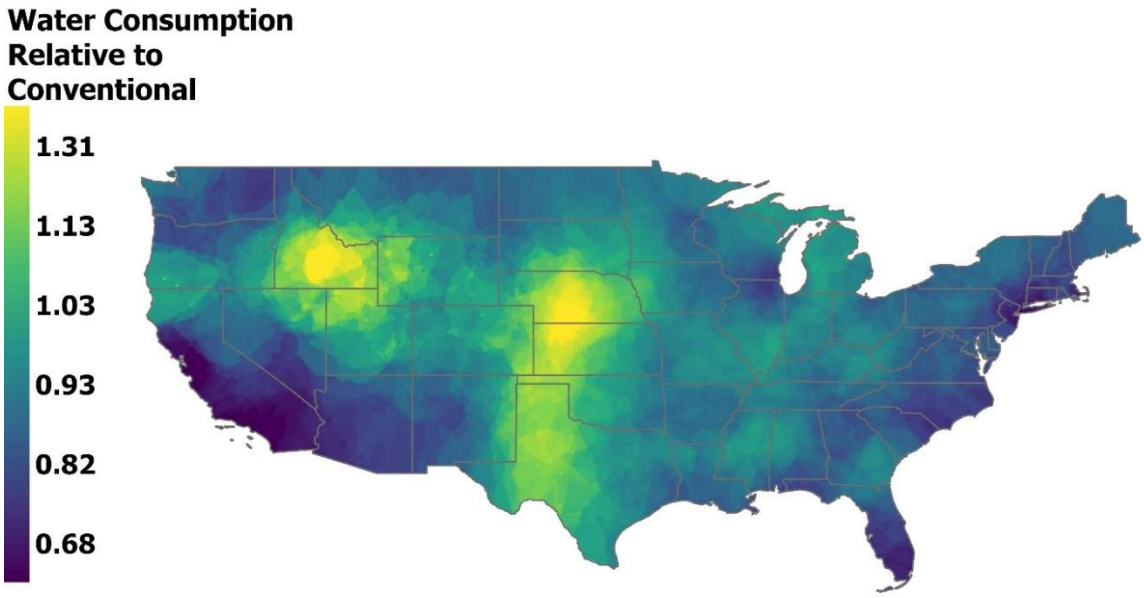

Figure A14*. Water consumption per kg of lettuce from a yield-weighted mix of local seasonal soil production and conventional production and transport, relative to conventional production and transport.*

Appendix A References

(1) Goldstein, B.; Hauschild, M.; Fernández, J.; Birkved, M. Testing the Environmental Performance of Urban Agriculture as a Food Supply in Northern Climates. *J. Clean. Prod.* **2016**, *135*, 984–994. https://doi.org/10.1016/j.jclepro.2016.07.004.

(2) Martin, M.; Molin, E. Environmental Assessment of an Urban Vertical Hydroponic Farming System in Sweden. *Sustainability* **2019**, *11* (15), 4124. https://doi.org/10.3390/su11154124.

(3) United States Department of Energy. EnergyPlus™ Version 9.5.0 Documentation, 2021. https://energyplus.net/ (accessed 2021-06-17).

(4) Dostal, J.; Baumelt, T. Model Predictive Control for Buildings with Active One-Pipe Hydronic Heating. *E3S Web Conf.* **2019**, *111*, 04050. https://doi.org/10.1051/e3sconf/201911104050.

(5) Engler, N.; Krarti, M. Review of Energy Efficiency in Controlled Environment Agriculture. *Renew. Sustain. Energy Rev.* **2021**, *141*, 110786. https://doi.org/10.1016/j.rser.2021.110786.

(6) Pennisi, G.; Sanyé-Mengual, E.; Orsini, F.; Crepaldi, A.; Nicola, S.; Ochoa, J.; Fernandez, J.; Gianquinto, G. Modelling Environmental Burdens of Indoor-Grown Vegetables and Herbs as Affected by Red and Blue LED Lighting. *Sustainability* **2019**, *11* (15), 4063. https://doi.org/10.3390/su11154063.

(7) European Commission PVGIS. [Dataset] PVGIS-NSDRB: 2005-2015, 2022. https://re.jrc.ec.europa.eu/pvg_tools/en/tools.html (accessed 2022-05-27).

(8) Stranghellini, C.; van 't Ooster, B.; Heuvelink, E. *Greenhouse Horticulture*; Wageningen Academic Publishers: Wageningen, 2019.

(9) Harbick, K.; Albright, L. D. Comparison of Energy Consumption: Greenhouses and Plant Factories. *Acta Hortic.* **2016**, No. 1134, 285–292. https://doi.org/10.17660/ActaHortic.2016.1134.38.

(10) Aldrich, R. A.; Bartok, J. W. *Greenhouse Engineering*; Northeast Regional Agricultural Engineering Service: Ithaca, NY, 1994.

(11) Zhang, Y.; Kacira, M. Comparison of Energy Use Efficiency of Greenhouse and Indoor Plant Factory System. *Eur. J. Hortic. Sci.* **2020**, *85* (5), 310–320. https://doi.org/10.17660/eJHS.2020/85.5.2.

(12) Engineering Toolbox. *Water - Heat of Vaporization vs. Temperature*. https://www.engineeringtoolbox.com/water-properties-d_1573.html (accessed 2022-10-19).

(13) Rufí-Salís, M.; Petit-Boix, A.; Villalba, G.; Ercilla-Montserrat, M.; Sanjuan-Delmás, D.; Parada, F.; Arcas, V.; Muñoz-Liesa, J.; Gabarrell, X. Identifying Eco-Efficient Year-Round Crop Combinations for Rooftop Greenhouse Agriculture. *Int. J. Life Cycle Assess.* **2020**, *25* (3), 564–576. https://doi.org/10.1007/s11367-019-01724-5.

(14) Barbosa, G.; Gadelha, F.; Kublik, N.; Proctor, A.; Reichelm, L.; Weissinger, E.; Wohlleb, G.; Halden, R. Comparison of Land, Water, and Energy Requirements of Lettuce Grown Using Hydroponic vs. Conventional Agricultural Methods. *Int. J. Environ. Res. Public. Health* **2015**, *12* (6), 6879–6891. https://doi.org/10.3390/ijerph120606879.

(15) Majid, M.; Khan, J. N.; Ahmad Shah, Q. M.; Masoodi, K. Z.; Afroza, B.; Parvaze, S. Evaluation of Hydroponic Systems for the Cultivation of Lettuce (Lactuca Sativa L., Var. Longifolia) and Comparison with Protected Soil-Based Cultivation. *Agric. Water Manag.* **2021**, *245*, 106572. https://doi.org/10.1016/j.agwat.2020.106572.

(16) Nelson, P. V. *Greenhouse Operation and Management*, 7th ed.; Prentice Hall: New York, 2011.

(17) Deru, M.; Field, K.; Studer, D.; Benne, K.; Griffith, B.; Torcellini, P.; Halverson, M.; Winiarski, D.; Liu, B.; Rosenberg, M.; Huang, J.; Yazdanian, M.; Crawley, D. U.S. Department of Energy Commercial Reference Building Models of the National Building Stock, 2010.

https://www.energy.gov/eere/buildings/commercial-reference-buildings (accessed 2021-12-01).
(18) Pacific Northwest National Laboratory. Building America and IECC Climate Zones by U.S. County Boundaries (Detailed), 2019. https://www.arcgis.com/home/item.html?id=8e5c3c6e1fa94e379553e199dcc4e777 (accessed 2022-01-06).
(19) Winkler, J.; Christensen, D.; Tomerlin, J. *Laboratory Test Report for Six ENERGY STAR® Dehumidifiers*; Technical Report 5500–52791; National Renewable Energy Laboratory: Golden, CO, 2011. https://doi.org/10.2172/1032386 (accessed 2021-12-01).
(20) Graamans, L.; Tenpierik, M.; van den Dobbelsteen, A.; Stanghellini, C. Plant Factories: Reducing Energy Demand at High Internal Heat Loads through Façade Design. *Appl. Energy* **2020**, *262*, 114544. https://doi.org/10.1016/j.apenergy.2020.114544.
(21) Katzin, D. Energy Saving by LED Lighting in Greenhouses : A Process-Based Modelling Approach, Wageningen University, 2021. https://doi.org/10.18174/544434.
(22) Kozai, T. Resource Use Efficiency of Closed Plant Production System with Artificial Light: Concept, Estimation and Application to Plant Factory. *Proc. Jpn. Acad. Ser. B* **2013**, *89* (10), 447–461. https://doi.org/10.2183/pjab.89.447.
(23) Plazit Polygal. Plazit-Polygal Double and Triple Layered Polycarbonate Sheets Product Datasheet, 2020. https://plazit-polygal.com/wp-content/uploads/filr/1449/DOUBLE%20AND%20TRIPLE%20LAYERED%20POLYCARBONATE%20EXTRUDED%20SHEETS_PRODUCT%20DATASHEET%20.pdf (accessed 2022-02-28).
(24) Sabic Innovative Plastics. Product Datasheet: WLMW Polycarbonate Sheet. http://www.polukarbonaat.ee/juhendid/docs/cerificate/WLMW_data_sheet.pdf.
(25) Pickens, J.; Wells, D. Controlling the Greenhouse Environment for Vegetable Crops, 2022. https://www.aces.edu/blog/topics/crop-production/controlling-the-greenhouse-environment-for-vegetable-crops/ (accessed 2023-01-25).
(26) Sanford, S. Greenhouse Unit Heaters— Types, Placement, & Efficiency, 2011. https://learningstore.extension.wisc.edu/products/greenhouse-unit-heaters-types-placement-and-efficiency-p135 (accessed 2023-01-25).
(27) Runkle, E. Evaporative Cooling, Part 1: Methods, 2022. https://www.canr.msu.edu/resources/evaporative-cooling-part-1 (accessed 2023-01-25).
(28) Bartok, J. *Reduce Greenhouse Humidity*. University of Connecticut College of Agriculture, Health, and Natural Resources. https://ipm.cahnr.uconn.edu/reduce-greenhouse-humidity/ (accessed 2023-01-24).
(29) Latimer, J. G. Dealing with the High Cost of Energy for Greenhouse Operations, 2018. https://www.pubs.ext.vt.edu/content/dam/pubs_ext_vt_edu/430/430-101/HORT-284.pdf (accessed 2023-01-24).
(30) Shelford, Ti.; Albright, L. D. Greenhouse Energy Model, 2019. https://cea.cals.cornell.edu/energy/greenhouse-energy-model-gem/.
(31) Nemali, K.; Langenhoven, P. Determining the Economic Value of Providing Supplemental Light to Lettuce During Winter Production, 2018. https://www.extension.purdue.edu/extmedia/HO/HO-283-W.pdf (accessed 2023-01-10).
(32) Engineering Toolbox. *Luminous Efficacy*. https://www.engineeringtoolbox.com/luminous-efficacy-d_1932.html (accessed 2022-10-19).
(33) Choudhury, A. K. R. Characteristics of Light Sources. In *Principles of Colour and Appearance Measurement*; Elsevier, 2014; pp 1–52. https://doi.org/10.1533/9780857099242.1.
(34) USDA National Agricultural Statistics Service. (Dataset) NASS - Quick Stats., 2017. https://quickstats.nass.usda.gov/ (accessed 2023-01-09).

(35) Smith, R.; Cahn, M.; Daugovish, O.; Koike, S.; Natwick, E.; Smith, H.; Subbarao, K.; Takele, E.; Turini, T. *Leaf Lettuce Production in California*; University of California, Agriculture and Natural Resources, 2011. https://doi.org/10.3733/ucanr.7216.
(36) Plawecki, R.; Pirog, R.; Montri, A.; Hamm, M. W. Comparative Carbon Footprint Assessment of Winter Lettuce Production in Two Climatic Zones for Midwestern Market. *Renew. Agric. Food Syst.* **2014**, *29* (4), 310–318. https://doi.org/10.1017/S1742170513000161.
(37) Venkat, K. Comparison of Twelve Organic and Conventional Farming Systems: A Life Cycle Greenhouse Gas Emissions Perspective. *J. Sustain. Agric.* **2012**, *36* (6), 620–649. https://doi.org/10.1080/10440046.2012.672378.
(38) IPCC. *2019 Refinement to the 2006 IPCC Guidelines for National Greenhouse Gas Inventories*; Buendia, E. C., Tanabe, K., Kranjc, A., Jamsranjav, B., Fukuda, M., Ngarize, S., Osako, A., Pyrozhenko, Y., Shermanau, P., Federici, S., Eds.; IPCC: Switzerland, 2019.
(39) IPCC. *2006 IPCC Guidelines for National Greenhouse Gas Inventories*; Eggleston, H. S., Buendi, L., Miwa, K., Ngara, T., Tanabe, K., Eds.; Institute for Global Environmental Strategies: Hayama, Japan, 2006.
(40) Vanuytrecht, E.; Raes, D.; Steduto, P.; Hsiao, T. C.; Fereres, E.; Heng, L. K.; Garcia Vila, M.; Mejias Moreno, P. AquaCrop: FAO's Crop Water Productivity and Yield Response Model. *Environ. Model. Softw.* **2014**, *62*, 351–360. https://doi.org/10.1016/j.envsoft.2014.08.005.
(41) Foster, T.; Brozović, N.; Butler, A. P.; Neale, C. M. U.; Raes, D.; Steduto, P.; Fereres, E.; Hsiao, T. C. AquaCrop-OS: An Open Source Version of FAO's Crop Water Productivity Model. *Agric. Water Manag.* **2017**, *181*, 18–22. https://doi.org/10.1016/j.agwat.2016.11.015.
(42) Amirouche, M. *Modeling of Nitrogen Use Efficiency in Lettuce Culture (Lactuca sativa): Isotopic Nitrogen (15 N) and AquaCrop | IntechOpen*. https://www.intechopen.com/chapters/73381 (accessed 2022-02-24).
(43) Ket, P.; Garre, S.; Oeurng, C.; Hok, L.; Degre, A. Simulation of Crop Growth and Water-Saving Irrigation Scenarios for Lettuce: A Monsoon-Climate Case Study in Kampong Chhnang, Cambodia. *Water* **2018**, *10* (5), 666. http://dx.doi.org/10.3390/w10050666.
(44) Sabzian, M.; Rahimikhoob, A.; Mashal, M.; Aliniaeifard, S.; Dehghani, T. Comparison of Water Productivity and Crop Performance in Hydroponic and Soil Cultivation Using AquaCrop Software. *Irrig. Drain.* **2021**, *70* (5), 1261–1272. https://doi.org/10.1002/ird.2600.
(45) Cornell University. *Growing Guide: Lettuce*. gardening.cornell.edu. http://www.gardening.cornell.edu/homegardening/scene9aa6.html (accessed 2022-10-20).
(46) Drost, D. Lettuce in the Garden, 2020.
(47) Oregon Vegetables. *Lettuce*. Oregon State University. https://horticulture.oregonstate.edu/oregon-vegetables/lettuce-0 (accessed 2022-10-20).
(48) Sanders, D. Horticulture Information Leaflets: Lettuce, 2019. https://content.ces.ncsu.edu/lettuce (accessed 2022-10-07).
(49) Thornton, M.M.; Shrestha, R.; Wei, Y.; Thornton, P.E.; Kao, S.; Wilson, B.E. Daymet: Daily Surface Weather Data on a 1-Km Grid for North America, Version 4. **2020**, 0 MB. https://doi.org/10.3334/ORNLDAAC/1840.
(50) Hufkens, K.; Talbert, C. Daymetpy: A Python Library for Accessing Daymet Surface Weather Data, 2018. https://github.com/bluegreen-labs/daymetpy (accessed 2022-07-06).
(51) Senay, G.; Kagone, S. Daily SSEBop Evapotranspiration Data from 2000 to 2018, 2019. https://doi.org/10.5066/P9L2YMV.
(52) North American Land Data Assimilation System. NLDAS Soils Datasets and Illustration [Dataset], 2022. https://ldas.gsfc.nasa.gov/nldas/soils (accessed 2022-05-18).
(53) Midwestern Regional Climate Center. Frost/Freeze Guidance: Climatology 1990-2020, 2021. https://mrcc.purdue.edu/VIP/indexFFG.html (accessed 2022-09-21).

(54) Bealmear, S. R.; Nolte, K. D. *Planting and Harvesting Calendar for Gardeners in Yuma County*; The University of Arizona Cooperative Extension, 2020; p 4. https://extension.arizona.edu/sites/extension.arizona.edu/files/pubs/az1615-2020.pdf (accessed 2023-05-17).
(55) Delaquis, P.; Fukumoto, L.; Toivonen, P.; Cliff, M. Implications of Wash Water Chlorination and Temperature for the Microbiological and Sensory of Fresh-Cut Iceberg Lettuce. *Postharvest Biol. Technol.* **2004**, *31*, 81–91. https://doi.org/10.1016/S0925-5214(03)00134-0.
(56) Tourte, L.; Smith, R.; Murdock, J.; Sumner, D. A. Sample Costs to Produce and Harvest Romaine Hearts, 2019. https://coststudyfiles.ucdavis.edu/uploads/cs_public/7a/c9/7ac93a02-6ad3-439a-a74d-2bcf9e40180c/2019romainehearts-final-7-8-2019.pdf (accessed 2023-01-19).
(57) The WebstaurantStore, Inc. *7" x 5" x 11" Low Density Polyethylene Lettuce Bag with Vent Holes - 1000/Case*. The WebStaurant Store. https://www.webstaurantstore.com/7-x-5-x-11-low-density-polyethylene-lettuce-bag-with-vent-holes-case/130VTD70511.html (accessed 2023-01-19).
(58) Stoessel, F.; Juraske, R.; Pfister, S.; Hellweg, S. Life Cycle Inventory and Carbon and Water FoodPrint of Fruits and Vegetables: Application to a Swiss Retailer. *Environ. Sci. Technol.* **2012**, *46* (6), 3253–3262. https://doi.org/10.1021/es2030577.
(59) Abejón, R.; Bala, A.; Vázquez-Rowe, I.; Aldaco, R.; Fullana-i-Palmer, P. When Plastic Packaging Should Be Preferred: Life Cycle Analysis of Packages for Fruit and Vegetable Distribution in the Spanish Peninsular Market. *Resour. Conserv. Recycl.* **2020**, *155*, 104666. https://doi.org/10.1016/j.resconrec.2019.104666.
(60) Tourte, L.; Smith, R.; Klonsky, K.; De Moura, R. Sample Costs to Produce Organic Leaf Lettuce, 2009. https://coststudyfiles.ucdavis.edu/uploads/cs_public/7d/96/7d96db67-49ca-442f-9543-4482187c9cd1/lettuceleaforganiccc09.pdf.
(61) Morgan, B.; Broadfoot, C.; Holmes, D.; Mahe, L.; McDonald, M.; Thorogood, S.; Wohltman, S.; McDonald, S. Google Maps Services for Python, 2022. https://github.com/googlemaps/google-maps-services-python (accessed 2022-04-28).
(62) Google. [Driving Directions from San Joaquin, California], n.d. https://www.google.com/maps (accessed 2021-08-05).
(63) Wernet, G.; Bauer, C.; Steubing, B.; Reinhard, J.; Moreno-Ruiz, E.; Weidema, B. The Ecoinvent Database Version 3 (Part I): Overview and Methodology. *Int. J. Life Cycle Assess.* **2016**, *21* (9), 1218–1230. https://doi.org/10.1007/s11367-016-1087-8.
(64) Iancu, I. E.; Moga, L. M. Life Cycle Analysis of Warehouse-Type Constructions. *CLIMA 2022 Conf.* **2022**, 2022: CLIMA 2022 The 14th REHVA HVAC World Congress. https://doi.org/10.34641/CLIMA.2022.329.
(65) UNEP Ozone Secretariat. Fact Sheet 9 - Large Air-Conditioning (Air-to-Air), 2015. https://ozone.unep.org/system/files/documents/FS%209%20Large%20air%20to%20air%20air-conditioning%20final.pdf (accessed 2023-01-31).
(66) Horomia, K.; Gordon-Smith, H. *2021 Global CEA Census Report*; WayBeyond Ltd and Agritecture LLC., 2021. https://www.waybeyond.io/census.
(67) Sandoval-Solis, S.; Orang, M.; Snyder, R. L.; Orloff, S.; Williams, K. E.; Rodriguez, J. M. *Spatial Analysis of Application Efficiencies in Irrigation for the State of California*; Water Management Research Group. University of California Davis.: Davis, CA., 2013. https://watermanagement.ucdavis.edu/research/application-efficiency/ (accessed 2023-05-15).
(68) Casey, L.; Freeman, B.; Francis, K.; Brychkova, G.; McKeown, P.; Spillane, C.; Bezrukov, A.; Zaworotko, M.; Styles, D. Comparative Environmental Footprints of Lettuce Supplied by

Hydroponic Controlled-Environment Agriculture and Field-Based Supply Chains. *J. Clean. Prod.* **2022**, *369*, 133214. https://doi.org/10.1016/j.jclepro.2022.133214.

(69) Körner, O.; Bisbis, M. B.; Baganz, G. F. M.; Baganz, D.; Staaks, G. B. O.; Monsees, H.; Goddek, S.; Keesman, K. J. Environmental Impact Assessment of Local Decoupled Multi-Loop Aquaponics in an Urban Context. *J. Clean. Prod.* **2021**, *313*, 127735. https://doi.org/10.1016/j.jclepro.2021.127735

APPENDIX B

B1. Fertilizer upstream LCA modeling

Within the 2023 harvest sample data, 22 unique fertilizers were identified, as summarized in **Table B1**. Depending on the fertilizer, different approaches were necessary to model upstream processes. First, seven fertilizers were found in the ecoinvent database and needed little additional modeling (see section **B1.1**). Additionally, eight fertilizers were determined to be blends of standard dry fertilizers (see section **B1.2**). Of the remaining fertilizers, two were unique compounds that required special modeling (see **B1.3**), two were compounds with a unique brand name provided (see **B1.4**), and three were NPK analysis values from which brands were assumed in order to source documentation (see **B1.5**). All models were constructed as processes in openLCA, using the appropriate ecoinvent flows to model upstream emissions in the production of one kg of fertilizer. Finally, some fertilizers were liquids reported in applied volumes; thus, densities were determined to translate these values into applied masses.

Table B1. *2023 harvest fertilizers with upstream modeling approach and density values for liquids. Citations are for sources of liquid fertilizer densities.*

Fertilizer name in data sample	Model Type	Density (if liquid)
Urea	ecoinvent standard	-
Urea Ammonium Nitrate Solution[1]	ecoinvent standard	11.1 lb. gal^{-1}
Monoammonium Phosphate 1	ecoinvent standard	-
Diammonium Phosphate 2	ecoinvent standard	-
Potash 60	ecoinvent standard	-
Ammonium Sulfate	ecoinvent standard	-
Ammonium Sulfate Sprayable (40%)[2]	ecoinvent standard	1.2 g cm^{-3}
180-65-45-12	Dry blend	-
100-40-10-20S	Dry blend	-
100/80/45-12S	Dry blend	-
115/90/60-15S	Dry blend	-
37.3-0-0-8.3	Dry blend	-
40.2-0-0-5.6	Dry blend	-
7.2-34.1-20.7-0	Dry blend	-
7.5-35.6-19-0	Dry blend	-
Ammonium Polyphosphate	Compound - special	-
Ammonium Thiosulfate 26[3]	Compound - special	11.1 lb. gal^{-1}
6-24-6 GoldStart[4]	Compound - brand	11.2 lb. gal^{-1}
XLR-RATE 7-23-5[5]	Compound - brand	11.1 lb. gal^{-1}
3-14-14 Starter[6]	Compound - assumed brand	1.3 SG
40-0-0	Compound - assumed brand	-
8-20-5-4S-0.5ZN[7]	Compound - assumed brand	11.01 lb. gal^{-1}

B1.1 Ecoinvent standard fertilizers

Among the standard fertilizers available in ecoinvent, two necessitated additional modeling considerations. Urea ammonium nitrate solution (UAN) can commonly have different NPK analysis values of 28-0-0 and 32-0-0[1]; in this study, a weighted average (42% and 58%, respectively) was created from the 2023 South Dakota state fertilizer report[8]. In addition, some

sites utilized a sprayable solution (40%) of ammonium sulfate (AS). Thus, a density of 1.2 g cm^{-3} was utilized from a corresponding safety data sheet[2].

B1.2 Blended fertilizers

Some fertilizers were reported not by mass percentage of NPK but by weights of each nutrient. Consulting with an agronomist with local expertise[9], it was determined that these indicated solid fertilizers that were blended at the farm, a common practice in South Dakota corn farming[10]. In this study, the ingredients were assumed to be monoammonium phosphate (MAP) to supply P, potassium chloride (KCl) to supply K, AS to supply S, and urea to supply any N not provided by MAP or AS. These ingredients were chosen because they are the most common for their respective nutrient in South Dakota[8], they are deemed common fertilizers by the local Extension office[10], and they are largely deemed compatible by Gilbertson & Vallin's solid fertilizer blending handbook[11]. These assumptions were further validated by an agronomist with local expertise[9]. Species mass balances were performed to determine the amount of each ingredient utilized with the results summarized in **Table B2**.

Table B2. *Ingredient summary of dry fertilizer blends utilized in the 2023 harvest sample.*

Given Blend Name		**Ingredient kg kg^{-1} blend**			
Provided Name	**Provided Unit**	**AS**	**KCl**	**MAP**	**Urea**
180-65-45-12	LBS	0.0849	0.1274	0.2124	0.5753
100-40-10-20S	LBS	0.2466	0.0493	0.2277	0.4764
100/80/45-12S	LBS	0.1145	0.1718	0.3524	0.3614
115/90/60-15S	LBS	0.1212	0.1939	0.3356	0.3492
7.2-34.1-20.7-0	LBS	0.0000	0.3447	0.6553	0.0000
7.5-35.6-19-0	LBS	0.0000	0.3163	0.6837	0.0000
37.3-0-0-8.3	LBS	0.3462	0.0000	0.0000	0.6538
40.2-0-0-5.6	LBS	0.2332	0.0000	0.0000	0.7668

B1.3 Special compound fertilizers

While other compound fertilizers in the 2023 harvest sample were derived from other fertilizers (i.e., labels and safety data sheets list ingredients like urea), two fertilizers were unique

chemicals (i.e., the only ingredient listed is the chemical itself). Thus, modeling these fertilizers – ammonium polyphosphate (APP) and ammonium thiosulfate (ATS) - required determining ingredients from chemistry and chemical engineering literature.

In the 2023 sample, APP was both applied as a solid fertilizer and used as an ingredient in other fertilizers. As a solid, APP has an NPK value of 15-60-0[12], and the chemical is typically synthesized from ammonia and phosphoric acid[13]. Thus, species balances were performed for N and P to determine inputs of 0.183 kg ammonia and 1.176 kg phosphoric acid to produce 1 kg of APP. Additionally, inputs for steam and electricity from the ecoinvent NPK fertilizer models[14] were used to approximate energy usage at the fertilizer production site.

Similarly to APP, ATS was both applied as a fertilizer in solution and used as an ingredient in other fertilizers. Solid ATS is typically formed by reacting ammonia, sulfur dioxide, and water to form ammonium sulfite, which is then reacted with sulfur[15], as shown in **Equation B1**:

Equation B1

$$2NH_3 + SO_2 + H_2O \rightarrow (NH_4)_2SO_3$$

$$(NH_4)_2SO_3 + S \rightarrow (NH_4)_2S_2O_3\ (ATS)$$

In solution, ATS can have NPK-S values of either 11-0-0-24 or 12-0-0-26[16]; given the farmer specified "Ammonium Thiosulfate 26," 12-0-0-26 was used in this study.

B1.4 Compound fertilizers with provided brand names

Two of the compound fertilizers in the 2023 harvest sample specified brand names: 6-24-6 GoldStart[4] and XLR-RATE 7-23-5[5]. The labels for these fertilizers included guaranteed

analyses that listed ammonia, urea, phosphoric acid, and potassium hydroxide as ingredients, including specifications for how much N came from ammonia and urea. Using these ingredients, material balances were performed for N, P, and K to determine the necessary amount of each ingredient to produce the fertilizers. Additionally, steam and electricity inputs from existing ecoinvent NPK fertilizer models[14] were included to approximate manufacturing energy demands.

B1.5 Compound fertilizers with assumed brands

Three fertilizers in the 2023 harvest sample were analysis values but did not provide a clear brand name. Thus, additional research was performed to identify fertilizers on the market that provide the same or similar nutrients per mass. Then, the ingredients listed in corresponding fertilizer labels and safety data sheets were used in species balances to provide the specified N, P, K, and S (see **Table B3**). In the case of the 3-14-14 Starter[6], "ammonium hydroxide" was represented as anhydrous ammonia and water, and the amount of N from ammonia and urea was averaged from similar liquid fertilizers[4,5]. Water was assumed to be deionized, and steam and electricity inputs from existing ecoinvent NPK fertilizer models[14] were included to approximate manufacturing energy demands.

Table B3. *Compound fertilizers with assumed brands found in the 2023 harvest sample.*

Fertilizer name in data sample	Assumed fertilizer – Manufacturer	Ingredients
3-14-14 Starter	3-14-14 w/sweetener – BlueStem Farm Supply	Ammonia (82% of N), urea (18% of N), phosphoric acid, potassium hydroxide, water
40-0-0	YaraVera Amidas 40-0-0 – Yara North America	Urea, ammonium sulfate
8-20-5-4S-0.5ZN	8-20-5-5S-.5Zn – MacroSource	APP, ATS, potassium chloride, water

B2. Soil dynamics modeling

B2.1 Fertilizer and crop residue nitrous oxide and carbon dioxide field emissions models

In order to reflect the different quantities of fertilizers applied to the 2023 harvest fields, Tier 1 GHG calculations were calculated on a site-by-site basis. Emissions considered included direct nitrous oxide emissions, indirect nitrous oxide emissions by volatilization and leaching, and carbon dioxide from urea applications. Where calculation factors varied by climate, the factors for "wet/mesic" climate were used to reflect the local geography.

Direct nitrous oxide emissions from nitrogen additions to the soil were calculated based on the USDA's adapted Tier 1 method[17]. Simplified for practices not included in this sample (e.g., nitrification inhibitors), **Equation B2** was used for synthetic fertilizers:

Equation B2

$$N_2O_{D,F} = \{[(F_{SN} * EF_{SN})] * [1 + S_{till}]\} * N_2O_{MW} * N_2O_{GWP}$$

Where:

- $N_2O_{D,F}$ is the direct N_2O soil emissions from fertilizer for the field (tons CO_2e)
- F_{SN} is the amount of synthetic fertilizer N applied (tons N)
- EF_{SN} is the emission factor for synthetic fertilizer N (tons N_2O-N tons^{-1} N)
- F_{CR} is the amount of N in crop residue left on the field (tons N)
- EF_{ON} is the emission factor for other nitrogen inputs (tons N_2O-N tons^{-1} N)
- S_{till} is the scaling factor for no-tillage (dimensionless)
- N_2O_{MW} is 44/28, the ratio of molecular weights for N_2O to N_2O-N (tons N_2O tons^{-1} N_2O-N)

- N_2O_{GWP} is 265, the AR5 GWP-100 value for N_2O (tons CO_2e tons^{-1} N_2O)

For nitrogen in crop residues left on the field, emissions were calculated on a corn-mass-produced basis as calculated with **Equation B3**:

Equation B3

$$N_2O_{D,R} = \{[(F_{CR} * EF_{ON})] * [1 + S_{till}]\} * N_2O_{MW} * N_2O_{GWP}$$

Where:

- $N_2O_{D,R}$ is the direct N_2O soil emissions from crop residue on a grain basis (tons CO_2e ton^{-1} corn)
- F_{CR} is the amount of N in crop residue left on the field on a grain basis (tons N ton^{-1} corn)
- EF_{ON} is the emission factor for other nitrogen inputs (tons N_2O-N tons^{-1} N)
- S_{till} is the scaling factor for no-tillage (dimensionless)
- N_2O_{MW} is 44/28, the ratio of molecular weights for N_2O to N_2O-N (tons N_2O tons^{-1} N_2O-N)
- N_2O_{GWP} is 265, the AR5 GWP-100 value for N_2O (tons CO_2e tons^{-1} N_2O)

The amount of N left per mass of corn grain was calculated using factors provided for corn grain systems as in **Equation B4**:

Equation B4

$$F_{CR} = \left(\left(\frac{DM}{HI} - 1\right) * N_a\right) * (1 - R_m) + \left(\frac{DM}{HI} * R * N_b\right)$$

Where:

- F_{CR} is the amount of N in crop residue left on the field on a grain basis (tons N ton^{-1} corn)

- DM is the dry matter content of harvested corn biomass (tons dry matter ton^{-1} corn biomass)
- HI is the ratio of crop yield to total aboveground biomass (tons corn biomass ton^{-1} corn yield)
- N_a is the nitrogen content of aboveground corn residue (tons N ton^{-1} dry matter)
- R_m is 0.8, the proportion of residue removed from the field[18] (tons dry matter removed ton^{-1} dry matter produced)
- R is the "root-to-shoot" ratio for corn (tons belowground dry matter ton^{-1} aboveground dry matter)
- N_b is the nitrogen content of belowground corn residue (tons N ton^{-1} dry matter)

Indirect emissions from fertilizer nitrogen volatilization were calculated as in **Equation B5**[19]:

Equation B5

$$N_2O_{vol} = (F_{SN} * Frac_{GASF}) * EF_{vol}$$

Where:

- N_2O_{vol} is the indirect soil N_2O emitted by the ecosystem receiving volatilized nitrogen (tons N_2O-N)
- F_{SN} is the synthetic nitrogen fertilizer applied (tons N)
- $Frac_{GASF}$ is the fraction of synthetic nitrogen that volatilizes as NH_3 and NO_x (tons N ton^{-1} nitrogen in synthetic fertilizer)
- EF_{vol} is the emission factor for volatilized nitrogen or proportion of nitrogen volatilized as NH_3 and NO_x that is transformed to N_2O in receiving ecosystem (tons N_2O-N ton^{-1} N)

Additionally, indirect emissions from fertilizers due to nitrogen leaching were calculated using **Equation B6**[19]:

Equation B6

$$N_2O_{leac\ ,SN} = F_{SN} * Frac_{leach} * EF_{leach}$$

Where:

- $N_2O_{leach,SN}$ is the indirect soil N_2O emitted by ecosystem receiving leached synthetic fertilizer nitrogen (ton N_2O-N)
- F_{SN} is the synthetic nitrogen fertilizer applied (tons N)
- $Frac_{leach}$ is the fraction of nitrogen inputs that is leached or runs off the land parcel (tons N ton^{-1} N in nitrogen inputs)
- EF_{leach} is proportion of leached and runoff nitrogen that is transformed to N_2O in the receiving ecosystem (tons N_2O-N ton^{-1} N)

Leaching of nitrogen from crop residues was similarly calculated as in **Equation B7**:

Equation B7

$$N_2O_{leach,CR} = F_{CR} * Frac_{leach} * EF_{leach}$$

Where:

- $N_2O_{leach,CR}$ is the indirect soil N_2O emitted by ecosystem receiving leached crop residue nitrogen (ton N_2O-N)
- F_{CR} is the amount of N in crop residue left on the field on a grain basis (tons N ton^{-1} corn)
- $Frac_{leach}$ is the fraction of nitrogen inputs that is leached or runs off the land parcel (tons N ton^{-1} N in nitrogen inputs)

- EF_{leac} is proportion of leached and runoff nitrogen that is transformed to N_2O in the receiving ecosystem (tons N_2O-N ton^{-1} N)

Finally, CO_2 emissions from fertilizers containing urea were calculated using **Equation B8**[17]:

Equation B8

$$C_{urea} = M * EF_{urea} * CO_2MW$$

Where:

- C_{urea} is the release of carbon from urea added to the soil (tons CO_2-eq)
- M is the amount of urea fertilization (tons of urea)
- EF_{urea} is the emission factor, based on the proportion of carbon in urea (tons CO_2-C ton^{-1} urea)
- CO_2MW is 44/12, the ratio of molecular weight of CO_2 to carbon (tons CO_2 ton^{-1} CO_2-C)

For fertilizers besides regular urea but which contain urea, different factors had to be applied to translate from the amount of fertilizer applied to the amount of urea applied (M). These factors, listed in **Table B4**, are calculated from the mass of urea utilized in the upstream lifecycle models except for UAN, which follows the IPCC best practice of assuming all UAN mass is urea if the actual amount is unknown[20].

Table B4. *Urea content in fertilizers found in the 2023 harvest sample used to calculate direct urea CO_2 emissions. Fertilizers not listed had zero urea content.*

Fertilizer name in data sample	Urea Content (kg urea kg^{-1})
Urea	1
Urea Ammonium Nitrate Solution	1
180-65-45-12	0.5753
100-40-10-20S	0.4764
100/80/45-12S	0.3614
115/90/60-15S	0.3492
40.2-0-0-5.6	0.7668
37.3-0-0-8.3	0.6538
3-14-14 Starter	0.0117
40-0-0	0.7708
6-24-6 GoldStart	0.0152
XLR-RATE 7-23-5	0.0370

B2.2 Land management practices in the Gevo corn production area

Using local Extension office documents, USDA statistics, and local agronomist validation, a set of land management practices were determined for the Gevo corn production area in southwest South Dakota and southwest Minnesota. For the modeled dates, planting occurred on April 15th while harvest occurred on November 15th [21]. Fields were set to be in corn-soy rotation[21,22] with no cover cropping[21,23]. Regarding nitrogen management, 30-50 lbs. N ac^{-1} were applied at planting while the rest was applied between emergence and silking in June[21,24,25], and no enhanced efficiency fertilizers were utilized[21]. Finally, the proportion of crop residue left on the field was assumed to be 20% after harvesting, baling, and grazing activities[18,21].

B3. Uncertainty modeling

B3.1 Tier 1 nitrous oxide and urea CO_2 field emissions uncertainty modeling

For each of the emissions factors indicated in **Appendix B Section 2.1**, the USDA[17] and IPCC[19,20] resources provided average values along with uncertainty data. These values were

applied as triangular distributions in the Python LCA model to generate randomized values for each Monte Carlo run. The values used to create these distributions are summarized in **Table B5**.

Table B5*. Triangular distribution values for Tier 1 soil emissions calculations. Values correspond to the factors and units indicated in Appendix B Section 2.1.*

Factor	Left Value	Center Value	Right Value
EF_{SN}	0.013	0.016	0.019
S_{till}	-0.16	-0.015	0.16
EF_{ON}	0	0.005	0.011
DM	0.844	0.86	876
HI	0.45	0.53	0.61
N_a	0.001	0.006	0.011
R	0.005	0.18	0.355
N_b	0.002	0.007	0.012
EF_{vol}	0.011	0.014	0.017
EF_{leach}	0	0.011	0.02
$Frac_{GASF}$	0.02	0.11	0.33
$Frac_{Leach}$	0.01	0.24	0.73
EF_{urea}	0.1	0.2	0.2

B4. Supplementary Figures

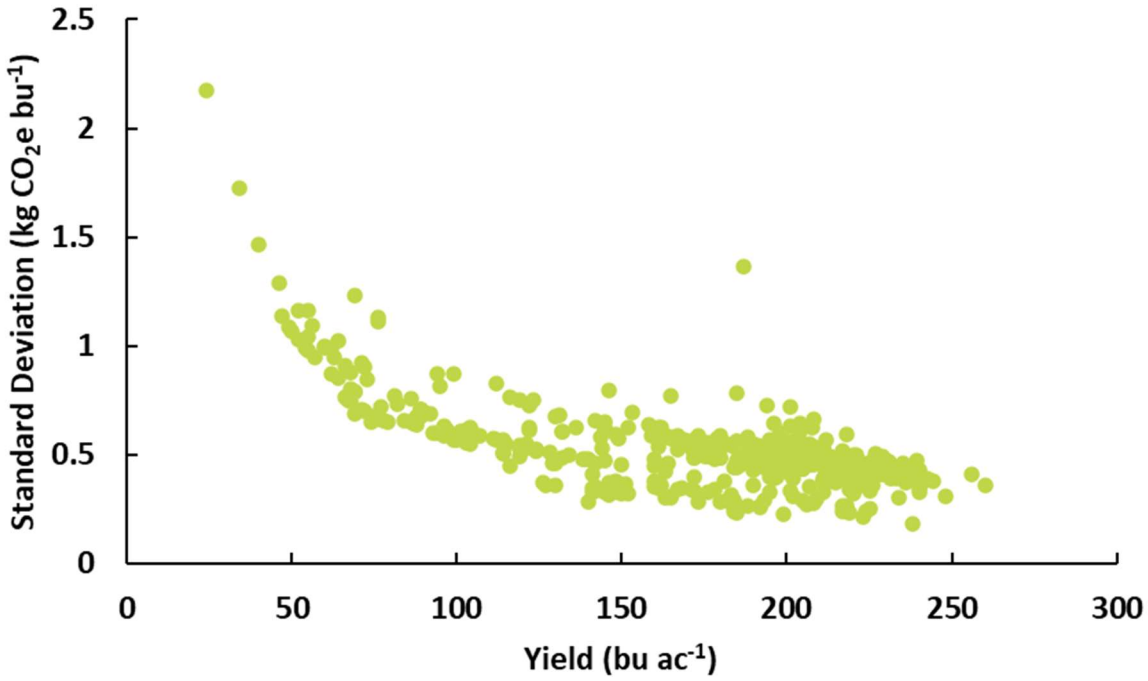

Figure B1. *Scatter plot of field-level yield vs. the standard deviation of GWP for that field. Generally, poor yields leave the LCA model more sensitive to input variations; thus, stochastic models return a broader distribution of results. The outlier at (187,1.36) was a field with exceptionally high reported fertilizer use per acre making the model sensitive to variations in upstream and soil emissions.*

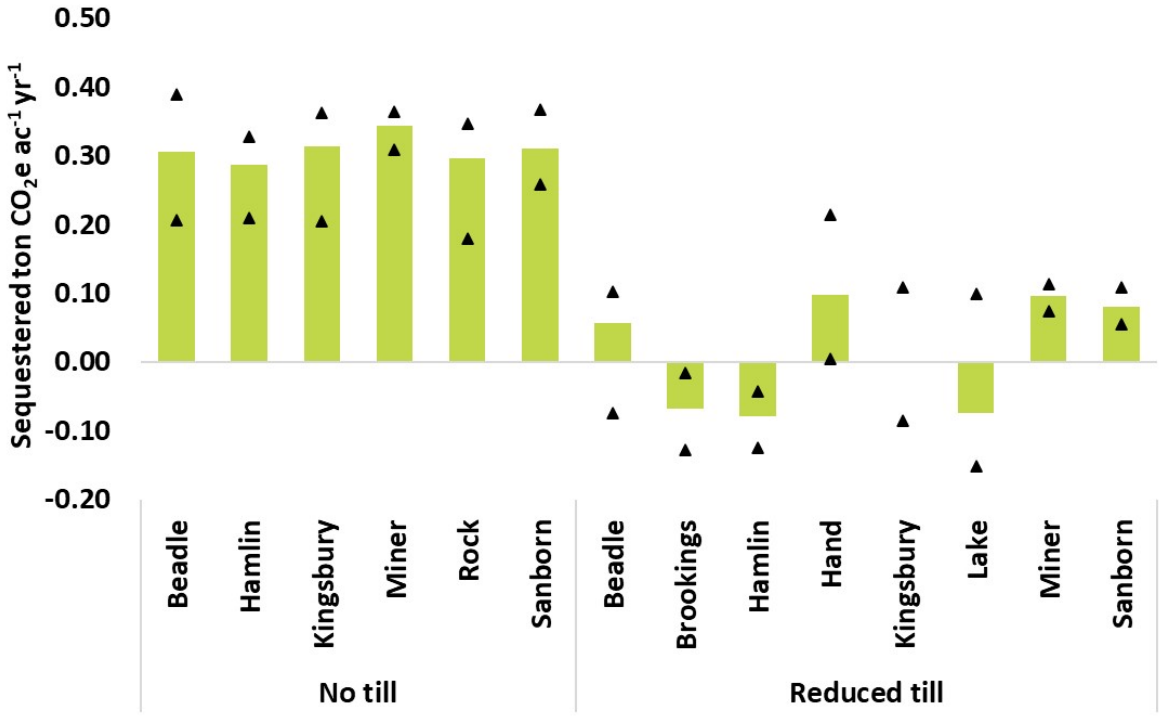

Figure B2. *Daycent SOC results by till type and county in the 2023 harvest area. Note these represent sequestered values, and thus negative values represent GHG emissions. Triangles represent the maximum and minimum result of simulated sites for that county.*

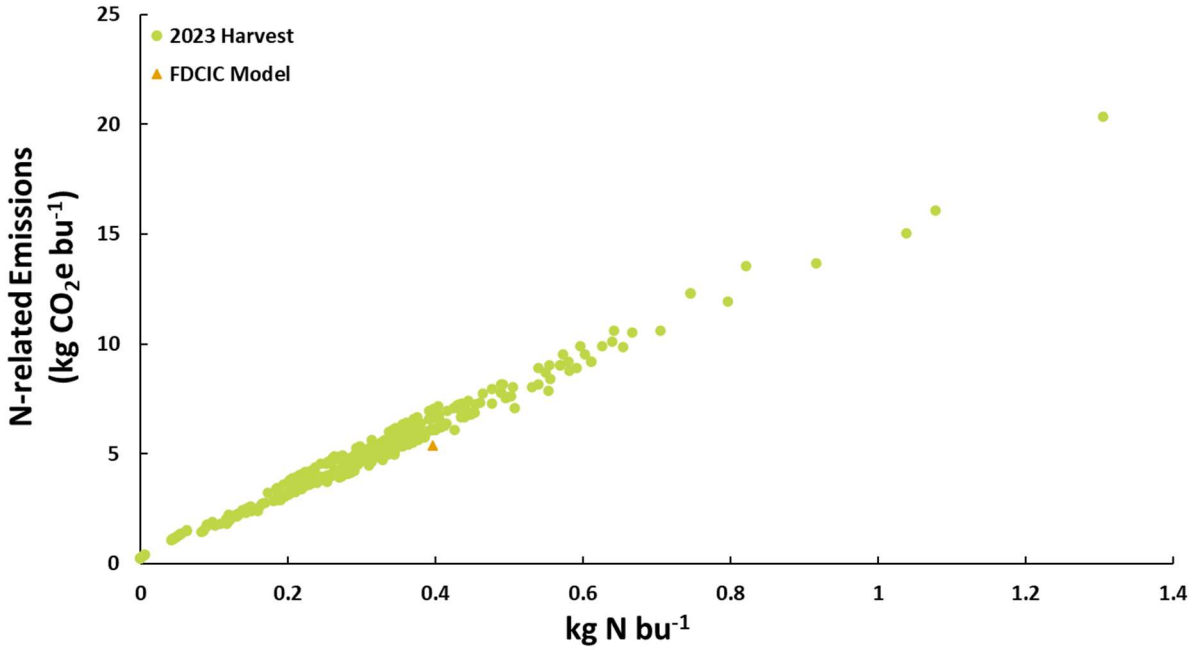

Figure B3. *Scatter plot of applied N per bushel vs. N-related emissions (upstream and on-field) for the 2023 harvest sites and the FDCIC default.*

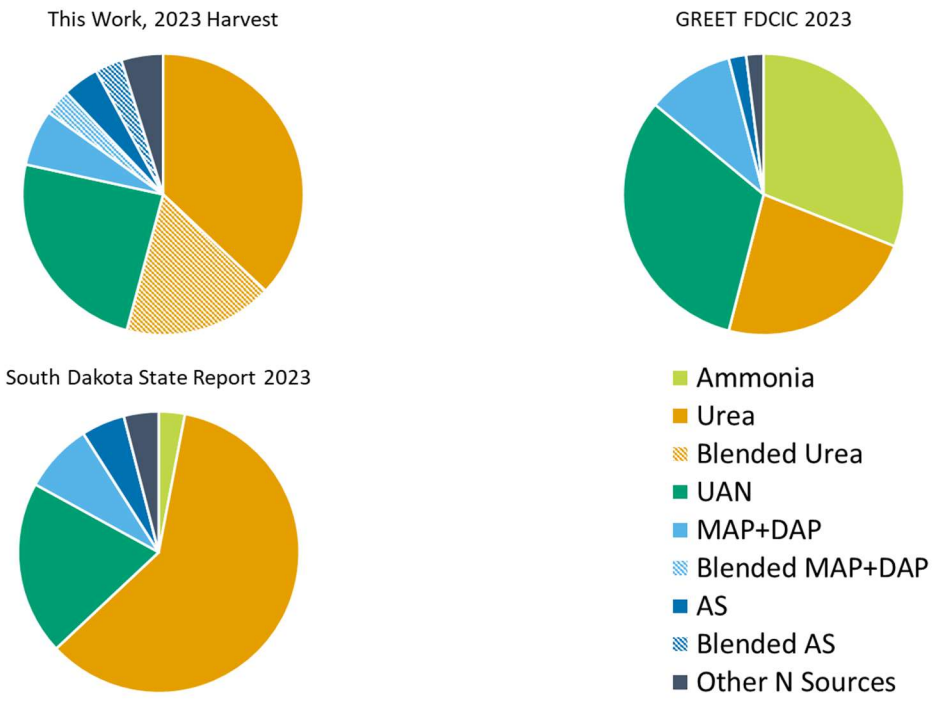

Figure B4. *Comparison of N fertilizer sources by mass N, comparing the 2023 harvest, the South Dakota state-level fertilizer report[8], and the GREET FDCIC 2023 model[26].*

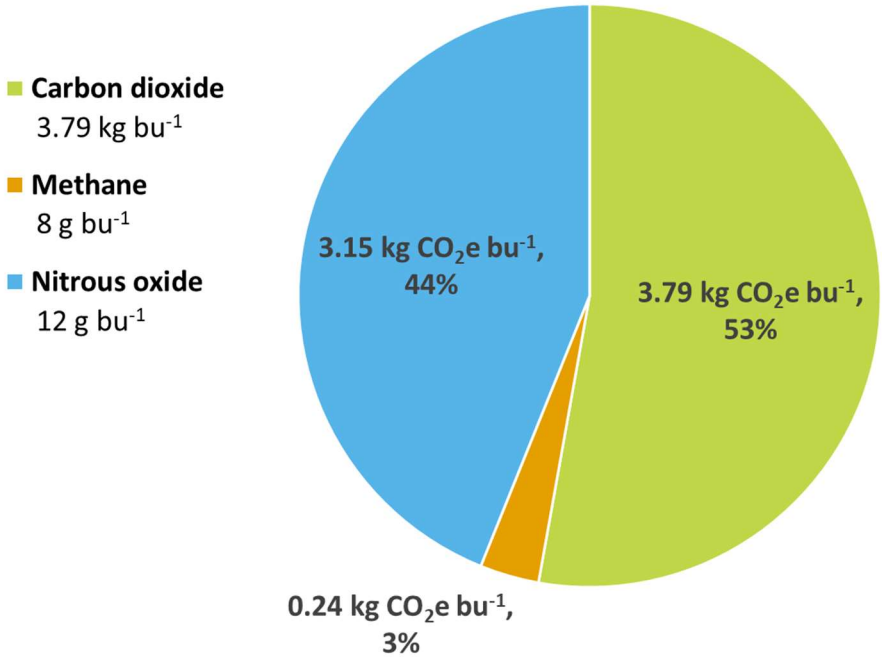

Figure B41. *FDCIC carbon footprint breakdown by GHG species. In the legend, mass of the gas emitted per bushel of corn is shown, while the chart values show GWP-100 values. Note in this chapter that AR5 GWP-100 values are used. 93% of N_2O emissions are on-field fertilizer emissions, 10% of CO_2 emissions are urea on-field emissions, and 17% of CO_2 emissions are on-field lime emission; such results emphasize the drastic effect chemical usage and efficiency can have on corn CI results.*

B5. Additional SAF Context

B5.1 Indirect emissions for corn SAF feedstock

While this study focused on an attributional feedstock analysis, federal tax credit guidelines provide factors to apply to capture consequential market effects[27]. For the ethanol ATJ pathway using U.S. corn, this includes:

- An indirect land use change emission of 1.324 kg CO_2e bu^{-1} corn, reflecting new cropland brought into production or changes in existing croplands;
- An "Other crops" emission of 0.093 kg CO_2e bu^{-1} corn, corresponding to changes in non-feedstock crop production following shifts in agricultural commodity markets; and
- A "Livestock" emissions reduction of -0.363 kg CO_2e bu^{-1} corn, due to changes in livestock and poultry production following shifts in agricultural commodity markets.

Altogether, these indirect effects add 1.054 kg CO_2e bu^{-1} corn or 6.049 kg CO_2e $MMBTU^{-1}$ in this study's jet fuel model.

B5.2 Alternative SAF feedstock carbon intensity context

To provide context to the carbon intensities measured in this work, values for other feedstocks may be considered using the International Civil Aviation Organization's CORSIA default emission values[28], shown in ***Figure B42***. Notably, the CORSIA estimate for corn ethanol ATJ is similar to the lower range of CI estimates in this study, reflecting different LCA modeling assumptions (e.g., global feedstock supply chains, conversion ratios, coproduct handling, etc.) Thus, the CORSIA corn grain ATJ estimate is included for direct comparison between default values. Generally, across conversion pathways and feedstocks, corn ethanol ATJ is highly

carbon-intensive, further demonstrating the need for farm-level and downstream mitigation measures.

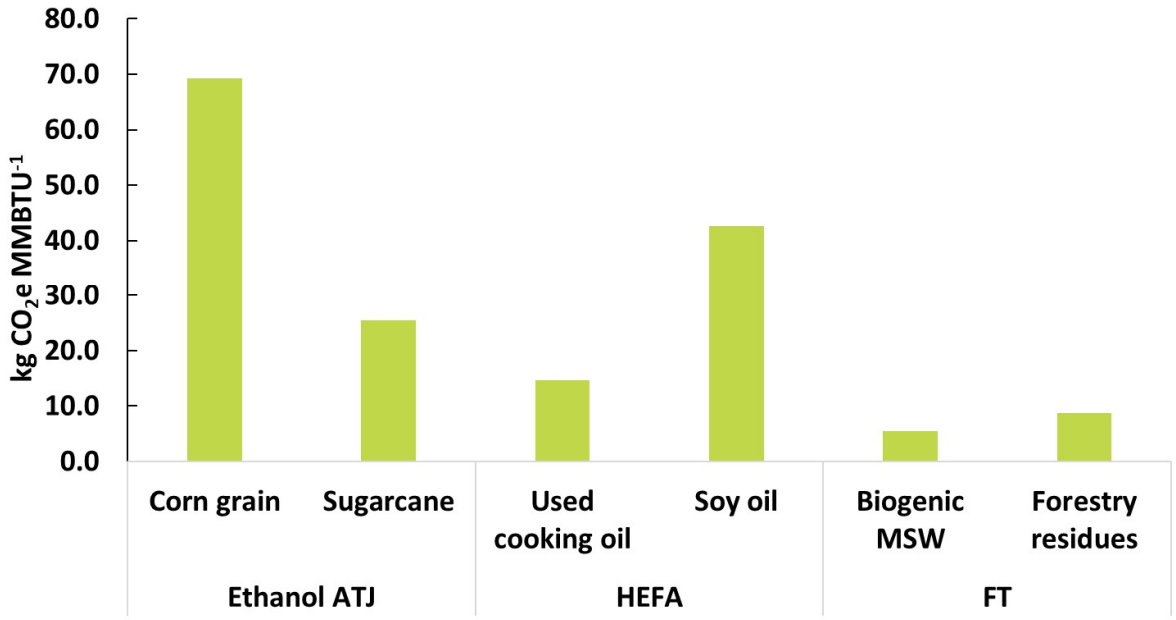

Figure B42. *CORSIA default emission values for select conversion pathways and feedstocks. Pathways considered are ethanol alcohol-to-jet (ATJ), hydrotreated esters and fatty acids conversion (HEFA), and Gasification Fischer-Tropsch conversion (FT). Biogenic municipal solid waste (MSW) refers to MSW without non-biogenic carbon content (e.g., no plastics).*

Appendix B References

(1) Leikam, D. F. Fluid Fertilizer Density, 2016. https://fluidfertilizer.org/density-of-fluid-fertilizers/fluid-fertilizer-density-2/ (accessed 2025-01-24).
(2) BASF Corporation. Safety Data Sheet Ammonium Sulfate 40%, 2022. https://www.google.com/url?sa=t&source=web&rct=j&opi=89978449&url=https://download.basf.com/p1/000000000030046449_SDS_GEN_US/en_US/Ammonium_sulfate_40%252525_30046449_SDS_GEN_US_en_4-0.pdf&ved=2ahUKEwiLj4aBo4-LAxVRNzQIHd90D7sQFnoECBAQAQ&usg=AOvVaw2LlBf3uRXTwkGGjr9VRL8- (accessed 2025-01-24).
(3) Plant Food Company, Inc. Ammonium Thiosulfate, 12-0-0, 26% Sulfur SDS, 2015. https://www.plantfoodco.com/golf-professional-turf/products/secondary-nutrients/ammthiosulfate-12-0-0/ (accessed 2025-02-03).
(4) The Andersons, Inc. 6-24-6 GoldStart Liquid Fertilizer, 2021.
(5) CHS Inc. XLR Rate 7-23-5 Liquid Fertilizer Label, 2020. https://www.chsagronomy.com/crop-nutrients/starter-fertilizers/xlr-rate#details (accessed 2025-01-24).
(6) BlueStem Farm Supply, LLC. Liquid Fertilizer 3-14-14 w/Sweetener Product Data Sheet, 2008. https://bluestemag.com/soil-amendments/ (accessed 2025-01-28).
(7) MacroSource. 8-20-5-5S-.5Zn Liquid Fertilizer SDS, 2024. https://ictulsa.com/safety-data-sheets/ (accessed 2025-01-28).
(8) South Dakota Department of Agriculture. *Fertilizer Annual Report*; Pierre, SD, 2023. https://danr.sd.gov/Agriculture/Inspection/FertilizerSoilAmendments/FertilizerProgram/default.aspx (accessed 2025-01-24).
(9) Jordan Keltgen. Confirming Dry Blend Ingredients in Brookings Area, 2025.
(10) Carlson, G.; Clay, D.; Reese, C. L. Common Fertilizers Used in Corn Production, 2019. https://extension.sdstate.edu/sites/default/files/2019-09/S-0003-28-Corn.pdf (accessed 2024-01-28).
(11) Gilbertson, J.; Vallin, E. HANDBOOK OF SOLID FERTILISER BLENDING Code of Good Practice for Quality, 2016. https://fertiliser-society.org/wp-content/uploads/2019/11/Blender-Handbook-2017-efba.pdf (accessed 2025-01-28).
(12) Nebraska Department of Agriculture. Fertilizer Codes, 2022. https://nda.nebraska.gov/plant/fertilizer/index.html.
(13) Wang, B.; Lv, Z.; Yu, M.; Liu, X.; Li, C.; Hua, Q.; Liu, Y.; Liu, P.; Shen, B.; Zhao, N.; Ding, J.; Tang, J. One-Pot Synthesis and Hydrolysis Behavior of Highly Water-Soluble Ammonium Polyphosphate. *ACS Sustain. Chem. Eng.* **2022**, *10* (39), 13037–13049. https://doi.org/10.1021/acssuschemeng.2c03169.
(14) Wernet, G.; Bauer, C.; Steubing, B.; Reinhard, J.; Moreno-Ruiz, E.; Weidema, B. The Ecoinvent Database Version 3 (Part I): Overview and Methodology. *Int. J. Life Cycle Assess.* **2016**, *21* (9), 1218–1230. https://doi.org/10.1007/s11367-016-1087-8.
(15) Barberá, J. J.; Metzger, A.; Wolf, M. Sulfites, Thiosulfates, and Dithionites. In *Ullmann's Encyclopedia of Industrial Chemistry*; Wiley-VCH, Ed.; Wiley, 2000. https://doi.org/10.1002/14356007.a25_477.
(16) Koch Fertilizer. Ammonium Thiosulfate Solution SDS, 2019. https://kochfertilizer.com/sds/ (accessed 2025-01-28).

(17) Ogle, S. M.; Adler, P. R.; Bentrup, G.; Derner, J.; Domke, G.; Grosso, S. D.; Lehmann, J.; Reba, M.; Woolf, D. Chapter 3: Quantifying Greenhouse Gas Sources and Sinks in Cropland and Grazing Land Systems. In *Quantifying greenhouse gas fluxes in agriculture and forestry: Methods for entity-scale inventory*; U.S. Department of Agriculture, Office of the Chief Economist.: Washington, DC, 2024.
(18) Gessner, H. Should We Sell Corn Stalks?, 2024. https://extension.sdstate.edu/should-we-sell-corn-stalks (accessed 2025-02-20).
(19) IPCC. *2019 Refinement to the 2006 IPCC Guidelines for National Greenhouse Gas Inventories*; Buendia, E. C., Tanabe, K., Kranjc, A., Jamsranjav, B., Fukuda, M., Ngarize, S., Osako, A., Pyrozhenko, Y., Shermanau, P., Federici, S., Eds.; IPCC: Switzerland, 2019.
(20) IPCC. *2006 IPCC Guidelines for National Greenhouse Gas Inventories*; Eggleston, H. S., Buendi, L., Miwa, K., Ngara, T., Tanabe, K., Eds.; Institute for Global Environmental Strategies: Hayama, Japan, 2006.
(21) Keltgen, J. Standard Land Management Practices in Southeast SD and Southwest MN, 2025.
(22) Wang, T. Economics of Different Crop Rotation Systems in South Dakota, 2022. https://extension.sdstate.edu/economics-different-crop-rotation-systems-south-dakota (accessed 2025-02-12).
(23) Wallander, S.; Bowman, M.; Rosenberg, A. B. More Farmers Are Adding Fall Cover Crops to Their Corn-for- Grain, Cotton, and Soybean Fields, 2022. https://www.ers.usda.gov/data-products/charts-of-note/chart-detail?chartId=103975 (accessed 2025-02-12).
(24) Graham, C.; Bly, A. Chapter 20: Corn Nitrogen Timing. In *iGrow Corn: Best Management Practices*; South Dakota State University, 2016.
(25) USDA National Agricultural Statistics Service. Crop Progress and Condition: Corn in South Dakota, 2023. https://www.nass.usda.gov/Charts_and_Maps/Crop_Progress_&_Condition/2023/ (accessed 2025-02-12).
(26) Liu, X.; Cai, H.; Kwon, H.; Wang, M. FEEDSTOCK CARBON INTENSITY CALCULATOR (FD-CIC) Model, 2023. https://greet.anl.gov/tool_fd_cic.
(27) Office of Energy Efficiency and Renewable Energy. Guidelines To Determine Life Cycle Greenhouse Gas Emissions of Clean Transportation Fuel Production Pathways Using 45ZCF-GREET, 2025. https://www.energy.gov/eere/greet (accessed 2025-01-24).
(28) International Civil Aviation Organization. *CORSIA Default Life Cycle Emissions Values for CORSIA Eligible Fuels*; ICAO, 2024. https://www.icao.int/environmental-protection/CORSIA/Pages/CORSIA-Eligible-Fuels.aspx (accessed 2025-05-13).

APPENDIX C

C1. Materials and Methods Supplementary Information

C1.1 Crop Production Model

Lettuce cultivation was simulated using the UN Food and Agriculture Organization's AquaCrop model[1] with the open source AquaCrop-OS[2] Python tool to enable simulation of multiple sites and years. AquaCrop parameters and location data were taken from a previously-published model[3], and relevant data for the locations considered in this work are summarized in **Table C1**. Daily weather data came from the Downscaled CMIP5 Climate and Hydrology Projections website[4], specifically the localized construct analogs (LOCA) for climate[5] and hydrology[6] daily projections, using the 32 RCP-4.5 climate models. In addition to temperature and precipitation data, these models provided inputs for soil moisture at planting, as well as data to derive reference evapotranspiration rates. The soil layers were deduced to be at depths of 0.1 m, 0.5 m, and 1.5 m based on the hydrology data source's reference to Liang et al.[7]. For reference evapotranspiration, version 1.2.0 of the pyfao56 tool was used[8] with some modifications for the data availability and formats in the LOCA resource. For each location, crop growth was simulated for each of the 32 climate models, then seasonal yield and irrigation results from all successful runs were averaged. In two years, one crop simulation failed for New York, reflecting a model that predicted particularly cold weather in the growing period. For more consistent comparison without the variation between different seasons, this LCA utilizes values for the spring seasons in the four large cities, the mid-December planting in Salinas, CA, and the mid-November planting in Yuma, AZ.

Table C1. *Location data for the sites simulated in this study, derived from Maynard et al. (2023).*

Location	TMY Station	Latitude	Longitude	Soil Texture	Elevation (m)	Planting Date
Salinas, CA	724917	36.667	-121.6	SANDY LOAM	16	Dec 15
Yuma, AZ	699604	32.65	-114.617	SAND	43	Nov 15
New York City, NY	725030	40.783	-73.883	LOAMY SAND	4	Mar 28
Los Angeles, CA	722956	33.917	-118.333	LOAMY SAND	89	Feb 28
Chicago, IL	725300	41.983	-87.917	LOAMY SAND	182	Apr 21
Houston, TX	722429	30.067	-95.55	SAND	15	Feb 14
				SANDY LOAM		

Figure C1 displays the yield results of AquaCrop simulations. Notably, while there is an overlap in error bars, there is also a clear trend from 2020 to 2050 of increasing yields as ambient temperatures increase, with some variation reflecting the different climate models.

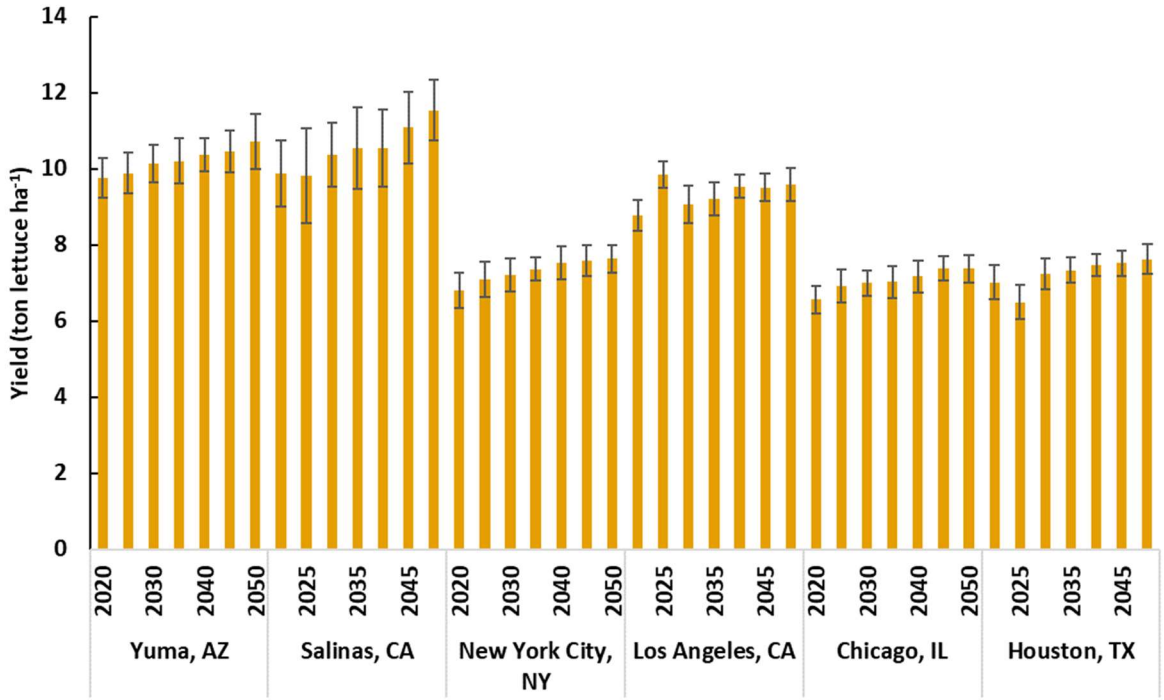

Figure C1. *AquaCrop lettuce model average yield results for all locations and years. Error bars represent standard deviation of results from 32 RCP-4.5 climate models.*

C1.2 Prospective LCI Modeling

C1.2.1 N Fertilizer Background Technosphere Transformation

USA market ammonia production mixes created by Boyce et al.[9] were obtained for the study years under the IMAGE SSP2 Base, RCP-2.6, and RCP-1.9 scenarios, including the 2020 baseline value. These were then combined with the greenhouse gas emissions associated with energy and transport as noted in Argonne National Laboratory's Feedstock Carbon Intensity Calculator (FD-CIC) model for urea fertilizer to determine upstream nitrogen fertilizer GWP-100 impacts [10].

Among the scenarios modeled by Boyce et al., the RCP-2.6 is modeled consistent with a 2 ^{0}C increase by the end of the century[9]; because this is consistent with the +2-3 ^{0}C trajectory observed by the UNEP[11], this scenario served as the baseline estimate. Meanwhile, the Base model (consistent with a +3 ^{0}C trajectory) was used for the conservative scenario. To consider more optimistic implementation of green hydrogen in fertilizer supply chains, the International Energy Agency (IEA) Net Zero Emissions projections for low-impact hydrogen demand as a percentage of total demand were considered[12]. The IEA report provided values for 2022, 2030, 2035, and 2050, reaching 98% of total hydrogen demand. Based off these values, an "S-curve" adoption model was created to estimate low-emissions hydrogen proportions in other study years. "S-curves," or technology diffusion curves, commonly occur in the adoption of technologies with a formative phase followed by a growth phase and then a saturation phase[13]. Based on these proportions, GHG intensities of urea fertilizer were calculated as a weighted mixture of the baseline value derived from the work of Boyce et al.[9] and the "Green" urea impact in the FD-CIC model[10].

C1.2.2 Renewable Diesel LCI and Adoption

Based on the work of Xu et al.[14], an LCA model of soy-based renewable diesel (RD) was developed with ecoinvent inputs[15]. For the soybean crude oil feedstock, this included incorporating the ecoinvent soybean meal inventory to account for the allocation assumptions in the ecoinvent model and instead aligning them with Xu et al.'s allocation methods. The ecoinvent description noted the basis of 1000 kg of oil. Using the mass fraction factors from Xu et al. (0.216 for oil, 0.784 for meal), this implied a total mass of 4630 kg (3630 kg of which is meal). Using the ecoinvent 3.9 IPCC 2021 GWP-100 factors, this translated to a total GHG impact of 2458 kg CO_2e for the process. Reallocating with Xu et al.'s mass factors as they did for soybean crushing in their study[14] yielded a reallocated GWP as shown in **Equation C1**:

***Equation C1**. Soy oil and meal allocation calculation used for RD feedstock GWP.*

$$GWP_{reallocated} = \frac{\left(M_{oil} * GWP_{oil} + \frac{M_{oil}}{AF_{oil}} * AF_{meal} * GWP_{meal}\right)}{M_{oil}} * AF_{oil}$$

Where:

- $GWP_{reallocated}$ is the GWP-100 of soy oil (kg CO_2e kg^{-1} oil) aligned with Xu et al.'s allocation factors.
- M_{oil} is the mass of oil in the ecoinvent basis (1000 kg oil).
- AF_{oil} is Xu et al.'s mass allocation fraction for oil in soy milling, 0.216.
- AF_{meal} is Xu et al.'s mass allocation fraction for meal in soy milling, 0.784.
- GWP_{oil} is the original ecoinvent GWP-100 factor for soy oil (kg CO_2e kg^{-1} oil).
- GWP_{meal} is the original ecoinvent GWP-100 factor for soy meal (kg CO_2e kg^{-1} oil).

Thus, this adjusted soy oil factor was combined with other ecoinvent flows (see **Table C2**) and Xu et al.'s allocation factors for the renewable diesel production stage to replicate Xu et al.'s

non-LUC GHG intensity results for soy-based renewable diesel. The proximity of this study's model result (0.0237 kg CO_2e MJ^{-1} diesel) to Xu et al.'s (0.0235 kg CO_2e MJ^{-1} diesel) provided validation of the allocation method and flows used[14].

Table C2. *Summary of the LCI for renewable diesel, based on the work of Xu et al.[14]. Note that "baseline" and "prospective" highlight if a different flow name was used between ecoinvent 3.9 cutoff database and the premise REMIND database (a higher resolution geography for natural gas and a "blue" hydrogen option in the prospective years).*

Input	Unit per kg RD	Amount	Inventory flow
Feedstock	kg	1.26	Soybean meal and crude oil production, US
Natural Gas	MJ	0.82	*Baseline:* heat production, natural gas, at industrial furnace low-Nox >100kW, RoW *Prospective:* heat production, natural gas, at industrial furnace low-Nox >100kW, USA
Electricity	MJ	0.43	Market for electricity, high voltage, US-MRO
Hydrogen	kg	0.04	*Baseline:* hydrogen production, steam reforming, RoW *Prospective:* hydrogen production, steam methane reforming of natural gas, with CCS (MDEA, 98% eff.), 25 bar, USA

With the result replicated for the 2020 basis, the calculation was repeated for each of the dynamic simulation years from 2025 to 2050 using the premise ScenarioLink REMIND SSP2-Base database[16]. Flow values and allocation factors were held constant, and the relevant inventory names were summarized in **Table C2**. Finally, the LUC factors listed by Xu et al. (see **Table C3**) were incorporated in the model; each is a selectable scenario, and the average of the three is used as the baseline scenario value.

Table C3*. ILUC values collected by Xu et al.[14] incorporated into this study's RD model, including which technology change case utilizes which value).*

Xu et al. (2022) Case	ILUC Factor (kg CO_2e MJ^{-1})	Scenario, This Study
CCLUB	0.0092	Optimistic
CARB	0.0291	Conservative
ICAO	0.020	-
Average	0.019	Baseline

With these dynamic characterization factors calculated, the extent of renewable diesel use in the lettuce model were modeled using projections from the U.S. Energy Information Administration Annual Energy Outlook[17]. Average daily production values for conventional diesel and renewable diesel were collected for each simulation year under 3 scenarios: the Reference case, the Low Oil Price case, and the High Oil Price case. Adoption of RD in the lettuce model was then calculated as the ratio of RD to both renewable and conventional diesel.

To consider more optimistic implementation of RD in agriculture, the Annual Energy Outlook renewable diesel production values were instead compared to the 2010-2020 average of diesel sales to farm consumers[18]. The ratio of RD production to farm consumption was used as the proportion of farm machinery energy demand met by renewable diesel; this represented an aggressive case which assumes farm consumers are prioritized for domestic RD supply over other sectors.

C1.2.3 Irrigation Electrification LCI and Adoption

As in previously published lettuce modeling work[3], 70% of irrigation demand was assumed to be met with sprinkler irrigation, while 30% was met by drip irrigation. Within the corresponding ecoinvent flows[15], some of the energy demands were modeled with a mix of diesel and electric pumps. These were then multiplied by the corresponding pump efficiencies used by Driscoll et al.[19] to calculate the total ideal energy demand for both drip and sprinkler systems. Then, the baseline mix of pump energy types was determined for each simulation using the Water Resource Regions acreage values in Table 13 of the 2018 Irrigation and Water Management Survey[20]. These proportions were then multiplied by the total ideal energy demands of the drip and sprinkler inventories and divided by the efficiency factors from Driscoll et al.[19] to

determine actual energy demand for each pump energy type. Fossil fuel energy demands were then multiplied by GWP-100 values for corresponding ecoinvent inventories, while electric energy demands were multiplied by corresponding subregional GWP-100 values derived from eGRID 2022[21]. Efficiency factors and flows used in these calculations are summarized in **Table C4**.

Table C4. *Efficiency factors (Driscoll et al., 2024) and ecoinvent flows (Wernet et al., 2016) used in irrigation LCI calculations.*

Fuel Type	Efficiency	Flow (ecoinvent cutoff 3.9)
Electric	88%	(N/A – eGRID and Cambium factors used)
LPG	25%	market for propane, burned in building machine | GLO
Gasoline	23%	market for petrol, unleaded, burned in machinery | GLO
Natural Gas	21%	market for natural gas, burned in gas turbine | GLO
Diesel	31%	diesel, burned in agricultural machinery | GLO

With the baseline determined, future energy mixes were derived for later simulation years. Driscoll et al. considered a case where the portion non-electric acreage declined by 5% each year[19]; this rate was adopted as the baseline scenario for this study. This decline assumed the proportion of each fossil fuel type to total fossil fuel usage stayed constant (e.g., if natural gas made up 50% of fossil fuel usage in the baseline, then it made up 50% of fossil fuel usage in all years thereafter). As with the baseline year, these proportions were combined with the total ideal energy demand and efficiency factors and then corresponding GWP-100 values, though electric demand was instead combined with regionalized factors from the National Renewable Energy Laboratory (NREL) Cambium dataset for appropriate years[22].

To consider a range of electric adoption scenarios, the pace of adoption assumed by Driscoll et al.[19] was adjusted to more conservative and more aggressive rates: 2.5% and 7.5% changeover from fuel pumps to electric pumps, respectively. These scenario variations caused

greater effects compared to the baseline in the near-term and in regions where electrification began at a low level; in regions with higher initial electrification and in later years, the GWP-reduction effects of the different rates converged (for example, see **Figure C2**).

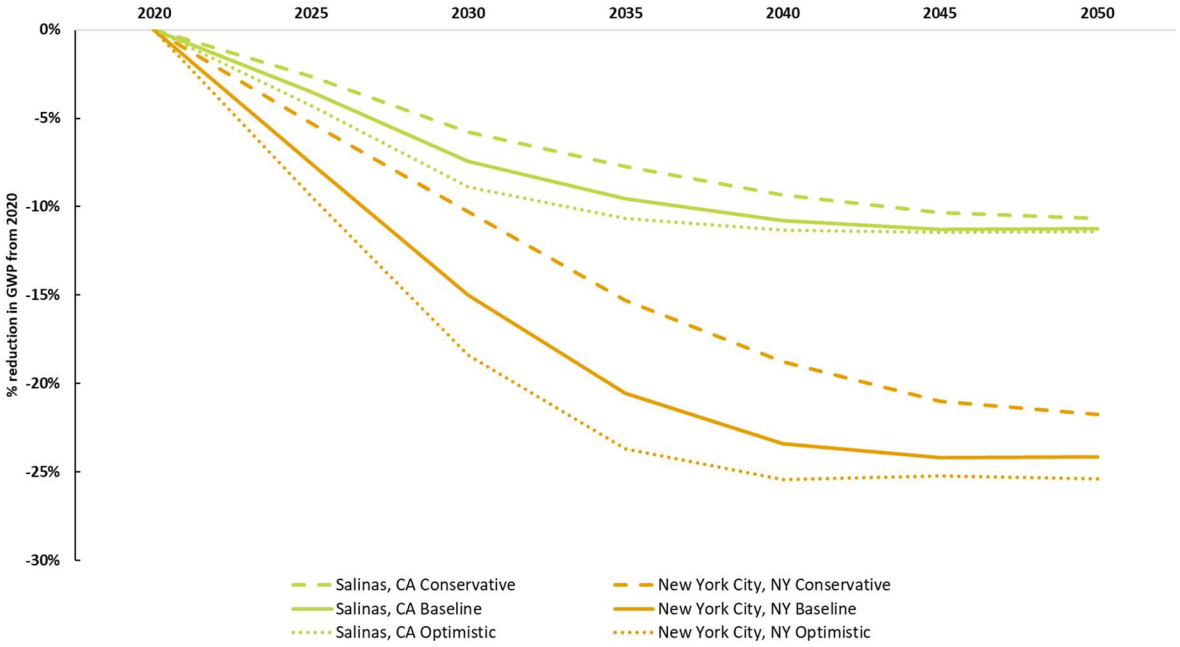

Figure C2. *Reductions in total GHG impact for lettuce grown in Salinas and New York under different irrigation transition rates. Salinas represents a high initial electrification percentage, while New York represents a low initial percentage. Note technology change cases include corresponding background grid transformation.*

C1.2.4 Machinery Electrification LCI and Adoption

When considering the electrification of heavy equipment in the agricultural sector, variations in size and power for different crop systems can be significant. For example, the ecoinvent agricultural tractor was noted at 4000 kg in weight[15], similar to the smaller 80 HP and 100 HP John Deere agricultural tractors considered for electrification in a CALSTART white paper focused on zero-emission off-road equipment in California[23]. In comparison, a John Deere 9R Series tractor can have as high as 620 HP ratings; in this equipment size range, the company is focused on biofuels instead of electrification[24]. Due to this range in power, different cropping systems that use different machines may electrify at different rates or not be candidates for

electrification at all. For lettuce systems, a recent California crop budget indicated equipment power ratings of 120 HP, 150 HP, and 205 HP[25], similar to the agricultural tractors and construction tractors Lund et al. considered feasible for battery electrification[23]. Thus, the use of the tractor size in ecoinvent was assumed appropriate, and this study assumed lettuce cropping systems would be feasible candidates for electrification.

The ecoinvent technosphere flows Into the heavy machinery activities described In Maynard et al.[3] were examined to determine the amount of diesel utilized per hectare of cultivated lettuce. Utilizing a lower heating value (LHV) of 135.522 MJ gal^{-1} and a density of 3.167 kg gal^{-1} [26], this was translated into energy usage, which was then adjusted by 0.4[27] to account for engine inefficiencies and calculate a theoretical energy demand per hectare. Electric adoption fraction for a given year would then be multiplied by this per hectare value and adjusted by an efficiency factor of 0.8[27]. This electricity demand per hectare would then be divided by yield per hectare for given location and year to get a per-mass electricity demand. This value would then be multiplied by the impact factor from eGRID 2022 for the baseline year[21] or the corresponding Cambium value for projected years[22].

In addition to electricity generation impacts, the impact of battery materials was also estimated using the NMC 111 lithium ion process from ecoinvent, including the density of 0.197 kWh of storage per kg of battery[15]. To translate impacts from an energy storage functional unit to an energy usage functional unit, the battery lifetime estimated by Lagnelov et al. for the electric replacement of a similarly-sized tractor (335 HP) was considered; however, Lagnelov et al. modeled the replacement as two lower-powered autonomous tractors[28]. Thus, as a conservative estimate, the lifetime was halved to 2000 cycles. Beyond the 2020 baseline, NMC 111 battery impact calculations were repeated for each of the dynamic simulation years from 2025 to 2050

using the premise ScenarioLink REMIND SSP2-Base database[16], though the energy density and lifetime cycle values were held constant as a conservative estimate.

Adoption of electrification in heavy duty farm machinery was estimated using new capacity addition values from NREL's Electrification Future Study[29]. The NREL study included a Reference case, Medium Electrification case, and High Electrification case across economic sectors and weight classes, including heavy-duty vehicles (HDVs). The Reference case assumed no electrification in the industrial sector (including agriculture), while the Medium Electrification case assumes limited industry adoption based on a "productivity benefit" heuristic, which the authors acknowledge "may result in conservative adoption assumptions for many electrotechnologies"[29]. Thus, this study adapts some of the modeled cases in order to explore a range of electrotechnology deployment in the agricultural sector. Mai et al. estimate agricultural machinery would reach 25% of new capacity additions by 2050; correspondingly, in the equivalent Moderate case heuristic, the adoption would be 10%[29]. This case and others are presented in **Table C5**; Mai et al. reported values for 2030, 2040, and 2050[29], so values for 2025, 2035, and 2045 were linearly interpolated.

Table C5. *Scenarios for portion of Heavy Machinery energy demand met by electricity, based on Mai et al.'s industry sector heuristics (p. 114, 2018).*

Year	Moderate Case, Moderate Benefits	Moderate Case, Large Benefits	High Case, High Benefits
2020	0.0%	0.0%	0.0%
2025	0.0%	5.0%	12.5%
2030	0.0%	10.0%	25.0%
2035	2.5%	15.0%	42.5%
2040	5.0%	20.0%	60.0%
2045	7.5%	22.5%	67.5%
2050	10.0%	25.0%	75.0%

To translate these projection cases into adoption scenarios, they were compared to Lund et al.'s more recent projections in California, where regulations target zero emissions for the sector by 2035[23]. Their near-term projections placed U.S.-wide sales of BEV's to make up 1% of tractor sales by 2029, while in California a higher proportion of 12% is expected. Comparing these projections to the work of Mat et al.[29] indicates the U.S. is on track for the "Moderate Case, Moderate Benefits" scenario while California specifically is on an accelerated track similar to the "Moderate Case, Large Benefits" scenario. California accounts for most of the lettuce produced in the United States: 76% of leaf lettuce from 2021-2023[30]. Because of this proportionally high impact compared to the rest of the country, the baseline adoption scenario was calculated as a weighted average between the California-representative scenario ("Moderate Case, Large Benefits") and the U.S.-wide scenario ("Moderate Case, Moderate Benefits"). Additionally, the "Moderate Case, Moderate Benefits" and "High Case, High Benefits" scenarios were considered as conservative and optimistic scenarios, respectively (see **Table C6** for summary of values used in this study).

Table C6. *BEV adoption scenario values used in this study, derived from projections by Mai et al. (2018) and Lund et al. (2022).*

Year	Conservative	Baseline	Optimistic
2020	0.0%	0.0%	0.0%
2025	0.0%	3.8%	12.5%
2030	0.0%	7.6%	25.0%
2035	2.5%	12.0%	42.5%
2040	5.0%	16.4%	60.0%
2045	7.5%	18.9%	67.5%
2050	10.0%	21.4%	75.0%

C1.2.5 Additional Input Dynamic Modeling

Beyond the main transitions of study (on-farm energy and upstream N fertilizer), upstream dynamic effects were incorporated to compare the extent of likely background dynamic impacts in 2050. Using the premise tool, particularly the ScenarioLink plugin for Activity Browser[16], the 2050 REMIND SSP2 Base case database was used for other inputs to the lettuce system (P fertilizer, K fertilizer, and pesticide upstream emissions) as well as inputs to the irrigation and machinery models (e.g., pump manufacturing and fossil fuel upstream emissions). These additional transitions were not considered in the main report, but the functionality remains in the LCA model for future consideration.

C1.3 Mitigation Cost Modeling

C1.3.1 Green Nitrogen Fertilizer Transition Costs

To calculate the transition costs of nitrogen fertilizer, the cost difference between green and conventional ammonia was estimated. Green ammonia prices were derived from the International Renewable Energy Agency's published range for 2020 production costs: the high cost case was used as the maximum of the range and the low cost case was used as the minimum[31]. The conventional ammonia cost maximum and minimum cases were derived from ten years of available data (2010-2020) from the United States Geological Survey National

Minerals Information Center Minerals Yearbook[32]. Then, the Argo Excel add-in was used to perform a 10,000 trial simulation of the difference between green and grey ammonia, varying the difference inputs on a uniform distribution[33]. The difference in ammonia cost was then multiplied by a stoichiometric ratio to get the difference in cost for urea (n.b. this assumes that, aside from ammonia sourcing costs, all costs in urea production are assumed equal.)

Green ammonia cost estimates vary significantly depending on assumptions, including the location and modeled year; therefore, other resources were surveyed to validate the IRENA estimates. Sousa et al.'s technoeconomic analysis[34] for production in Norway found a range of \$744 ton^{-1} to \$1786 ton^{-1} depending on electricity and equipment prices, with a reported main case of \$1486 ton^{-1}. A report by EPRI for 2030 in multiple US markets found a range of \$250 ton^{-1} to \$1250 ton^{-1}, particularly dependent on the continued implementation and effects of the Inflation Reduction Act[35]. Finally, recent S&P Global data for three months (April – June 2024)[36] quoted green ammonia from the US Gulf Coast delivered to Northwest Europe at an average of \$934 ton^{-1}. These values are displayed in **Figure C3**. While the variation demonstrates the highly dynamic nature of ammonia production costs during the energy transition, the overlap of these different sources of different types (peer-reviewed literature, grey literature, and price data) with the IRENA range of values provides validation of the modeled scenario values.

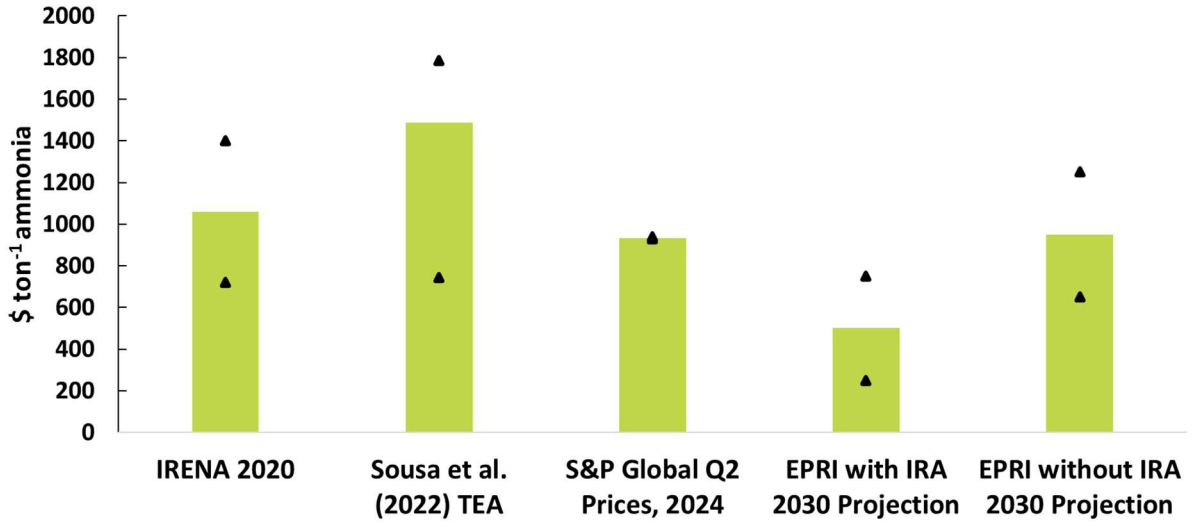

Figure C3. *Green ammonia price ranges reported in grey literature and technoeconomic literature, including maximum and minimum values (black triangles). The IRENA values were utilized in the abatement cost scenarios.*

The CI of both conventional and green ammonia-derived urea was calculated using the values found in the FD-CIC model[10].

C1.3.2 Irrigation Transition Costs

This study examined the cost of transitioning from fossil fuel-driven pumps to electric pumps in California. In particular, the transition from natural gas to electricity was examined. This decision was made to focus on transitioning from one energy supply network (natural gas pipelines) to another (electrical grids), as more remote locations would introduce greater uncertainties in the infrastructure cost considerations. To estimate energy prices per fuel unit, this study used a portion of the R code developed by Driscoll et al. along with updated 2023 EIA data[19] to determine maximum and minimum prices. Values for pump investment costs were taken from the 50 HP pumps case studies conducted by the Alabama Cooperative Extension System[37]. For the fossil fuel case, this included the pump and the $1000 dollar side mount generator. For the electrical case, this included the pump and the panel. Additionally, from these case studies included estimates of $10,000 and $5,500 for electrical utility connections. Conservatively,

$10,000 was applied for all simulations. Costs were then adjusted from 2019 to 2023 using the Chemical Engineering Plant Cost Index[38].

A net present cost analysis was then performed for both natural gas and electrical pumps over a 20-year lifetime. Following the example of Milhollin et al., investment cost was depreciated over the lifetime of the pump, and an interest costs were calculated with an 8.5% annual rate[39]. As in Morata et al.'s example, salvage value was assumed negligible[37]. In addition to energy expenditures, operational costs included maintenance and insurance costs, estimated at 0.5% and 3% [39]. Property tax cost was assumed to be zero, as farms may deduct local taxes on farm equipment as a business expense [40]. As with the LCA, the energy demand per m^3 of water was calculated from the ecoinvent irrigation inventories and adjusted by efficiency factors for different fuel types. These were then multiplied by the corresponding electricity and fuel costs at the state level. All costs were normalized per m^3 of water cost. The net present value calculation was then performed using an internal rate of return of 10% as the discount rate, based on information from the University of Minnesota Center for Farm Financial Management [41]. Finally, the Argo Excel add-in was used to perform a 10,000 trial simulation, varying energy prices on uniform distributions [33].

The emissions mitigation potential of a natural gas-to-electric transition was calculated on a per m^3 of water basis. Using the methods described in Section C.1.2.2, the efficiency-adjusted energy demand values for the sprinkler-drip irrigation mix were determined for a natural gas pump and an electric pump on a per m^3 basis. These were then multiplied by the emission factor of natural gas combustion[15] and the subregional GRID 2022 emission factor[21].

C1.3.3 Machinery Electrification Costs

While considering off-road machinery electrification, Lund et al. noted the importance of total cost of ownership (TCO) in the uptake of new technologies, identifying electric vs. diesel TCO values as a field of further study[23]. While such evaluations exist for other alternative fuel technology tractors[42] and small compact BEV tractors[43], studies were not yet found for BEV farm machinery in the lettuce system 100-200 HP range. Thus, more readily available and robust TCO estimates for heavy duty on-road machines were adapted and used as a proxy. This proxy was based on the similarity between the challenges for agricultural machinery electrification and long-haul trucking electrification. BEV farm machinery would need to meet high power demands (e.g., tilling), operate continuously for long hours (e.g., during planting and harvest), and balance battery weight tradeoffs like soil compaction concerns[44]. Similarly, long-haul trucking challenges include high power demands for heavy loads, large storage requirements for long hours of operation, and battery weight tradeoffs regarding payloads. Thus, factors that impact the cost of BEV trucks (battery weight, manufacturing cost, charging, etc.) could similarly impact the cost of BEV tractors. Notably, since the high power demands of long-haul trucking are similar to high power tractors like the 9R series (see Section C1.2.3), using this proxy was possibly conservative for the lower-power tractors used in this lettuce crop model.

TCO estimates were adapted from Argonne National Laboratory's work estimating class 8 sleeper cab costs in 2025[45]. Within this report, the financial analysis utilized a real discount rate of 3.0% to account for changes in price due to inflation while calculating TCO's for comparisons of actual costs. The main body of that report published values for a "high technology progress case" impacting aspects like vehicle costs and energy efficiency; this work used the "high technology progress case" as a minimum estimate and the "Model Year 2020" values as the high-

cost case. Other such adaptations of high-low-cost cases were adapted for this work and are summarized in **Table C7**.

Table C7. *Summary of input variations for electrified machinery transition cost cases.*

Cost Case	ANL Case	BEV M&R Multiplier	BEV Efficiency (mi/DGE)	Elec. Price ($/kWh)	EVSE Cost ($/mi)	TIH	Payload ($/mi)	Charger Power (kW)	Labor ($/hr.)
High	MY20	0.79	11.59	0.34	0.16	2%	0.10	400	30
Low	High Prog.	0.41	14.67	0.102	0	1%	0	2000	17.59

Alterations of note include:

- Electrical Vehicle Supply Equipment (EVSE): Burnham et al. estimated the cost of this equipment as $0.10 per mile if it is not "amortized over multiple vehicles"[45]. As a conservative estimate, this work's high-cost case assumed the full cost is borne by one owner, i.e. each farm purchases EVSE and no credit is taken for multiple machines from that farm sharing EVSE. In contrast, the low-cost case assumed the cost is negligible, e.g., the EVSE cost is amortized over many vehicles on the farm or shared by multiple farms.
- Tax, Insurance, and Housing (TIH): class 8 vehicles on highways would face significantly different fees, taxes, and insurance rates compared to farm equipment. Thus, in the low-cost case, these costs were estimated as 1% of machinery cost as indicated by Edwards[46]. The high-cost case added an additional percent, as Edwards suggested to estimate the varying rates of local property taxes.
- Payload: in Burnham et al.'s report, this category reflected lost payload weight due to battery weight[45]. It was retained in the high-cost estimate as an analogue for similar

weight considerations for farm equipment (e.g., hauling less fertilizer in a particular run, prompting the cost of additional refills).

- Labor: Burnham et al. included this category as an estimate of the paid time drivers receive while fueling, calculated with the modeled battery capacity divided by an assumed charging power and multiplied by an hourly wage rate[45]. It was included here to reflect similar additional work hours on a farm; the high-cost hourly rate conservatively used Burnham et al.'s estimate for driver wages, while the low-cost case used an estimate for agricultural equipment operators from the USDA Economic Research Service[47].

Finally, the Argo Excel add-in was used to perform a 10,000 trial simulation of the TCO calculation, varying all price inputs on uniform distributions[33].

These TCO values were on a per-mile basis, while the ecoinvent inventory data were on a per-hectare basis. Thus, the distance traveled was estimated by dividing the area-based activity values by corresponding tool widths listed either in ecoinvent[15] or a California Extension lettuce crop budget[25]. The change in per-mile carbon intensity was calculated moving from a 100% diesel case (using the ecoinvent diesel combustion inventory) to a 100% electric case (using the eGRID 2022 California CF).

C1.3.4 Renewable Diesel Transition Costs

Quarterly average prices for RD and conventional diesel were obtained from the United States Department of Energy's Clean Cities Alternative Fuel Price reports from January 2017 to April 2024[48]. The difference was converted from a diesel gallon equivalent basis (LHV: 128,488 BTU $gallon^{-1}$) to a per MJ basis[49]. The maximum and minimum difference values were considered for the high-cost and low-cost transition scenarios. Then, the Argo Excel add-in was

used to perform a 10,000 trial simulation of the calculation, varying the difference inputs on a uniform distribution[33].

The CI of conventional diesel was determined using the ecoinvent 3.9 cutoff inventory for diesel burned in agricultural machinery[15], while the GWP of renewable diesel was based on Xu et al.'s estimate for soy-based diesel with an average of their reported LUC factors[14].

C1.4 Impact contributions of different greenhouse gases

Considering the relative contributions of different GHG's to the lettuce system carbon footprint, as in ***Figure C46***, provides additional insights into what the considered technological changes accomplish and what other opportunities remain for DLCA analysis. Notably, the mitigation measures included in this work primarily result in reducing carbon dioxide emissions. This phenomenon reflects that the technology transformations reduce combustion (e.g., electric pumps and low-emission upstream electricity), replace fossil fuel combustion emissions with biofuel combustion (e.g., renewable diesel), or mitigate CO_2 process emissions (e.g., CO_2 from fertilizer hydrogen synthesis processes). While these measures accomplish overall GHG emission reductions, the large and unchanging footprint of N_2O should be considered in future dynamic modeling efforts. As noted in **Section 4.3.1**, the relative contribution of N_2O will grow as CO_2 mitigation measures proceed, and thus nitrogen-focused measures like nitrogen efficiency technologies will need to be implemented in the sector.

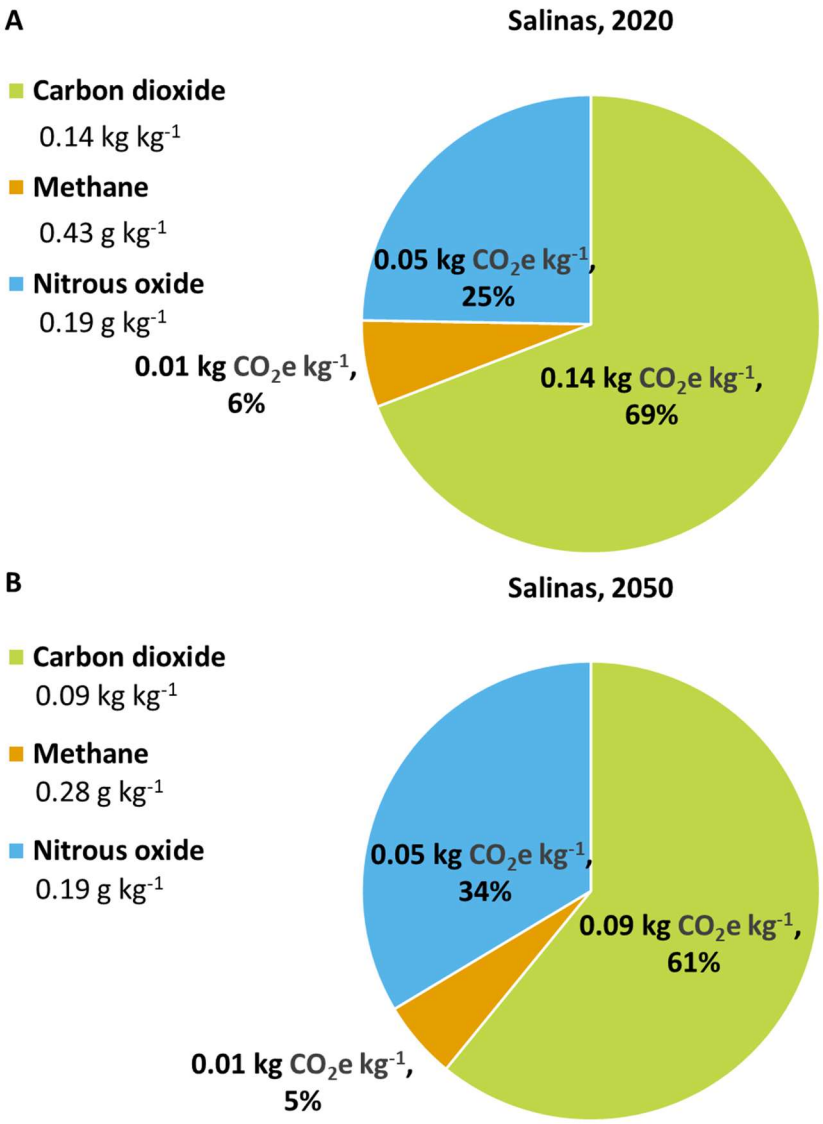

Figure C46. *Salinas, CA carbon footprint breakdowns for A) 2020 and B) 2050 (baseline change case) by GHG species. In the legend, mass of the gas emitted per kg of lettuce is shown, while the chart values show GWP-100 values. Note in this chapter that AR6 GWP-100 values are used.*

C2. Python codes used in dynamic process modeling

C2.1 Modified pyfao56 code

‘’’’’

~~~Rmaynard — adapted from pyfao56 for LOCA-CMIP5-Hydrology-daily dataset.
~~~

Changes of note:

Solar radiation: the LOCA dataset includes net shortwave and longwave radiation; rather than needing to calculate from total solar radiation by Eqs 16 and 17, just need to convert to perform Eq. 15, Rn=Rns-Rnl, and convert from W/m2 to MJ/m2/d. Note LOCA provides negative Rnl, so the calc is (+)

Due to limitations (i.e. the data available in loca) ea is calculated using the tmin method.

The refet.py module contains functions for computing short-crop or tall-crop reference evapotranspiration following the ASCE Standardized Reference Evapotranspiration Equation.

The ASCE Standarized Reference Evapotranspiration Equation is documented in the following publications: https://ascelibrary.org/doi/book/10.1061/9780784408056

ASCE Task Committee on Standardization of Reference Evapotranspiration (Walter, I. A., Allen, R. G., Elliott, R., Itenfisu, D., Brown, P., Jensen, M. E.,Mecham, B., Howell, T. A., Snyder, R., Eching, S., Spofford, T., Hattendorf, M., Martin, D., Cuenca, R. H., Wright, J. L.) , 2005. The ASCE Standardized Reference Evapotranspiration Equation. American Society of Civil Engineers, Reston, VA.

The refet.py module contains the following:

```
    ascedaily — function to compute daily ASCE Standardized Reference ET
    ascehourly — function to compute hourly ASCE Std. Reference ET

01/07/2016 Initial Python script by Kelly Thorp
11/04/2021 Finalized updates for inclusion in pyfao56 Python package
08/01/2022 Added the ASCE hourly reference ET algorithm
08/03/2022 Added functionality to input vapor pressure
-----------------------------------------------------------------------
"""

import math

def ascedaily(rfcrp,z,lat,doy,rns,rnl,tmax,tmin,
              wndsp=float('NaN'),wndht=2.0):
    """Compute daily ASCE Standardized Reference Evapotranspiration

    Parameters
    ----------
    rfcrp : str
        'S' for the short reference crop (0.12-m grass)
        'T' for the tall reference crop (0.50-m alfalfa)
    z : float
        Weather site elevation above mean sea level (m)
    lat : float
        Latitude of the weather site (decimal degrees)
    doy : float
        Day number of the year between 1 and 366
    rns : float
        net shortwave radiation (MJ m^-2 d^-1)
```

rnl : float

net longwave radiation (MJ m^-2 d^-1)

tmax : float

Daily maximum air temperature (deg C)

tmin : float

Daily minimum air temperature (deg C)

vapr : float, optional (but recommended)

Daily average vapor pressure (kPa) (default = NaN)

tdew : float, optional (but recommended)

Daily average dew point temperature (deg C) (default = NaN)

rhmax : float, optional

Daily maximum relative humidity (%) (default = NaN)

rhmin : float, optional

Daily minimum relative humidity (%) (default = NaN)

wndsp : float, optional (but recommended)

Daily average wind speed (m s^-1) (default = NaN)

wndht : float, optional (but recommended)

Height of wind measurement above the ground (m) (default = 2.0)

Returns

---

etsz : float

Daily standardized reference evapotranspiration for the

short or tall reference crop (mm)

“””

#tavg (float) : Mean daily air temperature (deg C)

#ASCE (2005) Eq. 2

```
tavg = (tmax+tmin)/2.0

#patm (float) : Mean atmospheric pressure at weather station (kPa)
#ASCE (2005) Eq. 3
patm = 101.3*((293.0-0.0065*z)/293.0)**5.26

#psycon (float) : Psychrometric constant (kPa (deg C)^-1)
#ASCE (2005) Eq. 4
psycon = 0.000665*patm

#Udelta (float) : Slope of the saturation vapor pressure
#temperature curve (kPa (deg C)^-1)
#ASCE (2005) Eq. 5
Udelta = 2503.0*math.exp(17.27*tavg/(tavg+237.3))
Udelta = Udelta/((tavg+237.3)**2.0)

#es (float) : Saturation vapor pressure (kPa)
#ASCE (2005) Eqs. 6 and 7
emax = 0.6108*math.exp((17.27*tmax)/(tmax+237.3))
emin = 0.6108*math.exp((17.27*tmin)/(tmin+237.3))
es = (emax+emin)/2.0

#ea (float): Actual vapor pressure (kPa) ASCE (2005) Table 3
   #ASCE (2005) Appendix E
tdew = tmin — 2.0
ea = 0.6108*math.exp((17.27*tdew)/(tdew+237.3))

#rns (float) : Net shortwave radiation (MJ m^-2 d^-1)
```

```
#ASCE (2005) Eq. 16
albedo = 0.23
# rns = (1.0-albedo)*israd

#ra (float) : Extraterrestrial radiation (MJ m^-2 d^-1)
#ASCE (2005) Eqs. 21-27
# latrad = lat*math.pi/180.0 #Eq. 22
# dr = 1.0+0.033*math.cos(2.0*math.pi/365.0*doy) #Eq. 23
# ldelta = 0.409*math.sin(2.0*math.pi/365.0*doy-1.39) #Eq. 24
# ws = math.acos(-1.0*math.tan(latrad)*math.tan(ldelta)) #Eq. 27
# ra1 = ws*math.sin(latrad)*math.sin(ldelta) #Eq. 21
# ra2 = math.cos(latrad)*math.cos(ldelta)*math.sin(ws) #Eq. 21
# ra = 24.0/math.pi*4.92*dr*(ra1+ra2) #Eq. 21

#rso (float) : Clear sky solar radiation (MJ m^-2 d^-1)
#ASCE (2005) Eq. 19
# rso = (0.75+2e-5*z)*ra

#rnl (float) : Net longwave radiation (MJ m^-2 d^-1)
#ASCE (2005) Eqs. 17 and 18
# ratio = sorted([0.3,israd/rso,1.0])[1]
# fcd = sorted([0.05,1.35*ratio-0.35,1.0])[1] #Eq. 18
# tk4 = ((tmax+273.16)**4.0+(tmin+273.16)**4.0)/2.0 #Eq. 17
# rnl = 4.901e-9*fcd*(0.34-0.14*math.sqrt(ea))*tk4 #Eq. 17

#rn (float) : Net radiation (MJ m^-2 d^-1)
#ASCE (2005) Eq. 15
rn = rns+rnl
```

```
    #g (float) : Soil heat flux (MJ m^-2 d^-1)
    #ASCE (2005) Eq. 30
    g = 0.0

    #u2 (float) : Wind profile relationship (m s^-1)
    #ASCE (2005) Eq. 33 and Appendix E
    if math.isnan(wndsp): wndsp = 2.0
    u2 = wndsp * (4.87/math.log(67.8*wndht-5.42))

    #Aerodynamic roughness and surface resistance constants
    #ASCE (2005) Table 1
    if rfcrp == 'S': #Short reference crop (0.12-m grass)
       Cn = 900.0  #K mm s^3 Mg^-1 d^-1
       Cd = 0.34   #s m^-1
    elif rfcrp == 'T': #Tall reference crop (0.50-m alfalfa)
       Cn = 1600.0 #K mm s^3 Mg^-1 d^-1
       Cd = 0.38   #s m^-1

    #etsz (float) : Standardized daily reference crop ET (mm d^-1)
    #ASCE (2005) Eq. 1
    etsz = 0.408*Udelta*(rn-g)+psycon*(Cn/(tavg+273.0))*u2*(es-ea)
    etsz = etsz/(Udelta+psycon*(1.0+Cd*u2))

    return etsz

def ascehourly(rfcrp,z,lat,lon,lzn,doy,sct,israd,tavg,vapr=float('NaN'),
            tdew=float('NaN'),rhum=float('NaN'),tmin=float('NaN'),
wndsp=float('NaN'),wndht=2.0,tl=1.0,csreq='D',fcdpt=1.0):
```

“””Compute hourly ASCE Standardized Reference Evapotranspiration

Parameters

---

rfcrp : str

‘S’ for the short reference crop (0.12-m grass)

‘T’ for the tall reference crop (0.50-m alfalfa)

z : float

Weather site elevation above mean sea level (m)

lat : float

Latitude of the weather site (decimal degrees)

lon : float

Longitude of the weather site (decimal degrees)

lzn : float

Longitude of the center of the local time zone (decimal degrees)

doy : float

Day number of the year between 1 and 366

sct : float

Standard clock time at the midpoint of the period (h)

For the period between 1400-1500 hours, sct = 14.5 h

israd : float

Incoming solar radiation (MJ m^-2 d^-1)

tavg : float

Average air temperature (deg C)

vapr : float, optional (but recommended)

Average vapor pressure (kPa) (default = NaN)

tdew : float, optional (but recommended)

Average dew point temperature (deg C) (default = NaN)

rhum : float, optional

Average relative humidity (%) (default = NaN)

tmin : float, optional

Daily minimum air temperature (deg C) (default = NaN)

wndsp : float, optional (but recommended)

Average wind speed (m s^-1) (default = NaN)

wndht : float, optional (but recommended)

Height of wind measurement above the ground (m) (default = 2.0)

tl : float, optional

Length of the calculation period (h) (default = 1.0)

csreq : str, optional

'S' for the simple Eq. 47 for clear sky solar radiation

'D' for the complex method in Appendix D (default = 'D')

fcdpt : float, optional

Cloudiness value (fcd) from previous timestep (default = 1.0)

Returns

---

etsz : float

Hourly standardized reference evapotranspiration for the

short or tall reference crop (mm)

fcd : Cloudiness value for possible use in next timestep

""

#patm (float) : Mean atmospheric pressure at weather station (kPa)

#ASCE (2005) Eq. 34

patm = 101.3*((293.0-0.0065*z)/293.0)**5.26

```
#psycon (float) : Psychrometric constant (kPa (deg C)^-1)
#ASCE (2005) Eq. 35
psycon = 0.000665*patm

#Udelta (float) : Slope of the saturation vapor pressure
#temperature curve (kPa (deg C)^-1)
#ASCE (2005) Eq. 36
Udelta = 2503.0*math.exp(17.27*tavg/(tavg+237.3))
Udelta = Udelta/((tavg+237.3)**2.0)

#es (float) : Saturation vapor pressure (kPa)
#ASCE (2005) Eq. 37
es = 0.6108*math.exp((17.27*tavg)/(tavg+237.3))

#ea (float): Actual vapor pressure (kPa) ASCE (2005) Table 4
if not math.isnan(vapr):
   #ASCE (2005) Table 4
   ea = vapr
elif not math.isnan(tdew):
   #ASCE (2005) Eq. 38
   ea = 0.6108*math.exp((17.27*tdew)/(tdew+237.3))
elif not math.isnan(rhum):
   #ASCE (2005) Eq. 41
   ea = es*rhum/100.
Else:
   #ASCE (2005) Appendix E
   tdew = tmin — 2.0
   ea = 0.6108*math.exp((17.27*tdew)/(tdew+237.3))
```

```
#rns (float) : Net shortwave radiation (MJ m^-2 h^-1)
#ASCE (2005) Eq. 43
albedo = 0.23
rns = (1.0-albedo)*israd

#ra (float) : Extraterrestrial radiation (MJ m^-2 h^-1)
#ASCE (2005) Eqs. 48-58
dr = 1.0+0.033*math.cos(2.0*math.pi/365.0*doy) #Eq. 50
ldelta = 0.409*math.sin(2.0*math.pi/365.0*doy-1.39) #Eq. 51
b = 2.0*math.pi*(doy-81.0)/364.0 #Eq. 58
sc = 0.1645*math.sin(2.0*b)-0.1255*math.cos(b)-0.025*math.sin(b) #57
wmid = math.pi/12.0*((sct+0.06667*(lzn-lon)+sc)-12.) #Eq. 55
w1 = wmid-math.pi*tl/24.0 #Eq. 53
w2 = wmid+math.pi*tl/24.0 #Eq. 54
latrad = lat*math.pi/180.0 #Eq. 49
ws = math.acos(-1.0*math.tan(latrad)*math.tan(ldelta)) #Eq. 59
if w1 < -1.0*ws: w1 = -1.0*ws #Eq. 56
if w2 < -1.0*ws: w2 = -1.0*ws #Eq. 56
if w1 > ws: w1 = ws #Eq. 56
if w2 > ws: w2 = ws #Eq. 56
if w1 > w2: w1 = w2 #Eq. 56
ra1 = (w2-w1)*math.sin(latrad)*math.sin(ldelta) #Eq. 48
ra2 = math.cos(latrad)*math.cos(ldelta) #Eq. 48
ra3 = math.sin(w2)-math.sin(w1) #Eq. 48
if wmid < -1.0*ws or wmid > ws:
    ra = 0.0
else:
```

```
    ra = 12.0/math.pi*4.92*dr*(ra1+ra2*ra3) #Eq. 48

#rso (float) : Clear sky solar radiation (MJ m^-2 h^-1)
#ASCE (2005) Eq. 47 and Appendix D
beta1 = math.sin(latrad)*math.sin(ldelta)
beta2 = math.cos(latrad)*math.cos(ldelta)*math.cos(wmid)
beta = math.asin(beta1+beta2) #Eq. 62 or D.6
if csreq == 'S':
    rso = (0.75+2e-5*z)*ra #Eq. 47
else:
    if beta < 0.3:
        rso = 0.0
    else:
        pwat = 0.14*ea*patm+2.1 #Eq. D.3
        kt = 1.0
        kb1 = -0.00146*patm/(kt*math.sin(beta))
        kb2 = 0.075*(pwat/math.sin(beta))**0.4
        kb = 0.98*math.exp(kb1-kb2) #Eq. D.2
        if kb >= 0.15:
            kd = 0.35-0.36*kb #Eq. D.4
        else:
            kd = 0.18+0.82*kb #Eq. D.4
        rso = (kb + kd)*ra #Eq. D.1

#rnl (float) : Net longwave radiation (MJ m^-2 h^-1)
#ASCE (2005) Eqs. 44, 45, and 62
if beta < 0.3 or rso <= 0.0: #nighttime
    fcd = fcdpt
```

```
else: #daytime
    ratio = sorted([0.3,israd/rso,1.0])[1] #Eq. 45
    fcd = sorted([0.05,1.35*ratio-0.35,1.0])[1] #Eq. 45
tk4 = (tavg+273.16)**4.0 #Eq. 44
rnl = 2.042e-10*fcd*(0.34-0.14*math.sqrt(ea))*tk4 #Eq. 44

#rn (float) : Net radiation (MJ m^-2 h^-1)
#ASCE (2005) Eq. 42
rn = rns+rnl

#g (float) : Soil heat flux (MJ m^-2 h^-1)
#ASCE (2005) Eqs. 65 and 66
#Aerodynamic roughness and surface resistance constants
#ASCE (2005) Table 1
if rfcrp == 'S': #Short reference crop (0.12-m grass)
    Cn = 37.0 #K mm s^3 Mg^-1 h^-1
    if rn < 0.0: #nighttime
        g = 0.5*rn
        Cd = 0.96 #!s m^-1
    else: #daytime
        g = 0.1*rn
        Cd = 0.24 #!s m^-1
elif rfcrp == 'T': #Tall reference crop (0.50-m alfalfa)
    Cn = 66.0 #K mm s^3 Mg^-1 h^-1
    if rn < 0.0: #nighttime
        g = 0.2*rn
        Cd = 1.7 #!s m^-1
    else: #daytime
```

```
        g = 0.04*rn
        Cd = 0.25 #!s m^-1

    #u2 (float) : Wind profile relationship (m s^-1)
    #ASCE (2005) Eq. 67 and Appendix E
    if math.isnan(wndsp): wndsp = 2.0
    u2 = wndsp * (4.87/math.log(67.8*wndht-5.42))

    #etsz (float) : Standardized daily reference crop ET (mm h^-1)
    #ASCE (2005) Eq. 1
    etsz = 0.408*Udelta*(rn-g)+psycon*(Cn/(tavg+273.0))*u2*(es-ea)
    etsz = etsz/(Udelta+psycon*(1.0+Cd*u2))

    return (etsz, fcd)
```

C2.2 AquaCrop code

```
# -*- coding: utf-8 -*-
“””
Created on Wed Apr 24 10:42:40 2024

@author: mrmaynar
“””

#%% Package cell
import math
import refet_RM as RET
import pandas as pd
import os
from tqdm import tqdm
```

```
from pathlib import Path

from aquacrop import AquaCropModel, Soil, Crop, InitialWaterContent, IrrigationManagement

from aquacrop.utils import prepare_weather, get_filepath


#%% Targets Cell

yearnum = 2020

if yearnum ==2035:#to handle a quirk with years just before a leap year. In this 5 year step initial set, only 2035-36 has the issue.

    Endday = 30#for seasons that cross new year, the first year's data are copypasted

else: #but in a year before leap year, 365 copypasted doesn't fill all 366 days

    endday = 31#AquaCrop won't work if data are missing in sim period; this workaround cuts out the "missing day"


year = year = str(yearnum) #What year we are running

Targetlist = '\\Target_Locations_Seasons_25April2024.xlsx' #What list of locations/seasons we are running

Specialtag = '25April2024' #Helps identify scenarios


#%% Location target cell

listpath = 'C:\\Users\\mrmaynar\\Documents\\Python Scripts\\Dynamic LCA'

locationdf = pd.read_excel(listpath+Targetlist,sheet_name='Initial')#Import I locations/seasons list

copyofloc = locationdf.copy(deep=True)

output = copyofloc.drop(['Lat','Elevation(m)','soildatebit'],axis=1)#preparing an output df

output['Year'] = yearnum

output['ActualHarvestDate'] = 999

output['DryYield(tons)'] = 999

output['Irrigation(mm)'] = 999
```

dummypath = listpath+'\\'+year+'_format_new.xlsx' #This is to point to "dummy" Excel files that format the file for AC (min,max,pr,ET0,Date) for particular year (different year files for handling leap year)

"New" refers to creating a two year range to allow for new year rollover seasons

path = Path(listpath) #Path for os tools

pathforcwd = os.getcwd()

#Variable names to help

climatevs = ['tasmin','tasmax','pr'] #climate variable names

hydrovs = ['shortwave_net','longwave_net','windspeed'] #hydrology variable names

soilvs = ['soilMoist1','soilMoist2','soilMoist3']#soil moisture var names

mmlayer = [100,400,1100]#mm depths in loca5, needed to adjust to fraction

rfcrp = 'S' #S for short reference, T for tall reference in ET calcs

#List of loca5 climate mnodel names, for later scenario/uncertainty work

scenarios = pd.read_csv('COLS_loca.txt')

scenariolist = list(scenarios['Scenarios'])

#%% AquaCrop Setup

#Irrigation Settings

Maxperday=25 #Maximum depth (mm) that can be applied each day

#Maxperseason = 340 #Maximum depth (mm) if testing droughts

SM = 70 # Soil moisture targets (%TAW)

AE = 90 #Application eff

seeds = 388000 #previous work 388000. CA Extension: 258k — 582k

#%%

runscount = len(scenariolist)*len(locationdf)

#lists to append to

loclist = []

```
TMYlist = []
Yearlist = []
Seasonlist = []
modellist = []
yieldlist= []
irriglist = []
faillist = []

for y in tqdm(range(len(locationdf))):#run through all location/seasons in targetlist. Includes pull-ins used for ET and AquaCrop

    Location = locationdf.at[y,'Location']
    Season = 'Season'+str(locationdf.at[y,'Season'])
    print(Location, Season)
    TMY = locationdf.at[y,'TMY']
    soiltag = locationdf.at[y,'Soil']
    simsoil = Soil(soil_type=soiltag) #AquaCrop Soil
    strt = locationdf.at[y,'Start'] #Simulation start date for this loc/season
    hrvst = locationdf.at[y,'End'] #Simulation end date for this loc/season
    soilmoday = locationdf.at[y,'soildatebit'] #Helps pull start date soil moisture
    rollover = locationdf.at[y,'YearRollover'] #Helps handle seasons that cross into new year
    endyear = yearnum+rollover
    z = locationdf.at[y,'Elevation(m)']
    lat = locationdf.at[y,'Lat']
    datapath =  os.path.join(path, Location)#Path to place where location climate and hydro files are

    #Setup crop, including plant/harv date
    lettuce = Crop('TomatoGDD',
```

```
                planting_date=strt,harvest_date=hrvst,CropType=1,
                b_HI = -9,CCx = 0.75,CDC = 0.008,CGC=0.01281,
                dHI0 = -9,Emergence = 210,exc=20,Flowering=-999,
                fshape_w1 = 1,fshape_w4 = 3,GDD_up=11.1,GDDmethod=2,
                HI0=0.95,Histart=600,Maturity=1130,MaxRooting=830,
                p_up1=0.25,p_up3=0.85,p_up4=0.9,PlantMethod=1,
                PlantPop=388000,SeedSize=5.0,Senescence=1020,
                SwitchGDD=1,Tbase=4.4,Tmin_up=8,TrColdStress=1,
                Tupp=30,WP=17,YldForm=230,Zmax=0.7)
    #Irrigation
    #irr_mngt =
IrrigationManagement(irrigation_method=1,SMT=[SM,SM,SM,SM],MaxIrrSeason=Maxperseas
on,AppEff=AE)
    irr_mngt =
IrrigationManagement(irrigation_method=1,SMT=[SM,SM,SM,SM],MaxIrr=Maxperday,AppEf
f=AE)
    #drought_mngt =
IrrigationManagement(irrigation_method=1,SMT=[SM,SM,SM,SM],MaxIrrSeason=Maxperseas
on,AppEff=AE)
```

```
    for c in range(32):#there are 32 climate models in loca5
        try:
            dftest = pd.read_excel(dummypath,sheet_name='Climate') #from dummy, prepare a df to
hold climate data
            climateout= dftest.columns.values.tolist() #list to handle incoming data
            dfhydro = pd.read_excel(dummypath,sheet_name='Hydrology') #from dummy, prepare a
df to hold hydro data
            hydroout= dfhydro.columns.values.tolist() #list to handle incoming data
```

```
dfsoil = pd.read_excel(dummypath,sheet_name='SoilMoisture') #from dummy, prepare a df to hold soil m data

soilout= dfsoil.columns.values.tolist() #list to handle incoming data


#Now work up the climate data

for x in range(len(climatevs)):#for each climate variable

    vpath = os.path.join(datapath,'Climate'+year,'loca5', climatevs[x]+'.csv')#csv path

    tasmin = pd.read_csv(vpath,header=None)#open the climate data csv

    cleaned = tasmin.drop([0,1,2],axis=1) #drop the dates

    cop = cleaned.copy(deep=True) #Create a copy to help with rollover seasons

    twoyearc = pd.concat([cleaned,cop],ignore_index=True)#twoyear long df

    dftest[climateout[x]]=twoyearc[c+3]#average all scenarios <-could be wear choose model of 32 instead

for x in range(len(hydrovs)):#for each hydro variable

    vpath = os.path.join(datapath,'Hydro'+year,'loca_hydro5', hydrovs[x]+'.csv')

    tasmin = pd.read_csv(vpath,header=None)#open the hydro data csv

    cleaned = tasmin.drop([0,1,2],axis=1) #drop the dates

    cop = cleaned.copy(deep=True) #Create a copy to help with rollover seasons

    twoyearh = pd.concat([cleaned,cop],ignore_index=True)#twoyear long df

    dfhydro[hydroout[x]]=twoyearh[c+3]#average all scenarios <-could be wear choose model of 32 instead

for x in range(len(soilvs)):#for each soil variable

    vpath = os.path.join(datapath,'Hydro'+year,'loca_hydro5', soilvs[x]+'.csv')

    tasmin = pd.read_csv(vpath,header=None)#open the soil data csv

    cleaned = tasmin.drop([0,1,2],axis=1) #drop the dates

    cop = cleaned.copy(deep=True) #Create a copy to help with rollover seasons

    twoyears = pd.concat([cleaned,cop],ignore_index=True)#twoyear long df

    dfsoil[soilout[x+1]]=twoyears[c+3]/mmlayer[x]#average all scenarios, convert to fraction <-could be wear choose model of 32 instead. "x+1" is due to there being a date in position 0
```

```
for I in range(len(dfhydro.index)):#Creating the ET0 for each day
    Tmax = dftest.at[I,'MaxTemp']
    Tmin = dftest.at[I,'MinTemp']
    Tavg = (Tmax+Tmin)/2
    day = i+1
    rns = dfhydro.at[I,'rns']*86400/1000000#net shortwave radiation, 180issou W/m2->MJ/d/m2
    rnl = dfhydro.at[I,'rnl']*86400/1000000 #net longwave radiation
    wndsp = dfhydro.at[I,'wndsp']
    #vapr = PL.GetVapPresFromRelHum(Tavg, RH)*0.001
    Etref = RET.ascedaily(rfcrp,z,lat,day,rns,rnl,Tmax,Tmin,wndsp,2.0)
    dftest.at[I,'ReferenceET'] = Etref #Completing the data that input to AquaCrop

#************With climate data worked up, time to run AquaCrop*********************
weather_data = dftest.copy(deep=True) #copy to make consolidation simple for now
weather_data.ReferenceET.clip(lower=0.1, inplace=True) #copied from "prepare weather" tool

####Soil moisture options
#Type 1
#InitWC = InitialWaterContent(value=['FC'])
#Type 2
SM_data = dfsoil.copy(deep=True) #copy to make consolidation simple for now
soilymd = year+soilmoday
soildate = (SM_data['Date'] == soilymd)
soiliWC = SM_data.loc[soildate]
L1=round(soiliWC.iloc[0]['0.1m'],3)
```

```
L2=round(soiliWC.iloc[0]['0.5m'],3)
L3=round(soiliWC.iloc[0]['1.6m'],3)
InitWC = InitialWaterContent(wc_type = 'Num',
                             method = 'Depth',
                             depth_layer= [0.1,0.5,1.6],
                             value = [L1, L2, L3])



simstart = f'{yearnum}/01/01'#added 3/20
simend= f'{endyear}/12/{endday}'#added 3/20
model = AquaCropModel(sim_start_time=simstart,
                      sim_end_time=simend,
                      weather_df=weather_data,
                      soil=simsoil,
                      crop=lettuce,
                      initial_water_content=InitWC,
                      irrigation_management=irr_mngt)
model.run_model(till_termination=True)
result2050=[model._outputs.final_stats]
growth2050 = [model._outputs.crop_growth]
flux2050 =[model._outputs.water_flux]
df2050 = result2050[0] #a small df with the yield and irrigation for this location/season in
this year


#**********now that AquaCrop is run, time to send this result for the location/season
in this year somewhere**********
result2050 = df2050.copy(deep=True) #copy to make consolidation simple for now
loclist.append(Location)
Yearlist.append(year)
```

```
            Seasonlist.append(Season)
            modellist.append(scenariolist[c])
            TMYlist.append(TMY)
            Yield = result2050.at[0,'Dry yield (tonne/ha)']
            yieldlist.append(Yield)
            Irr = result2050.at[0,'Seasonal irrigation (mm)']
            irriglist.append(Irr)
        except:
            f = Location + '_'+Season+'_'+scenariolist[c]
            faillist.append(f)
            pass

d = pd.DataFrame()
d['Location'] = loclist
d['Year'] = Yearlist
d['TMY'] = TMYlist
d['Climate Model'] = modellist
d['Dry yield (tonne/ha)'] = yieldlist
d['Seasonal irrigation (mm)'] = irriglist

d2=d.copy(deep=True)
#set up a season-specific output dataframe
dseason=d.copy(deep=True)
dseason['Season'] = Seasonlist
dseason2=dseason.copy(deep=True)
#And a raw output for deeper exploration, if desired
allresults=dseason.copy(deep=True)
d = d.groupby(['TMY']).agg({'Year': 'first',
```

```
                'Location': 'first',
                'Climate Model': 'first',
                'Dry yield (tonne/ha)': 'mean',
                'Seasonal irrigation (mm)': 'mean'})
d2 = d2.groupby(['TMY']).agg({'Year': 'first',
                'Location': 'first',
                'Climate Model': 'first',
                'Dry yield (tonne/ha)': 'std',
                'Seasonal irrigation (mm)': 'std'})
dseason = dseason.groupby(['TMY','Season']).agg({'Year': 'first',
                'Location': 'first',
                'Climate Model': 'first',
                'Dry yield (tonne/ha)': 'mean',
                'Seasonal irrigation (mm)': 'mean'})
dseason2 = dseason2.groupby(['TMY','Season']).agg({'Year': 'first',
                'Location': 'first',
                'Climate Model': 'first',
                'Dry yield (tonne/ha)': 'std',
                'Seasonal irrigation (mm)': 'std'})
failures = pd.DataFrame()
failures['Failed Runs'] = faillist


outname =
os.path.join(pathforcwd,'Outputs','Summaries','Results_'+year+'_'+Specialtag+'_multimodel'
+'.xlsx')
writer = pd.ExcelWriter(outname)
d.to_excel(writer, sheet_name = 'Average',index=True)
d2.to_excel(writer, sheet_name = 'stdev',index=True)
dseason.to_excel(writer, sheet_name = 'Season Average',index=True)
```

```
dseason2.to_excel(writer, sheet_name = ‘Season stdev’,index=True)

allresults.to_excel(writer, sheet_name = ‘Raw’,index=True)

failures.to_excel(writer, sheet_name = ‘FailedRuns’,index=True)

writer.close()

# #outname =
os.path.join(pathforcwd,’Outputs’,’Summaries’,’Initialtargetresults_’+Specialtag+’_model_’+sc
enariolist[0]+’.xlsx’)  #for running multiple climate models
```

Appendix C References

(1) Vanuytrecht, E.; Raes, D.; Steduto, P.; Hsiao, T. C.; Fereres, E.; Heng, L. K.; Garcia Vila, M.; Mejias Moreno, P. AquaCrop: FAO's Crop Water Productivity and Yield Response Model. *Environ. Model. Softw.* **2014**, *62*, 351–360. https://doi.org/10.1016/j.envsoft.2014.08.005.

(2) Foster, T.; Brozović, N.; Butler, A. P.; Neale, C. M. U.; Raes, D.; Steduto, P.; Fereres, E.; Hsiao, T. C. AquaCrop-OS: An Open Source Version of FAO's Crop Water Productivity Model. *Agric. Water Manag.* **2017**, *181*, 18–22. https://doi.org/10.1016/j.agwat.2016.11.015.

(3) Maynard, R.; Burkhardt, J.; Quinn, J. C. Sustainability of Lettuce Production: A Comparison of Local and Centralized Food Production. *J. Clean. Prod.* **2023**, *428*, 139224. https://doi.org/10.1016/j.jclepro.2023.139224.

(4) Maurer, E. P.; Brekke, L.; Pruitt, T.; Duffy, P. B. Fine-resolution Climate Projections Enhance Regional Climate Change Impact Studies. *Eos Trans. Am. Geophys. Union* **2007**, *88* (47), 504–504. https://doi.org/10.1029/2007EO470006.

(5) Pierce, D. W.; Cayan, D. R.; Thrasher, B. L. Statistical Downscaling Using Localized Constructed Analogs (LOCA)*. *J. Hydrometeorol.* **2014**, *15* (6), 2558–2585. https://doi.org/10.1175/JHM-D-14-0082.1.

(6) Vano, J.; Hamman, J.; Gutmann, E.; Wood, A.; Mizukami, N.; Clark, M.; Pierce, D. W.; Cayan, D. R.; Wobus, C.; Nowak, K.; Arnold, J. *Comparing Downscaled LOCA and BCSD CMIP5 Climate and Hydrology Projections — Release of Downscaled LOCA CMIP5 Hydrology*; 2020. https://gdo-dcp.ucllnl.org/downscaled_cmip_projections/techmemo/LOCA_BCSD_hydrology_tech_memo.pdf (accessed 2024-01-11).

(7) Liang, X.; Wood, E. F.; Lettenmaier, D. P. Surface Soil Moisture Parameterization of the VIC-2L Model: Evaluation and Modification. *Glob. Planet. Change* **1996**, *13* (1–4), 195–206. https://doi.org/10.1016/0921-8181(95)00046-1.

(8) Thorp, K. R.; Brekel, J.; DeJonge, K. C. Version 1.2.0 — Pyfao56: FAO-56 Evapotranspiration in Python. *SoftwareX* **2023**, *24*, 101518. https://doi.org/10.1016/j.softx.2023.101518.

(9) Boyce, J.; Sacchi, R.; Goetheer, E.; Steubing, B. A Prospective Life Cycle Assessment of Global Ammonia Decarbonisation Scenarios. *Heliyon* **2024**, *10* (6), e27547. https://doi.org/10.1016/j.heliyon.2024.e27547.

(10) Liu, X.; Cai, H.; Kwon, H.; Wang, M. FEEDSTOCK CARBON INTENSITY CALCULATOR (FD-CIC) Model, 2023. https://greet.anl.gov/tool_fd_cic.

(11) United Nations Environment Programme. *Emissions Gap Report 2023: Broken Record – Temperatures Hit New Highs, yet World Fails to Cut Emissions (Again)*; United Nations Environment Programme, 2023. https://doi.org/10.59117/20.500.11822/43922.

(12) IEA. *Hydrogen*; IEA: Paris, 2023. https://www.iea.org/reports/hydrogen-2156 (accessed 2024-02-12).

(13) Arvidsson, R.; Tillman, A.; Sandén, B. A.; Janssen, M.; Nordelöf, A.; Kushnir, D.; Molander, S. Environmental Assessment of Emerging Technologies: Recommendations for Prospective LCA. *J. Ind. Ecol.* **2018**, *22* (6), 1286–1294. https://doi.org/10.1111/jiec.12690.

(14) Xu, H.; Ou, L.; Li, Y.; Hawkins, T. R.; Wang, M. Life Cycle Greenhouse Gas Emissions of Biodiesel and Renewable Diesel Production in the United States. *Environ. Sci. Technol.* **2022**, *56* (12), 7512–7521. https://doi.org/10.1021/acs.est.2c00289.

(15) Wernet, G.; Bauer, C.; Steubing, B.; Reinhard, J.; Moreno-Ruiz, E.; Weidema, B. The Ecoinvent Database Version 3 (Part I): Overview and Methodology. *Int. J. Life Cycle Assess.* **2016**, *21* (9), 1218–1230. https://doi.org/10.1007/s11367-016-1087-8.

(16) van der Meide, M.; Sacchi, R. ScenarioLink: An Activity Browser Plugin for Scenario-Based LCA Databases, 2024. https://github.com/185isso/ScenarioLink.

(17) U.S. Energy Information Administration. Annual Energy Outlook 2023 Table 11. Petroleum and Other Liquids Supply and Disposition, 2023.

https://www.eia.gov/outlooks/aeo/data/browser/#/?id=11-AEO2023&region=0-0&cases=ref2023&start=2021&end=2050&f=A&linechart=~~ref2023-d020623a.27-11-AEO2023~ref2023-d020623a.53-11-AEO2023&map=&ctype=linechart&sourcekey=0 (accessed 2024-08-07).
(18) U.S. Energy Information Administration. U.S. No 2 Diesel Adj Sales/Deliveries to Farm Consumers, 2022. https://www.eia.gov/dnav/pet/hist/LeafHandler.ashx?n=PET&s=K2DVAFNUS1&f=A (accessed 2024-08-07).
(19) Driscoll, A. W.; Conant, R. T.; Marston, L. T.; Choi, E.; Mueller, N. D. Greenhouse Gas Emissions from US Irrigation Pumping and Implications for Climate-Smart Irrigation Policy. *Nat. Commun.* **2024**, *15* (1), 675. https://doi.org/10.1038/s41467-024-44920-0.
(20) National Agricultural Statistics Service. *2018 Irrigation and Water Management Survey*; AC-17-SS-1; United States Department of Agriculture: Washington, DC, 2019. https://www.nass.usda.gov/Publications/AgCensus/2017/Online_Resources/Farm_and_Ranch_Irrigation_Survey/index.php (accessed 2024-04-10).
(21) United States Environmental Protection Agency (EPA). *Emissions & Generation Resource Integrated Database (eGRID), 2020.*; Office of Atmospheric Protection, Clean Air Markets Division: Washington DC, 2022. https://www.epa.gov/egrid (accessed 2024-05-01).
(22) Gagnon, P.; Cowiestoll, B.; Schwarz, M. *Cambium 2022 Scenario Descriptions and Documentation*; NREL/TP-6A40-84916, 1915250, MainId:85689; 2023; p NREL/TP-6A40-84916, 1915250, MainId:85689. https://doi.org/10.2172/1915250.
(23) Lund, J.; Slosky, J.; Whitson, J.; McLane, R. *Technology and Market Assessment of Zero-Emission Off-Road Equipment*; CALSTART, 2022. https://calstart.org/off-road-assessment/ (accessed 2024-09-03).
(24) John Deere & Company. 2023 Business Impact Report, 2023. https://about.deere.com/en-us/sustainability#download-reports (accessed 2024-07-30).
(25) Tourte, L.; Smith, R.; Murdock, J.; Goodrich, B. Sample Costs to Produce and Harvest Romaine Hearts Lettuce, 2023. https://coststudies.ucdavis.edu/current/commodities/lettuce (accessed 2024-08-27).
(26) Wang, M.; Elgowainy, A.; Lee, U.; Baek, K.; Balchandani, S.; Benavides, P.; Burnham, A.; Cai, H.; Chen, P.; Gan, Y.; Gracida-Alvarez, U.; Hawkins, T.; Huang, T.-Y.; Iyer, R.; Kar, S.; Kelly, J.; Kim, T.; Kolodziej, C.; Lee, K.; Liu, X.; Lu, Z.; Masum, F.; Morales, M.; Ng, C.; Ou, L.; Poddar, T.; Reddi, K.; Shukla, S.; Singh, U.; Sun, L.; Sun, P.; Sykora, T.; Vyawahare, P.; Zhang, J. Greenhouse Gases, Regulated Emissions, and Energy Use in Technologies Model ® (2023 Excel), 2023. https://doi.org/10.11578/GREET-EXCEL-2023/DC.20230907.1.
(27) Hjelkrem, O. A.; Arnesen, P.; Aarseth Bø, T.; Sondell, R. S. Estimation of Tank-to-Wheel Efficiency Functions Based on Type Approval Data. *Appl. Energy* **2020**, *276*, 115463. https://doi.org/10.1016/j.apenergy.2020.115463.
(28) Lagnelöv, O.; Larsson, G.; Larsolle, A.; Hansson, P.-A. Life Cycle Assessment of Autonomous Electric Field Tractors in Swedish Agriculture. *Sustainability* **2021**, *13* (20), 11285. https://doi.org/10.3390/su132011285.
(29) Mai, T. T.; Jadun, P.; Logan, J. S.; McMillan, C. A.; Muratori, M.; Steinberg, D. C.; Vimmerstedt, L. J.; Haley, B.; Jones, R.; Nelson, B. *Electrification Futures Study: Scenarios of Electric Technology Adoption and Power Consumption for the United States*; NREL/TP—6A20-71500, 1459351; 2018; p NREL/TP—6A20-71500, 1459351. https://doi.org/10.2172/1459351.
(30) National Agricultural Statistics Service. *Vegetables 2023 Summary*; United States Department of Agriculture, 2024. https://usda.library.cornell.edu/concern/publications/02870v86p (accessed 2024-09-05).
(31) IRENA; AEA. *Innovation Outlook: Renewable Ammonia*; International Renewable Energy Agency, Ammonia Energy Association: Abu Dhabi, Brooklyn, 2022.

(32) USGS National Minerals Information Center. Nitrogen Statistics and Information, 2024. https://www.usgs.gov/centers/national-minerals-information-center/nitrogen-statistics-and-information (accessed 2024-08-26).
(33) Booz Allen Hamilton. Argo, 2021. https://boozallen.github.io/argo/ (accessed 2024-09-01).
(34) Sousa, J.; Waiblinger, W.; Friedrich, K. A. Techno-Economic Study of an Electrolysis-Based Green Ammonia Production Plant. *Ind. Eng. Chem. Res.* **2022**, *61* (39), 14515–14530. https://doi.org/10.1021/acs.iecr.2c00383.
(35) Venkatesh, A. U.S. Low-Carbon Ammonia: Costs and Resource Requirements, 2024. https://www.epri.com/research/products/000000003002028977 (accessed 2024-07-23).
(36) Edwardes-Evans, H.; Perez, M.; Burgess, J. *Interactive: Platts Ammonia price chart*. S&P Global. https://www.spglobal.com/commodityinsights/en/market-insights/latest-news/energy-transition/051023-interactive-ammonia-price-chart-natural-gas-feedstock-europe-usgc-black-sea (accessed 2024-07-23).
(37) Morata, G.; Goodrich, B.; Ortiz, B. V. Investment Costs of Center Pivot Irrigation in Alabama—Three Scenarios, 2019. https://www.aces.edu/blog/topics/crop-production/investment-costs-of-center-pivot-irrigation-in-alabama-three-scenarios/ (accessed 2024-07-09).
(38) Chemical Engineering Magazine. *Chemical Engineering Plant Cost Index*. Chemical Engineering. https://www.chemengonline.com/pci-home (accessed 2024-08-14).
(39) Milhollin, R.; Kientzy, D.; Hamilton, S.; Lock, R. Forage Crop Irrigation Systems and Economics, 2023. https://extension.missouri.edu/publications/g1697 (accessed 2024-07-25).
(40) Internal Revenue Service. Publication 225 (2023), Farmer's Tax Guide, 2023. https://www.irs.gov/publications (accessed 2024-07-25).
(41) Center for Farm Financial Management. Farm Finance Scorecard, 2022. https://www.cffm.umn.edu/farm-management-publications/ (accessed 2024-08-27).
(42) Ahluwalia, R. K.; Wang, X.; Star, A. G.; Papadias, D. D. Performance and Cost of Fuel Cells for Off-Road Heavy-Duty Vehicles. *Int. J. Hydrog. Energy* **2022**, *47* (20), 10990–11006. https://doi.org/10.1016/j.ijhydene.2022.01.144.
(43) Proctor, K. W. *Total Cost of Ownership of a Compact Battery Electric Agricultural Tractor*; Oregon State University, 2022. https://static1.squarespace.com/static/5eab584a296dca09a66e85a6/t/627946f6c12c786debe434c7/1652115191705/TCO_report_May+2022.pdf.
(44) Keller, T.; Sandin, M.; Colombi, T.; Horn, R.; Or, D. Historical Increase in Agricultural Machinery Weights Enhanced Soil Stress Levels and Adversely Affected Soil Functioning. *Soil Tillage Res.* **2019**, *194*, 104293. https://doi.org/10.1016/j.still.2019.104293.
(45) Burnham, A.; Gohlke, D.; Rush, L.; Stephens, T.; Zhou, Y.; Delucchi, M.; Birky, A.; Hunter, C.; Lin, Z.; Ou, S.; Xie, F.; Proctor, C.; Wiryadinata, S.; Liu, N.; Boloor, M. *Comprehensive Total Cost of Ownership Quantification for Vehicles with Different Size Classes and Powertrains*; ANL/ESD-21/4, 1780970, 167399; 2021; p ANL/ESD-21/4, 1780970, 167399. https://doi.org/10.2172/1780970.
(46) Edwards, W. Estimating Farm Machinery Costs, 2015. https://www.extension.iastate.edu/agdm/crops/html/a3-29.html (accessed 2024-08-07).
(47) USDA Economic Research Service. *Farm Labor*. USDA Economic Research Service. https://www.ers.usda.gov/topics/farm-economy/farm-labor/ (accessed 2024-08-27).
(48) United States Department of Energy. *Clean Cities and Communities Alternative Fuel Price Report*; Alternative Fuels Data Center, 2024. https://afdc.energy.gov/fuels/prices.html (accessed 2024-08-15).
(49) United States Department of Energy. *Fuel Properties Comparison*. Alternative Fuels Data Center. https://afdc.energy.gov/fuels/properties?fuels=GS,DS,BD,LPG,CNG,LNG,ETH&properties=energy_ratio,energy_comparison,energy_content_higher_value (accessed 2024-08-22)

APPENDIX D

D1. Overview of LCA tools and models utilized

D1.1 The ecoinvent database

The ecoinvent database is a collection of life cycle inventory data for hundreds of products and activities across different sectors[1]. Within this dataset, flows of different technospheric flows (e.g. “one kg of urea”) and ecospheric flows (e.g., “one kg of carbon dioxide emitted to air”) are accounted for in production processes (e.g., “production of urea.”) Within these production processes, upstream activities within the database are incorporated, e.g., accounting for the generation of electricity and the synthesis of ammonia used at a urea production plant. These production systems may be specified by geography, such as Global or US processes, and may be in “market” processes, which incorporate a mix of upstream sources as well as an estimate of transportation services utilized. By utilizing this database, LCA practitioners incorporate upstream supply chain complexities while modeling their production system of study.

Within this work, different versions of ecoinvent were utilized based on the licenses available at the time of the research as well as the capabilities of each version. In the first research phase, version 3.7.1 was utilized. In the second research phase, version 3.8 was utilized, including the uncertainty estimates within processes that allow for stochastic modeling. In the third research phase, version 3.9 was utilized both in its original form as well as versions transformed by the “premise” methodology for prospective analysis. This methodology, including the work of Sacchi et al.[2] and Boyce et al.[3], applies transformations to certain upstream processes based on integrated assessment models. For example, the “2050 SSP2-RCP2.6”

transformation of ecoinvent 3.9 built by Boyce et al. makes changes to hydrogen production processes, incorporating future low-carbon hydrogen production technologies like water electrolysis and carbon capture predicted by the year 2050.

D1.2 The openLCA software

The openLCA software is a free, open-source software for LCA[4] that was used in this research to access the ecoinvent database and build product system models. Users of openLCA can import different life cycle impact methods[5] to translate ecoinvent's ecosphere flows to impacts measures; for example, the IPCC's AR6 factors can convert flows of carbon dioxide, methane, and nitrous oxide into carbon dioxide-equivalents to represent the global warming potential caused by a production process. Additionally, openLCA allows the creation of user-generated processes that incorporate upstream processes from ecoinvent. For example, a user-created process to produce one bushel of corn can specify quantities of ecoinvent-sourced inputs like fertilizers, thus including upstream chemical manufacturing emissions in the analysis.

In this research, openLCA was utilized in the first and second research phases. In the first research phase, openLCA was used to calculate GWP and water consumption characterization factors for upstream inputs in the lettuce production LCA's. For example, as indicated in **Table A8**, kg CO_2e MJ^{-1} and m^3 water MJ^{-1} values were calculated in openLCA for natural gas usage; these characterization factors were then transcribed to a spreadsheet model, where they were multiplied by the respective natural gas usage model estimates at each site. In the second research phase, processes in the openLCA software were created for each of the fertilizers applied, as discussed in **Appendix B Section B1.** Along with preexisting ecoinvent processes (e.g., diesel consumption in agricultural machinery), characterization factors were created to be applied in the Python model, including stochastic model averages and standard deviations

calculated using openLCA's Monte Carlo functionality. Further, the FDCIC comparison model was constructed and run directly in openLCA to estimate per-bushel carbon intensity. Thus, both within the software and in tandem with spreadsheet calculations, openLCA facilitated the life cycle impact estimates in this research.

D1.3 The Activity Browser program and ScenarioLink plugin

In the third research phase, Activity Browser was used to access ecoinvent instead of openLCA. Activity Browser is a Python-based software[6] which served the same purpose as openLCA did in the preceding research phases with the notable added capability of the ScenarioLink plugin. ScenarioLink allowed access to the "premise" versions of the ecoinvent database[7], wherein Sacchi et al.[2] and Boyce et al.[3] applied integrated assessment modeling to upstream processes. As in previous research phases, characterization factors were derived for input materials and activities and transcribed to a spreadsheet where calculations for different locations, years, and technology change cases were performed.

D2. Overview of energy and crop modeling tools utilized

D2.1 EnergyPlus modeling of CEA building energy demand

In the first research phase, plant factory and greenhouse energy demand models were estimated using v9.5.0 of the EnergyPlus software[8]. Within the software's integrated development environment (IDE), the design specifications for each building type were encoded into design files. These specifications included aspects such as the building dimensions, building materials, HVAC equipment, and HVAC setpoints. Outside of the IDE, Dostal and Baumelt's cosimulation tool was used in the MATLAB programming language[9]. This tool allowed for efficient iteration through each of the study locations, as MATLAB would input a weather data

file into the building design file, receive and save the energy demand outputs from the building design file, then input the weather data for the next location. Further, the cosimulation tool allowed monitoring of controlled variables and thus enabled control system responses beyond those included in the standard EnergyPlus software. For example, in the greenhouse simulation, humidity could be monitored at each time step; if the humidity exceeded setpoints, the MATLAB code would prompt a change in the building design file to ventilate the space. EnergyPlus outputs thus provided annual estimates for natural gas and electricity usage which were then transcribed to a spreadsheet LCA model.

D2.2 AquaCrop modeling of crop growth

In the first and third research phases, the AquaCrop model10 was used to simulate the growth and irrigation demand of lettuce in soil production systems. Within the open-source version of AquaCrop, AquaCrop-OS11, horticultural parameters for the simulated crop were entered in TXT files; as described in Appendix A Section A1.5, such parameters for lettuce were derived from previous AquaCrop applications in the literature. Additionally, AquaCrop requires TXT files that describe the growing environment, such as soil texture, weather data, and planting schedules. In the first research phase, to allow for iteration through multiple locations, the MATLAB version of the open-source AquaCrop-OS software was utilized. Similarly, in the third research phase, the Python version of AquaCrop-OS was used for site and year iterations. Further, within the Python code, the pyfao56 code package12 was used to calculate evapotranspiration values from future weather data sets. By utilizing AquaCrop for different locations and time points, per-hectare estimates for lettuce yield and irrigation demand were generated and transcribed to spreadsheet-based LCA models.

Appendix D References

(1) Wernet, G.; Bauer, C.; Steubing, B.; Reinhard, J.; Moreno-Ruiz, E.; Weidema, B. The Ecoinvent Database Version 3 (Part I): Overview and Methodology. *Int. J. Life Cycle Assess.* **2016**, *21* (9), 1218–1230. https://doi.org/10.1007/s11367-016-1087-8.

(2) Sacchi, R.; Terlouw, T.; Siala, K.; Dirnaichner, A.; Bauer, C.; Cox, B.; Mutel, C.; Daioglou, V.; Luderer, G. PRospective EnvironMental Impact asSEment (Premise): A Streamlined Approach to Producing Databases for Prospective Life Cycle Assessment Using Integrated Assessment Models. *Renew. Sustain. Energy Rev.* **2022**, *160*, 112311. https://doi.org/10.1016/j.rser.2022.112311.

(3) Boyce, J.; Sacchi, R.; Goetheer, E.; Steubing, B. A Prospective Life Cycle Assessment of Global Ammonia Decarbonisation Scenarios. *Heliyon* **2024**, *10* (6), e27547. https://doi.org/10.1016/j.heliyon.2024.e27547.

(4) GreenDelta. openLCA, 2024. https://www.openlca.org/ (accessed 2024-10-01).

(5) Rodríguez, C.; di Noi, C.; Srocka, M.; Ciroth, A. openLCA LCIA Methods 2.1.3, 2017. https://nexus.openlca.org/database/openLCA%20LCIA%20methods (accessed 2023-02-28).

(6) Steubing, B.; De Koning, D.; Haas, A.; Mutel, C. L. The Activity Browser — An Open Source LCA Software Building on Top of the Brightway Framework. *Softw. Impacts* **2020**, *3*, 100012. https://doi.org/10.1016/j.simpa.2019.100012.

(7) van der Meide, M.; Sacchi, R. ScenarioLink: An Activity Browser Plugin for Scenario-Based LCA Databases, 2024. https://github.com/polca/ScenarioLink.

(8) United States Department of Energy. EnergyPlus™ Version 9.5.0 Documentation, 2021. https://energyplus.net/ (accessed 2021-06-17).

(9) Dostal, J.; Baumelt, T. Model Predictive Control for Buildings with Active One-Pipe Hydronic Heating. *E3S Web Conf.* **2019**, *111*, 04050. https://doi.org/10.1051/e3sconf/201911104050.

(10) FAO. *AquaCrop, the crop water productivity model*. Food and Agricultural Organization of the United Nations. https://www.fao.org/aquacrop/en/ (accessed 2022-05-18).

(11) Foster, T.; Brozović, N.; Butler, A. P.; Neale, C. M. U.; Raes, D.; Steduto, P.; Fereres, E.; Hsiao, T. C. AquaCrop-OS: An Open Source Version of FAO's Crop Water Productivity Model. *Agric. Water Manag.* **2017**, *181*, 18–22. https://doi.org/10.1016/j.agwat.2016.11.015.

(12) Thorp, K. R.; Brekel, J.; DeJonge, K. C. Version 1.2.0 — Pyfao56: FAO-56 Evapotranspiration in Python. *SoftwareX* **2023**, *24*, 101518. https://doi.org/10.1016/j.softx.2023.101518.